FACULDADE DE ENGENHARIA DA UNIVERSIDADE DO PORTO

Quantitative assessment of motor performance during robot-aided rehabilitation: preliminary results from NEUROPROBEs project

Débora Marisa Araújo da Silva Pereira

DISSERTATION

MSC IN BIOENGINEERING - BIOMEDICAL ENGINEERING

Supervisor: Prof. Dr. Silvestro Micera, SSSA (Pisa, Italy)

Co-Supervisor: Prof. Dr. João Paulo Cunha, INESC TEC, FEUP (Porto, Portugal)

September, 2017

Quantitative assessment of motor performance during robot-aided rehabilitation: preliminary results from NEUROPROBEs project

Débora Marisa Araújo da Silva Pereira

MSc in Bioengineering - Biomedical Engineering

September, 2017

Abstract

Stroke refers to an episode of neurological dysfunction caused by a non-traumatic and permanent vascular complication in the Central Nervous System. A typical consequence of such event, hemiparesis, is observed in abnormal patterns of movement coordination and task execution with the impaired upper limb. As so, stroke survivors have a reduced quality of life, losing their independence and ability to perform basic daily tasks.

Motor therapy, a component of neurorehabilitation, helps these patients to restore and maintain their motor ability. Recently, innovative technologies like robots have been adopted to assist motor rehabilitation, inclusively for the upper limb. Among other existing techniques, robotic therapy has become popular, because these devices provide movement assistance and controllability, measurement reliability, and help physiotherapists to simultaneously supervise several patients more easily. In addition, robotics has allowed rehabilitation to evolve towards the personalization of the treatment for each patient, because movement execution can be quantified using robotics kinematics and motor performance can be continuously estimated over the rehabilitation time. However, treatment customization is emerging and needs yet to be validated concerning its effectiveness over the standard therapy. Moreover, quantification of motor impairment is usually done disregarding the neuromuscular state of the patient (the level of recovery of nondisabled neural patterns), considering only the consequences of that state (movement execution skills).

This dissertation assessed the neurobiomechanical state of acute/sub-acute stroke patients during robotic-assisted motor rehabilitation of the upper limb, using a novel exoskeleton (ALEx Rehab Station), in the scope of Neuroprobes project. To achieve this purpose, electromyographic signals of 8 healthy subjects and 4 stroke patients were acquired while they executed 3D point-to-point reaching movements wearing ALEx, as well as their arm trajectories. From this data, muscle coordination and motoneural activity in the spinal cord were assessed and task execution was quantified.

Patients who received the robotic treatment clearly improved their motor performance in terms of accuracy, efficiency, smoothness, easiness and independence to accomplish a task. Nevertheless, their muscular organization and neural activity did not progress towards the one characterizing nondisabled persons.

In this regard, this work studied the possibility to include information about the patient's muscular organization in a recently developed algorithm for the personalization of the robotic treatment with ALEx. Additionally, the present thesis proposes new kinematic parameters for the same algorithm to improve the estimation of motor impairment: MDH (to measure accuracy), RMP (to measure smoothness) and Assisted-distance (to measure robotic-assistance dependence). Finally, recommendations are provided to improve the rehabilitation protocol with ALEx.

Keywords: Stroke, Robot-aided Motor Rehablitation, Arm exoskeleton, Quantitative assessment, kinematics, Muscle Synergies, Spinal Maps

Acknowledgments

I would like to express my appreciation to both Prof. Dr. Silvestro Micera and Prof. Dr. João Paulo Cunha for their support, supervision and good cooperation across countries that made possible to accomplish the goals of my thesis.

I am very grateful to Prof. Micera for giving me the opportunity to work with his excellent team of researchers, engineers and clinicians, in the scope of such an interesting project. I also thank prof. Cunha for his guidance in spite of the distance imposed by the project location.

I also deeply thank to Camilla Pierella, Martina Coscia, Peppino Tropea and Vito Monaco for guiding me towards the success of my work, for all suggestions that contributed to be a better professional and a better person and, of course, for their endless patience to answer my questions!

Finally, I thank my family and Luís Castro very much for sharing with me both the moments of joy and difficulty during the course of my work, and for their constant support.

Débora Pereira

"Research is what I'm doing when I don't know what I'm doing."

Wernher von Braun

Contents

List of Figures

List of Tables

Abbreviations and Symbols

ADL	Activity of Daily Living
ALEx	Arm Light Exoskeleton
BICL	Long head of biceps brachii muscle
BICS	Short head of biceps brachii muscle
BMI	Brain-machine interface
BRAD	Brachioradialis muscle
BWSTT	Body weigh support treadmill training
CIT	Constraint-induced therapy
CNS	Central Nervous System
DANT	Anterior head of deltoid muscle
DMED	Medial head of deltoid muscle
DoF	Degree of Freedom
DOT	Normalized dot product
DPOS	Posterior head of deltoid muscle
EE	End-effector
EEG	Electroencephalogram / Electroencephalografic signal
EMG	Electromyogram / Electromyographic signal
ICH	Intracerebral Hemorrhage
INFRA	Infraspinatus muscle
LAT	Latissimus dorsi muscle
MDH	Mean Distance to the Healthy Path
MN	Motoneurons / Motoneural
MRI	Magnetic Ressonance Imaging
PEC	Pectoralis major muscle
PRO	Pronator muscle
RHO	Rhomboid major muscle
RMP	Ratio Between the Mean Acceleration and the Peak Acceleration
S1/S2/...	Synergy 1, 2, ...
SAH	Subarachnoid Hemorrhage
SAL	Spectral Arc-Length
sEMG	Surface EMG
T1/.../T18	Target 1/.../Target 18
TIA	Transient Ischemic Attacks
TRAPM	Middle fibers of trapezium muscle
TRAPS	Upper fibers of trapezium muscle
TRILAT	Lateral fibers of triceps brachii muscle
TRILONG	Long head of triceps brachii muscle
WHO	World Health Organization

Chapter 1

Introduction

1.1 Context and Motivation

Functional recovery from stroke demands a long period of physical rehabilitation. Investigating the mechanisms of motor relearning and cortical reorganization supported the definition of suitable methods to restore the arm functional movements. Additionally, the development of new technologies such as robotics has provided an opportunity to improve therapy delivery. In fact, robot-aided neurorehabilitation can provide the intensive and repetitive training needed to relearn upper-limb movements, by assisting the patient while performing motor tasks and by allowing the therapist to supervise several patients at the same time. (Basteris et al., 2015; Panarese et al., 2012)

Above all, motor therapy must be challenging to effectively promote motor recovery and maintain patient's attention and motivation, but, at the same time, it should be tailored on patient's residual abilities (Panarese et al., 2012). Given the fact that stroke population is highly heterogeneous (concerning, for example, the level of disability, the time course of recovery, the location, extension and type of lesion, the patient's age, and other reasons) (Basteris et al., 2015), an adaptive training, based on each individual needs and continuous progress, is believed to improve the outcome of the rehabilitative treatment (Krebs et al., 2003; Novak et al., 2011; Panarese et al., 2012; Papaleo et al., 2013; Metzger et al., 2014).

However, so far, tailoring exercises to the individual's performance demands a physiotherapist to evaluate the patient progress and adapt therapy accordingly, because customization capability of current robotic systems is limited (Panarese et al., 2012; Guglielmelli et al., 2009; Wu et al., 2016).

With this concern, the present work is being developed within the NEUROPROBEs project - Effect of an Automatic Personalized Robot-assisted Rehabilitation on Cortical Organization and Clinical Recovery After Stroke.

The project aims to develop an automatic and personalized robot-based protocol of motor rehabilitation for the upper limb. The personalization of the robot-aided treatment is expected to better promote brain plasticity and, consequently, increase speed and quality of the patient's recovery, compared to a standard physiotherapist or robot-assisted training.

In detail, the scope of the project is to continuously tailor the rehabilitative task assisted by a robotic device on the residual abilities of the patient. The exercise proposed by the customization algorithm is expected to contain only those movements that are useful for the patient's training, thus, focusing the treatment on meaningful exercises and continuously adapting it to the status of the patient, increasing also his/her motivation to continue the training.

Following this, another goal is to assess the safety and clinical efficacy of a new upper limb exoskeleton (ALEx RS) in assisting stroke patients during robotic-rehabilitation, compared to conventional therapy. ALEx was selected among the available upper limb exoskeletons, because it is the one presenting the highest "transparency" (Pirondini et al., 2016) and accessibility to the arm of the patient. This last feature was essential, because it allows the recording of neurophysiological measures, such as the electromyographic signals, which are necessary to characterize motor recovery after stroke. However, ALEx is a research prototype and its use on patients has never been tested before, requiring a further characterization and evaluation within the clinical environment of stroke patients rehabilitation.

For these purposes, a clinical trial is being conducted with 48 acute and subacute stroke patients at two hospitals - HUG (*Hôpitaux Universitaires Genève*) and Pisa University Hospital (*Azienda Ospedaliero Universitaria Pisana - Neurorehabilitation Unit*). Additionally, 48 healthy persons participate in the trial as part of a control group.

This trial is a collaboration between the Geneva-based Wyss Center, Wearable Robotics © (robot manufacturer and study sponsor), the group of the Bertarelli Foundation Chair in Translational NeuroEngineering at the *École polytechnique fédérale de Lausanne* (EPFL), the Swiss National Centre of Competence in research Robotics (NCCR) and the two participating hospitals.

Results of a pilot study on healthy subjects demonstrate that, when wearing ALEx, the exoskeleton allows arm movements similar to natural ones and, in an active mode (i.e. when ALEx provides assistance), the exoskeleton moves the arm of the subject in such a way to emulate trajectories and speed profiles similar to the natural arm movements, for a variety of tasks. This study provided clues about the influence of different rehabilitative approaches on motion and muscle coordination. (Pirondini et al., 2016)

An algorithm has already been develop, by Panarese et al. (2012), to track the motor improvement of the patients and to adopt therapist-like decision rules for varying task difficulty based on the patient's performance at a sub-task level. This algorithm was re-adapted for 3D movements and included in the online control system of ALEx, so that, for each treatment session with this robot, the motor tasks are automatically selected according to the patient's level of difficulty.

However, this implementation ought to be tested within the NEUROPROBEs trials and further analyzed, to verify if it will be beneficial for stroke subjects and more effective than conventional and standard robotic therapies in promoting arm motor recovery after stroke.

Moreover, the current algorithm only estimates the motor performance based on the consequences of the motor impairment, i.e., based on the kinematic performance of the patient. This project intents to go further and look for metrics able to define the impairment. As so, during the study, a multimodal neurophysiological assessment is carried out in order to evaluate the motor recovery not only in terms of kinematics, but also muscle and brain activity: kinematic data, magnetic resonance imaging (MRI) data, electroencephalographic (EEG) and electromyographic (EMG) signals are, thus, recorded. This extended evaluation will provide enough data to search for biomarkers of motor recovery in the muscle and brain activity, which may be included as parameters of an improved version of the personalization algorithm.

1.2 Thesis Goals

This thesis contributes to one of the main aims of NEUROPROBEs project, i.e. the definition of the neurobiomechanical state of post-stroke patients during robot-aided motor rehabilitation of the upper limb. With this purpose, the present work consisted in quantifying motor improvement of acute/sub-acute stroke patients during the treatment, using kinematics and muscular activity.

To achieve this, it was necessary to:

1. Define the framework (a structured methodology) for the analysis of kinematic data and muscle activity;
2. Identify meaningful indicators (quantitative metrics) of motor recovery and motor performance in kinematic data and muscle activity of stroke patients.

Detailing the first point, the goal was to study the variability in movement execution and muscle activity of healthy persons and, later, of stroke patients, while performing 3D point-to-point reaching movements in different conditions (different directions, and targets). It was necessary to explore this aspect since not enough information about 3D point-to-point reaching movements is reported in the literature, and because data collected in the stroke population during the treatment is constrained by the patients' ability, so this data refers to different movement conditions, for each subject and for each session of treatment.

Finally, the second goal of this work was to compare the two groups of subjects to identify which metrics related to kinematics and muscle activity can be used to quantify motor impairment and recovery.

It must be noted that the work developed was fully experimental and goes from data acquisition to data analysis, which provided an opportunity to practically learn how to perform recordings of electromyographic signals in hospital environment, during robot-aided rehabilitation.

This thesis was developed under the supervision of Prof. Dr. João Paulo Cunha [1], prof. Dr. Silvestro Micera [2] and collaborators (Martina Coscia [3], Camilla Pierella [4], Peppino Tropea [5]), at the Biorobotics Institute of the Scuola Superiore Sant'Anna (in Pontedera - Pisa, Italy).

1.3 Dissertation Structure

This dissertation is organized in nine chapters, including the current contextualization chapter.

Chapter 2 describes theoretical concepts of anatomy and physiology in the context of Stroke, and reviews the impact of this neural disorder in human society.

Chapter 3 introduces the main element of this work, Motor Rehabilitation of the Upper Limb for post-stroke patients. This chapter goes from the concept of motor recovery to the personalization of the treatment in Robotic-aided therapy. The necessary background theory is detailed for a good comprehension of each section and a review of the state of the art is provided for the three main branches of Motor Therapy addressed in this thesis.

Given that quantitative assessment are keywords of this work, two chapters (5 and 4) describe the current methods of kinematic evaluation of arm movements and analysis of muscle activity of the upper limb.

From Chapter 6 to Chapter 8, the work developed is reported: description of materials and methods, report of results obtained with 8 healthy and 4 acute/sub-acute post-stroke patients, as well as the respective discussion.

Chapter 9 presents the final conclusions of the thesis and future perspectives for Neuroprobes project.

[1] PhD, INESC TEC, Faculty of Engineering of the University of Oporto

[2] PhD, Bertarelli Foundation Chair in Translational Neuroengineering, Center for Neuroprosthetics and Institute of Bioengineering, École Polytechnique Fédérale de Lausanne (EPFL), Lausanne, Switzerland; Scuola Superiore Sant'Anna, BioRobotics Institute, Pisa, Italy

[3] PhD, Wyss Center for Bio- and Neuro-Engineering, Geneva, Switzerland; Bertarelli Foundation Chair in Translational Neuroengineering, Center for Neuroprosthetics and Institute of Bioengineering, École Polytechnique Fédérale de Lausanne (EPFL), Lausanne, Switzerland

[4] PhD, Wyss Center for Bio- and Neuro-Engineering, Geneva, Switzerland; Bertarelli Foundation Chair in Translational Neuroengineering, Center for Neuroprosthetics and Institute of Bioengineering, École Polytechnique Fédérale de Lausanne (EPFL), Lausanne, Switzerland

[5] PhD, Scuola Superiore Sant'Anna, BioRobotics Institute, Pisa, Italy

Chapter 2

Stroke

This chapter provides background information about the pathological condition of the study (Stroke), presenting a general overview of the anatomy and the pathophysiology relevant to this disorder, as well as an analysis of its impact on today's society.

2.1 Background concepts

Hemorrhage, ischemia and infarction of the central nervous system (CNS), as well as the relation between these phenomena, are important in the context of stroke. Thanks to advances in neuroimaging, neuropathology and basic science, they are now better understood.

Ischemia is a restriction in blood flow to an organ, leading to oxygen and glucose insufficiency (as well as inadequate removal of metabolites) and, consequently, causing the death of that tissue, i.e. infarction (NIH, 2009; Steward, 2000).

Specifically, CNS infarction is defined as brain, spinal cord, or retinal cell death caused by evident[1] ischemia (Sacco et al., 2013).

An hemorrhage is a focal collection of blood within a tissue, resulting from rupture of an hypertensive, weakened small-vessel and consequent bleeding (Donnan et al., 2008).

Specifically, CNS hemorrhage is defined as an hemorrhage within the brain, spinal cord or retinal tissue. Ischemia may occur due to a focal CNS hemorrhage and, this way, a CNS hemorrhage may lead to cell death - CNS hemorrhagic infarction (Sacco et al., 2013).

Additionally, an hemorrhage may also take place within the brain parenchyma or the ventricular system - Intracerebral Hemorrhage (ICH) -, or into the subarachnoid space (i.e. the space between the arachnoid membrane and the pia mater of the brain or spinal cord) - Subarachnoid Hemorrhage (SAH).

[1] That is, ischemia diagnosed by an objective (imaging, pathological or other) evidence, or by a clinical evidence (symptoms of neurological déficit present for 24h or more, or death).

Ischemia may also occur due to occlusion or stenosis of CNS blood vessels caused by either local embolism (that is, an atherosclerotic plaque which breaks away, travels with the blood flow and blocks the blood stream) or thrombosis (formation of a blood clot which obstructs the blow flow) (Dorland, 2011).

All of the mentioned conditions (ischemia, hemorrhage, infarction), and their anatomical variations in the CNS, lead to cell death, damaging the CNS and altering its normal function. This lesion may be symptomatic or not. When it is, the patient suffers from neurological deficit expressed by the clinical evidences to be described in Section 2.2.2. When the lesion is assymptomatic, the condition is called silent: silent CNS infarction; silent cerebral hemorrhage.

Stroke is a broad term referring to an episode of neurological dysfunction caused by a non-traumatic vascular complication in the CNS (Figure 2.1 [2]), as those described above. According to the Stroke Council of the American Heart Association (AHA)/American Stroke Association (ASA) (Sacco et al., 2013), this complication identifies the type of stroke:

- a CNS infarction (being hemorrhagic or not) defines an Ischemic Stroke;
- an intracerebral hemorrhage defines a Stroke caused by ICH;
- a subarachnoid hemorrhage defines a Stroke caused by SAH;
- a cerebral venous thrombosis (CVT) defines a Stroke caused by CVT.

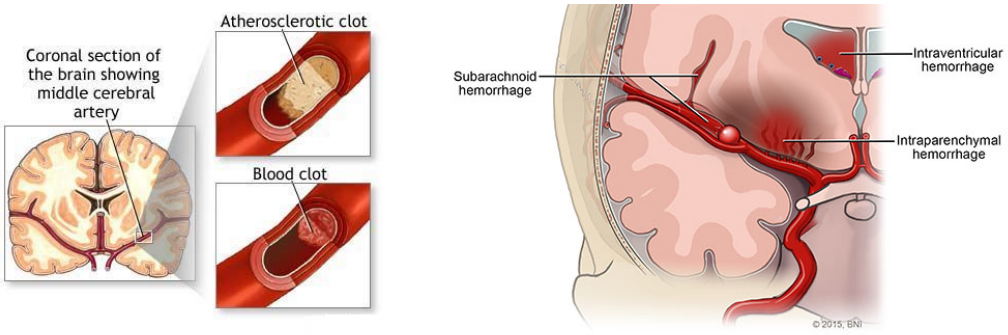

Figure 2.1: Possible vascular complications preceding stroke. (1) Subarachnoid hemorrhage takes place when a weakened blood vessel of the brain ruptures, leaking blood into the subarachnoid space and, consequently, narrowing adjacent blood vessels; (2) Intraparenchymal hemorrhage occurs typically due to abnormal development of an important cerebral area in infants or high blood pressure in adults - blood precipitates and breakdown products are deposited in the brain; (3) Intraventricular hemorrhage, besides injuring the brain, results in hydrocephalus (increase of fluid in the brain); (4) embolism - atherosclerotic clot blocks blood stream; (5) cerebral venous thrombosis - blood clot interrupts blood flow.

[2] https://ncats.nih.gov/exrna/projects/biomarkers2015#brain; https://www.verywell.com/lupus-as-a-cause-of-stroke-3146038

Silent infarction and silent hemorrhage are also considered to be stroke, as well as events of neurological deficit for which few information is available to further classify the stroke as one of the above definitions.

A stroke caused by some hemorrhage in the CNS may generally be called an hemorrhagic stroke. ICH or SAH can be considered subtypes of this definition.

It must also be noted that the definition of stroke assumes episodes of neurological deficit persisting during 24h or more (that is, a permanent damage to the CNS), or until death (Sacco et al., 2013). Temporary vascular-related episodes of neurological dysfunction (that is, a "transient" expression of stroke symptoms) are, otherwise, termed “transient ischemic attacks” (TIA) (which “may last from a few seconds up to several hours, the most common duration being a few seconds up to 5 or 10 minutes”, as stated by C.M. Fisher during the Second Princeton Cerebrovascular Disease Conference (Fisher, 1958)).

2.2 Stroke Anatomy and Pathophysiology

Different parts of the CNS have a critical role in the activation of muscles to produce voluntary movement, such as the spinal cord, the cerebellum, the brain, and the brain stem. The resulting motor behavior is affected by lesions in these regions, after ischemic or hemorrhagic events, as it happens with stroke patients. (Cheung et al., 2009)

2.2.1 Relevant Anatomy of the Central Nervous System in Stroke

The cerebellum, the brain and the brain stem are components of the encephalon, the part of the CNS contained in the skull.

Cerebellum is important in balance and muscle coordination, and is involved in motor control learning. The brain stem, in turn, has an important role in controlling functions like breathing, heart rate, and alertness/consciousness. The brain is the main center of processing of sensory information. (Rod R. Seeley, 2003)

More specifically about the brain, the gray matter in its exterior surface is the cortex, and deeper, are the basal nuclei.

Basal nuclei (which includes the caudate nucleus, putamen and globus pallidus) control automatic motor functions like walking, running and swallowing.

Brain cortex is divided by the middle line in right and left hemispheres, each of which is divided in lobes (see Figure 2.2 [3]). Frontal lobe has a crucial role in voluntary motor function, motivation, sense of smell, mood/emotions/attention and speech production. Parietal lobe is responsible for processing most of the sensory stimuli concerning the sense of touch, pain and temperature. Occipital lobe processes visual information and temporal lobe deals with hearing information, speech comprehension and memory.

[3] https://inside-the-brain.com/2013/03/07/what-is-attention-and-where-is-it-in-the-brain/

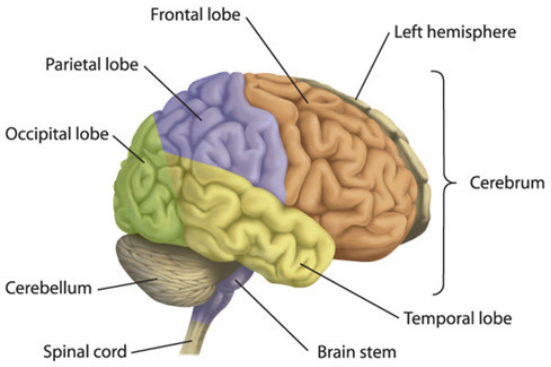

Figure 2.2: Brain lobes.

More specifically in the frontal lobe, the motor cortex is the region responsible for integrating information about the body position and the surrounding environment, and for defining the best plan to move the body for a given purpose. Thus, it controls voluntary movement. (Steward, 2000)

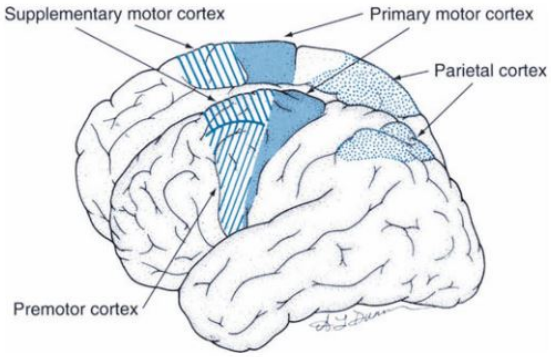

Figure 2.3: Cerebral motor cortex.

It is believed the motor cortex is divided in sub-regions (Figure 2.3) responsible for specific features of motion (Binder et al., 2009c; Steward, 2000):

- The primary motor cortex (also called M1) has a key role in controlling fine movements of the hand and fingers (manual dexterity), as well as face and tongue, which also demand skilled movements;
- The premotor cortex plans the strategy of complex movement involving proximal muscles, and has a key role in defining the orientation of the body to prepare some movement;
- The supplementary motor area has a similar role to the premotor cortex, for distal muscles;
- The posterior parietal cortex combines diverse sensory information to define the motor behavior relatively to the surrounding environment.

Sub-regions of the motor cortex are somatotopically organized, meaning that local stimulation generates movement of a particular part of the body. The lower limb, the upper limb, trunk, face

and tongue are represented in large areas of the primary motor cortex, situated in the precentral gyrus of the cerebral motor cortex (see Figure 2.4).

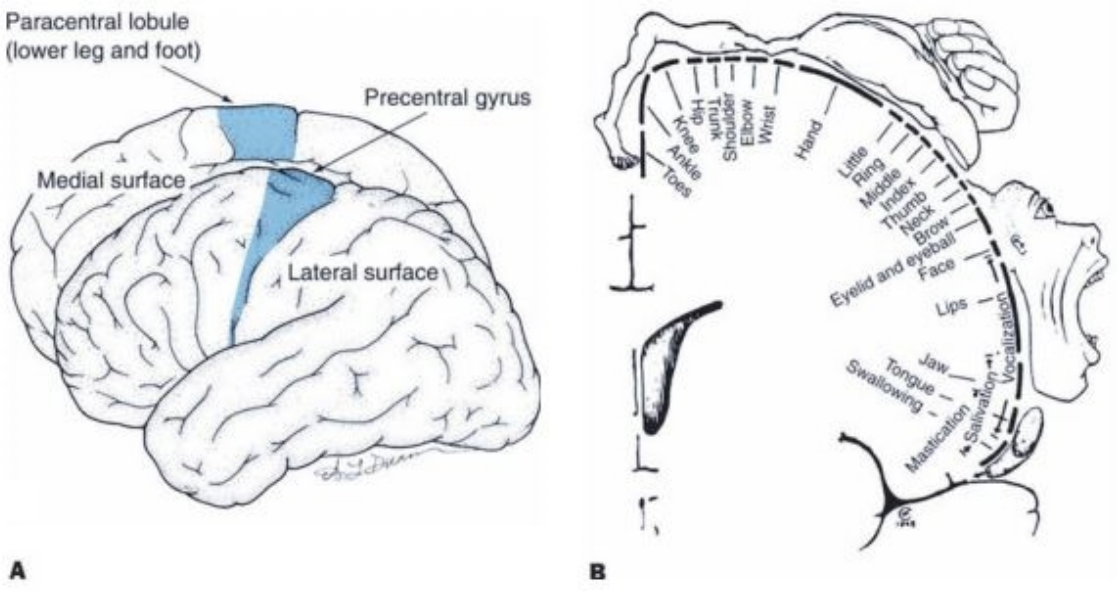

Figure 2.4: A - The primary motor cortex is localized in the precentral gyrus. B - Somatotopically organization of the primary motor cortex.

In what concerns the spinal cord, it is organized in different segments, each of which plays a role in the control of and is linked to some part of the body by the sensory and motor nerves that emerge from that segment. (Steward, 2000) For example, cervical segments of the spinal cord are known to control arm movements. (Riehle and Vaadia, 2004)

There are 8 cervical segments, from C1 to C8, 12 thoracic segments, T1 to T12, 5 lumbar segments, L1 to L5, and 5 sacral segments, S1 to S5. This division in segments is a mere terminology used to define and discuss the location of lesions in the spinal cord, and there are no actual boundaries limiting these spinal zones.

Neurons of the gray matter of the spinal cord are neither motor nor sensory but interneurons. Thus, lesions in the spinal cord gray matter cause sensory/motor deficits in particular body segments, and lesions in its white matter break the communication between the brain and the body, leading to sensory deficits and/or paralysis below the level of the lesion. (Steward, 2000)

2.2.2 Pathophysiology of Stroke

During Ischemic Stroke, when blood flow reduces in the CNS, part of the tissue (called the core of the infarct) is irreversibly damaged and dies within minutes, by experiencing mechanisms like excitotoxicity [4], ionic imbalance (eg, increased intracellular calcium, following ischemia), oxidative/nitrosative stress, inflammation, apoptosis and peri-infarct depolarization (Hakimelahi and González, 2009; Sacco et al., 2013). The peripheral tissue, however, may be perfused by collateral circulation and remain viable for some time. This region (called ischemic penumbra) must be promptly treated, otherwise, it will infarct as well, rapidly increasing the core tissue volume. (Hakimelahi and González, 2009)

In turn, when hemorrhage occurs, the leaked blood increases pressure in adjacent cells, injuring them and causing their death (hemorrhagic stroke). Alternatively, the excessive volume of leaked blood surrounding cells may reduce the blood flow in nearby vessels feeding the tissue (ischemia) and, this way, cause hemorrhagic infarction (ischemic stroke). (Steward, 2000)

Vessel breach may be caused, for example, by some vascular malformation, by high blood pressure (chronic hypertension) or by the presence of aneurysms[5] which eventually rupture. (NIH, 2009; Donnan et al., 2008)

Concerning hemorrhagic strokes as defined in the previous section, and, specifically, those caused by ICH, the hematoma is located in the brain parenchyma or ventricules, but pressure resulting from the mass effect of the hemorrhage may injure the neighbouring cerebral tissue and the global intracranial pressure may also increase. Similarly, a SAH produces the same result and debilitates cerebral autoregulation. (Sacco et al., 2013; Liebeskind, 2017)

The injury location in the CNS determines the type and level of neurological deficit. Typically, damage in the right hemisphere leads to contralateral hemiparesis [6], left hemisensory loss, right gaze preference and left visual field cut. Accordingly, the opposite side is similarly affected by an injury in the left hemisphere. Nevertheless, symptoms resulting from damage in the right hemisphere of the brain are not always detected by patient or medical doctor. (Liebeskind, 2017; Sacco et al., 2013)

An injury in the internal capsule (or in the corticospinal tract) may lead to hemiparetic face, arm and leg equally, whereas damage in the motor cortex leads to a more focal hemiparesis, predominantly affecting the face and the arm (MCA cortical territory). However, stroke severity does not necessarily determine the weakness severity.

[4] Excitotoxicity is a pathological mechanism of killing/damaging neurons by excessive excitation with neurotransmitters like glutamate (endogenous excitotoxin). Glutamate accumulates in the extracellular liquid, after ischemia, in stroke, and, along with the diminished nutrients and oxygen, leads nerve cells to die.

[5] Aneurym is a bulge developed in the wall of a blood vessel, due to its dilatation, which is filled with fluid or clotted blood. - from *Aneurysm* at *Dorland's Medical Dictionary (2011)*

[6] If the right hemisphere is damaged, the left side of the body is weakened, and the arm and leg movements are debilitated.

Specifically, hemiparesis is observed in abnormal patterns of movement coordination and unnatural posture, as well as a reduced strength of the impaired limb (Lennon and Ashburn, 2000). This is the main concern in physical therapy, during neurorehabilitation of the patient, to be discussed in Chapter 3.

2.3 Epidemiology and Economic Impact

Stroke is highly prevalent in the world, affecting 15 million people each year (WHO, 2002). According to the World Health Organization, in 2015, 6.24 million people suffered stroke worldwide and died, being the Stroke the second most common cause of death (approx. 11% of all deaths) after ischemic heart disease (WHO, 2017). The average age-adjusted stroke mortality for developed countries is about 50–100 per 100 000 persons per year (Donnan et al., 2008). However, this is variable between countries, which may indicate that prevalence of risk and genetic factors, as well as management of stroke, are geographically different (Donnan et al., 2008). In addition, although the risk increases with age, a stroke may occur at any age. For example, in 2009, in the United States of America, 34% of hospitalized stroke suffers were less than 65 years old (Hall et al., 2012).

Nevertheless, thanks to improved living standards and an enhanced control of stroke risk factors (especially high blood pressure and cigarette smoking) in developed countries, stroke mortality has been constantly decreasing over last 50 years (mostly since late 1960s, about 5% per year). Trends in developing countries are uncertain. (Donnan et al., 2008)

Additionally, stroke is the leading cause of impairment around the world: it is estimated that by 2030 disabilities associated to stroke in western countries will be considered the fourth critical cause of reduced disability-adjusted life-years (DALYs — "the sum of life-years lost as a result of premature death and years lived with disability adjusted for severity") (Donnan et al., 2008). Stroke survivors have a reduced quality of life, and population follow-up studies have verified that neurological impairment, dementia and recurrent stroke affect these patients after the first stroke (Mendis, 2013). According to Carod-Artal et al. (2000), evaluation of stroke survivors' life 1 year after the incident, 2/3 of these patients present impaired reaching movements. 73-88% of first time stroke survivors experience modifications in their upper limb function, as well as 55-77% of chronic post-stroke patients (Donnan et al., 2008; Clarke et al., 2002) . Therefore, the vast majority loses their independence in daily routines, being incapable to perform basic tasks with their paretic limb (Pirondini et al., 2016).

In fact, it is estimated that about 500 per 100 000 persons live with such severe consequences of stroke and, once stroke mortality seems to be falling faster than stroke incidence, this number will probably raise together with health-care demands (Donnan et al., 2008).

Around the world, 2-4% of total costs in health-care are dedicated to stroke care. In industrialized countries, direct costs of stroke care are higher than 4%: estimated at £7.6 billion in the UK,

AUS$1.3 billion in Australia, and US$40.9 billion in the USA, which is equivalent to US$100 per head of population per year (Donnan et al., 2008). Notwithstanding, World Health Organization reports a need for improvements in stroke care and rehabilitation, even among developed countries in favor of a reduction of post-stroke disability (Mendis, 2013).

Chapter 3

Upper Limb Motor Rehabilitation following Stroke

This chapter introduces the main concepts and current strategies in motor therapy of the upper limb and motor recovery of post-stroke patients. It goes from theory on motor control, neuroplasticity, and motor learning, to a review of the state of the art in methods and tools (such as robotics) used in motor therapy.

3.1 Motor Control, Motor Learning and Motor Recovery after Stroke

Motor control is the process by which the CNS (Central Nervous System) integrates sensory information in order to stimulate and coordinate the necessary set of muscles to execute some movement (Reviews, 2016). In this context, motor skill can be understood as "the ability to plan and execute a movement goal", as defined by Krakauer (2006).

An action or movement has an associated geometry and speed (kinematics) and requires the application of forces (dynamics). In this sense, motor skill is achieved (and improved by added practice) by minimizing movement execution errors of kinematic and dynamic nature, using visual and proprioceptive[1] senses, and, thus, minimizing energy and time spent. Motor learning comprises this concept of skill learning, motor adaptation and decision making (to be able to choose the appropriate movement for a specific situation) (Krakauer, 2006; Kitago and Krakauer, 2013).

One of the most currently accepted theories states that motor control is modular, which means that any movement (such as a reaching movement) is controlled by a sequence of individual operations (modules): an action trajectory may be previously planned disregarding the limb forces (as it believed, for example with reaching tasks (Krakauer, 2005)); lately, the action is performed by stimulating muscles to apply the adequate forces, according to the viscoelastic and inertial properties of the limb (Krakauer, 2005).

[1] Proprioception is the perception of stimuli within the organism itself, especially regarding the position and movement of the body and its elements.

Each of those modules of motor control may be neglected by some injury, as it happens in stroke. Following to such event, most patients experience spontaneous recovery to some extent which is variable across patients (Kwakkel et al., 2006). Previous experiments and analysis of recovery assessment indexes have shown that spontaneous recovery is maximized at early weeks after stroke, but it also takes place during the subacute and chronic phases (Ganguly et al., 2013; Krakauer, 2006; Di Pino et al., 2014).

This mechanism of natural neurological repair (as well as the one promoted by motor therapy) is believed to occur due to a combination of processes like brain reorganization, restoration of ischemic penumbra and recovery from diaschisis[2] (Krakauer, 2006).

In particular, the motor cortex has redundant functional regions (and is also able to create new functional regions), allowing a new brain area to get the responsibility to stimulate muscles previously recruited by the damaged brain area. This ability of the CNS to reorganize its functions and structure (by activation of new neural pathways and neurogenesis) is frequently denominated neuroplasticity (Krakauer, 2006; Di Pino et al., 2014; Ganguly et al., 2013; Hatem et al., 2016).

In fact, it has been previously observed that brain reorganization may involve intact, adjacent or distant, brain regions to the injury (in the same and/or opposite hemispheres) (Feydy et al., 2002; Erik Ween, 2008; Rehme et al., 2012). In the beginning (when only spontaneous recovery occurs), functional reorganization may involve several parts of the brain, but, with increasing therapy, reorganization tends to be more focal (near or distant from the original brain area responsible for that function) (Krakauer, 2005).

Moreover, spontaneous recovery is commonly insufficient and, additionally, patients often develop compensatory ways to execute some movements, using alternative muscles of the affected limb or favoring the use of the unaffected limb, due to their inability to recruit the same muscles as before stroke (Krakauer, 2006; Ganguly et al., 2013; Soekadar et al., 2014). For example, often the shoulder is excessively elevated and retracted to lift the arm due to a decreased range of motion of the shoulder flexion. Another example is the increased displacement of the trunk forward or its rotation in reaching or pointing movements when the range of motion of the elbow extension is limited (Levin et al., 2009).

Oppositely, true motor recovery presupposes the patient reacquires his ability to move the affected limb in a natural way. Recovery is, therefore, characterized by the reappearance of similar movement patterns to the ones of non-disabled subjects (the same end-effectors and joints, comparable ranges of motion, similar muscle co-activation patterns and spatio-temporal interjoint coordination, and normal muscle tone, i.e. reduced spasticity), as well as the ability to complete different tasks (Levin et al., 2009). Notwithstanding, the promotion of fully motor recovery as defined here is still an open question, because it is not certain that recovering all the patterns previous

[2]Diaschisis is "a temporary loss of function produced by acute focal brain damage in an adjacent region or in a region connected through fiber tracts." - from *Diaschisis* at *INS Dictionary of Neuropsychology and Clinical Neurosciences (2015)*

to injury result in a better performance of daily living activities.

In any case, these points explained in the two paragraphs above highlight the need for motor therapy after stroke and, given that investigation with human and animal models suggests that mechanisms involved in brain reorganization are similar to the ones in motor learning (Krakauer, 2005; Kitago and Krakauer, 2013; Di Pino et al., 2014), therapeutic methods which promote motor re-learning are expected to achieve better outcomes.

In addition, as reviewed in Krakauer (2006), there are experimental evidences that, after practice (repeated execution of the same movement) and consequent learning of some type of movement, the CNS has designed internal models which map the limb conditions (level of external forces, initial position, and other) to the respective muscle forces to be commanded for the movement execution. Moreover, experiments have also demonstrated that these internal models can answer to different type of movements from those used to learn. This generalization capacity is reflected in a consequent ability of the patient to perform not only the particular tasks trained during rehabilitation, but also any activity of daily living (ADL), as reviewed by Krakauer (2006).

Finally, it is necessary to understand that motor recovery after stroke is heterogeneous in respect to functional outcome. Individuals in acute phase affected by mild to moderate paresis of the upper limb are expected to achieve a good level of motor recovery: around 71% of these patients recover their dexterity to a considerable extent at 6 months after stroke (Nijland et al., 2010). On the contrary, severely affected patients have a bad prognosis: about 60% of them fail to recover their dexterity at 6 months after stroke (Kwakkel et al., 2003). In the worst scenario, patients with paralysis are poorly expected to recover a functional use of their arm (Hatem et al., 2016).

3.2 Physical Therapy of the Upper Limb

3.2.1 Background concepts

Neurorehabilitation is a complex medical process which applies basic and clinical neuroscience research in helping patients who have suffered damage in the nervous system. Its main purpose is to maximize functional recovery, and to minimize/compensate for any functional alterations[3] caused by the neurological injury (Ganguly et al., 2013). This is fundamental for a stroke survivor to have back a self-sustainable life and to engage in society. (Mendis, 2013)

As emphasized by the World Health Organization (Mendis, 2013), the article 26 of the United Nations Convention on the Rights of Persons with Disabilities appeals for "appropriate measures, including through peer support, to enable persons with disabilities to attain and maintain maximum independence, full physical, mental, social and vocational ability and full inclusion and participation in all aspects of life". Therefore, neurorehabilitation considers the patient well-being in all its aspects, being interdisciplinary: includes physical, occupational, psychological, vision, speech and language therapies, and other. Therefore, several rehabilitative programs, whether conducted in hospitals or specialized clinics, gather specialists of diverse fields in order to provide the best treatment to the patient. (Veerbeek et al., 2014; Lipovsek et al., 2012)

A general timeline of neurorehabilitation is often considered as presented in Figure 3.1 (Proietti et al., 2016). As the rehabilitative program evolves, the patient progresses and executes movements more independently, becoming more active during physical training. More objectively, three phases of stroke recovery may be considered in neurorehabilitation, according to Sullivan 's recommendation, and used in previous studies of stroke rehabilitation: the acute phase (0-7 days from the stroke onset); the subacute phase (7 days to 6 months); chronic phase (6 months until years post-stroke) (Sullivan, 2007). This distinction must be taken into account when developing rehabilitative treatments, specially in robotic-aided rehabilitation, where the control of robotic devices must be adapted to each phase.

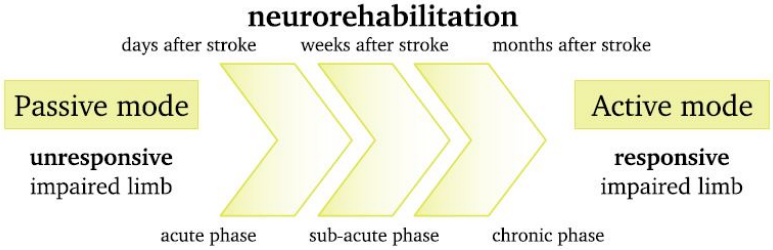

Figure 3.1: Global timeline of neurorehabilitation. The terms "Active" and "Passive" refer to the patient (see Section 3.3.1, Table 3.3).

[3] In the context of injury-induced functional modifications, it is important to note that impairment and disability are different concepts. Throughout this dissertation, these terms are used according to their definition by the WHO in The International Classification of Impairments, Disabilities, and Handicaps (1980):
- Impairment: "any loss or abnormality of psychological, physiological or anatomical structure or function."
- Disability: "any restriction or lack (resulting from an impairment) of ability to perform an activity in the manner or within the range considered normal for a human being."

Physical therapy, one of the above-mentioned components of neurorehabilitation, focus on restoring and maintaining the ADLs, commonly lasting from the early phase to the chronic phase of post-stroke rehabilitation (Veerbeek et al., 2014). This is important since stroke survivors, being physically debilitated, have their quality of life considerably reduced. Impairment of the upper limbs specifically limits their performance in basic activities like feeding and self-care, consequently reducing the independence of these individuals. In detail, paresis of the upper extremity is associated to weakness, loss of dexterity, spasticity, abnormal muscle synergies and, thus, abnormal motor control (Krakauer, 2005; Kitago and Krakauer, 2013).

So far, only a modest advance has been reported in functional outcomes of stroke survivors rehabilitation, despite the considerable improvements in stroke prevention, early diagnosis and acute treatment (Ganguly et al., 2013). As so, a more comprehensive knowledge about recovery from stroke is essential when studying any new technique to rehabilitate post-stroke patients.

3.2.2 State of the Art

Currently, it is generally accepted that a rehabilitative treatment must be adaptive to the patient's progress, following four main steps cyclically (Ganguly et al., 2013):

1. Needs screening;
2. Definition of realistic objectives;
3. Plan therapy program according to patient capabilities;
4. Assessment of improvements.

Moreover, it has been demonstrated that an assisted training is more effective than just encouragement of the patient to execute tasks on his/her own based on the therapist advices (this method may be, however, successful with patients with mild hemiparesis, being at least capable to partially perform the tasks) (Lum et al., 2002). Nevertheless, only assisted training is not also the best approach to induce motor relearning, so the modern therapists combines assistance with coaching (Barnes and Good, 2013).

Oppositely to strategies based on intuition applied in the past, modern motor rehabilitation is based on knowledge from experimental evidence or principles of evidence-based medicine (specially, conclusions from analysis of randomized controlled trials) (Barnes and Good, 2013).

A repetitive training is considered to have a major role in motor recovery. Thus, independently of the physical therapy strategy being followed, treadmill training seems to be essential. (Ganguly et al., 2013; Barnes and Good, 2013; Lum et al., 2002; Proietti et al., 2016; Maciejasz et al., 2014).

The following techniques are the state of the art of physical therapy of the upper limb after stroke, referring to methods of motor training. Some of them (such as constraint-induced therapy, EMG-triggered neuromuscular stimulation, or even interactive robotic-therapy) were developed based on motor learning theory (see Section 3.1), other are based on clinical and empiric evidences.

1. **classical Bobath approach**: The original concept proposes re-education over compensation - therapists re-educate the patient to regain normal movements with the affected arm, instead of teaching compensatory strategies with the unaffected arm (Graham et al., 2009);

2. **evolved Bobath approach**: Currently, knowledge on neuroplasticity, motor learning and motor control is added to the classical Bobath concept, so therapists guide the patient to develop optimal (not just "typical") movement patterns (Lennon and Ashburn, 2000);

3. **practice of repetitive and stereotyped exercises**: several studies have reported effectiveness of implementing this type of training (as mentioned by Lum et al. (2002)), but several more recent experiments have shown that the patient's ability to execute the learned tasks, retention of this ability, as well as capability of generalization to learn new actions are improved by including variability of exercises (Krakauer, 2006). Even though, repetitive training has brought good results in recovering subacute stroke patients, patients with chronic hemiparesis, and even patients with complete hemiplegia[4] (Barnes and Good, 2013).
   Additionally, it has been found that repetitions must be frequently interleaved by prolonged rest, so that learning is optimized (Krakauer, 2006).

4. **body weight support treadmill training (BWSTT)**: Practice of repetitive and stereotyped exercises with body weight support, that is, with the effect of gravity (weight) being compensated by some apparatus (the arm is suspended). BWS reduces the torque magnitude produced in the limb joints when some action is being performed (Coscia et al., 2014; Van Vliet et al., 2005).

5. **practice of repetitive and stereotyped exercises together with techniques to facilitate movement execution**: EMG-triggered neuromuscular stimulation[5], supra-threshold electric stimulation of hand and wrist muscles[6], application of loads (external loads) are examples of techniques combined with treadmill training. This approach is usually indicated for more severely affected patients.
   Past investigation has verified that repetitive movements (of hand and fingers) against loads have lead to increased motor ability when compared to Bobath approach or electrical stimulation treatments. (Lum et al., 2002) However, in more recent studies, EMG-triggered neuromuscular stimulation has demonstrated effectiveness in the three phases of neurorehabilitation mentioned in Figure 3.1. Oppositely, supra-threshold electric stimulation (being independent of movement intention by the patient) results in little functional outcomes. (Krakauer, 2006)

[4] Hemiplegia means "paralysis affecting only one side of the body". (Steward, 2000)

[5] In EMG-triggered neuromuscular stimulation, EMG surface electrodes provide input to a microprocessor, which outputs an electrical signal for neuromuscular stimulation when an intention to move the arm is detected. So, the patient initiates a voluntary contraction to execute an action and, when the muscle activity crosses some pre-defined threshold, the muscle is electrically stimulated to assist the movement.

[6] The electrical stimulation is provided independently from an intention of the patient to execute an action. Supra-threshold simply means the electrical stimulus is a voltage sufficiently high to generate the action potential in muscle fibers.

6. **Impairment-oriented training (IOT)**: This method includes two subtypes: arm ability training and arm basis training. The first targets patients with mild hemiparesis, the latter is adequate for patients with severe hemiparesis. (Barnes and Good, 2013) Training tasks promote abilities like "hand grip, finger individuation, arm-hand steadiness, aimed reaching, tracking, and wrist-finger speed", as mentioned in Krakauer (2006).

7. **task specific training**: Normal human behaviour results form goal-oriented actions. This fact and a concern on improvements in ability to perform activities of daily living (ADLs) originated this approach. Tasks are intensively repeated but tasks' difficulty may be varied. Task-oriented repetitive movements have proved positive outcomes, such as improved movement coordination and muscle strengthening. (Pirondini et al., 2016; Ganguly et al., 2013; Van Vliet et al., 2005; Kitago and Krakauer, 2013)

8. **constraint-induced therapy (CIT)**: Training of the impaired limb is stimulated by constraining the unaffected one (Maciejasz et al., 2014; Lum et al., 2002). This can induce an increased use of the impaired limb in ADLs (Lum et al., 2002; Kitago and Krakauer, 2013), but is still controversial, because the main improvement seems to be due to the intensity of therapy (massive repetition of exercises) and not due to the constrain, and because eligible patients for this therapy must have at least 10^{o} of wrist and finger extension, excluding many other patients Krakauer (2006); Barnes and Good (2013).

9. **interactive robotic-therapy**: Robots can be used to generate load against movement, to assist the patient actions and trajectory, and to correct them, and allow the application and combination of various techniques above enumerated (with improved intensity and repeatability, and with precise force patterns and accurate control of tasks execution (Pirondini et al., 2016)).
   For example, using force-fields produced by some robot, the patient's ability to adjust to disturbances to the movement is promoted[7] (Krakauer, 2006; Maciejasz et al., 2014; Pirondini et al., 2016).
   On the other hand, and with extreme importance for the work in the present thesis, robots add precision to therapy evaluation (offering kinematic variables to quantitatively analyze motor performance/improvement), and making possible to immobilize the patient trunk so that compensation with trunk movements does not affect the evaluation (Krakauer, 2006).

It must be noted that other methods of physical therapy for the upper extremity are available (like mental training or neuromodulation approaches). However, they are not so relevant to introduce robotic-aided rehabilitation and its assessment (the main context of this dissertation), since they are not usually applied in combination with robotic devices in post-stroke motor recovery. For a larger review on this matter, further reading of Barnes and Good (2013) is advised.

[7] The same theory of assistance-when-needed, as with EMG-triggered neuromuscular stimulation, but muscles involving movement of more than one joint are assisted at the same time.

Other important aspects are dose (amount of practice) and timing of physical therapy, which is yet a concern, nowadays. For example, it has been demonstrated that starting rehabilitation 5 days after injury is considerably more effective than after 1 month (Krakauer, 2005), and more studies provided similar evidences that early and intensive rehabilitation is more beneficial (Kwakkel et al., 1999; Kitago and Krakauer, 2013). However, other studies have proved the opposite, showing, for example, that an intensive therapy in the first hours and days after stroke does not achieve a good outcome (Nijland et al., 2011; Dromerick et al., 2009). As so, this topic is still under debate, being unknown the correct dose-timing relation, specially considering that each patient is different from another one (Lang et al., 2015).

As stated in Lang et al. (2015), it is urgently necessary to perform preclinical and clinical investigation in order to design an effective prescription system of physical training. Currently, according to the data analysis conducted by Lang et al. (2015) from various studies, one can say that:

- each patient requires a different optimal dose according to his/her clinical presentation;
- there is a limited relation between dose and positive functional outcomes, suggesting that usually larger amounts of physical training incomes better recovery;
- dose and timing may be connected - individuals at 2 to 3 months after stroke may benefit from large doses, but it might not be recommended for patients at the acute and sub-acute phase (days, weeks after stroke).

All of the above-mentioned characteristics in physical therapy must be considered to accurately assess any rehabilitative method (with any device, just like with the exoskeleton of the present work).

3.3 Robot-aided Motor Therapy of the Upper Limb

3.3.1 Background concepts

Recently, innovative technologies have been adopted to support the motor rehabilitation of the upper limb after stroke. They include, for example, robotics, brain computer interfaces, virtual reality games, functional electrical stimulation and brain stimulation (Maciejasz et al., 2014).

In particular, robotic technology has advanced towards faster and more powerful computers, novel approaches in computation, as well as more sophisticated electro-mechanical components, facilitating the integration of robotics into rehabilitation treatments. (Esquenazi and Packel, 2012; Chang and Kim, 2013)

Robot-aided rehabilitation is a physical therapeutic method supported by robotic devices having sensors, actuators and control units. Among many existing techniques of physical therapy for the upper limb (see Section 3.2.2), rehabilitation supported by robotics has attracted attention of researchers and therapists, because robots can provide an intensive (longer and independent of the physiotherapist's level of fatigue) and reproducible therapy, movement assistance and controllability, and measurement reliability. In addition, they allow physiotherapists to simultaneously supervise several patients more easily (Maciejasz et al., 2014; Huang and Krakauer, 2009; Lo and Xie, 2012).

Regarding the mechanical structure of robotic devices, there are two main classes, according to the mode of movement transfer from the robot to the patient (see Figure 3.2 [8] and Table 3.1): end-effector-based and exoskeleton-based devices. There are combinations of these two designs in more-than-one-robot systems: some parts of the robots are attached to and independently control the joints, and other parts are controlled simultaneously. Specifically, two-robots systems make it possible to mimic the usual assistance of a therapist with two hands (Maciejasz et al., 2014) - see Figure 3.3.

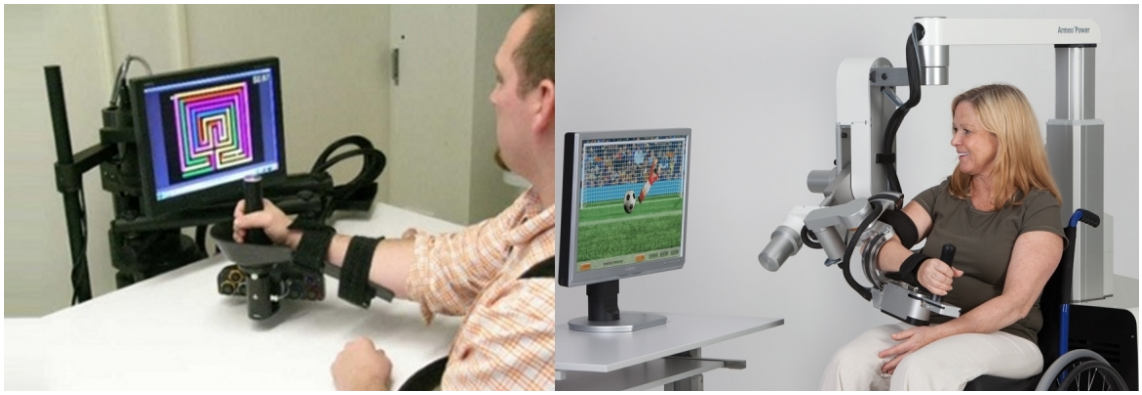

Figure 3.2: Examples of the two main classes of robotic devices: at left, an end-effector-based (named MIT-MANUS), and at right, an exoskeleton-based robot (named ArmeoPower).

[8] Source of the left image: https://www.strokengine.ca/intervention/robotics-introduction/; Source of the right image: http://products.iisartonline.org/productinfo.php?go=22

Table 3.1: Mechanical design of robotic devices in rehabilitation. (Huang and Krakauer, 2009; Maciejasz et al., 2014)

End-effector-based device	It is usually only a robotic arm (a "manipulandum") or a joystick. Patient and robot only have contact at the most distal component of the device. Being so simple, it is easy to fabricate and easy to fit the arm of any patient.
Exoskeleton-based device	It is similar to a suit, having several limb-mirroring components that wrap the segments of the human arm like an exoskeleton. Each component of the device is attached to the respective limb segment. This design has more degrees of freedom (DOF) and, thus, provides precise and independent control of each limb joint movement.

Robotic devices like exoskeletons demand more complex control algorithms and also more setup time before using the device, because each component has to be adjusted to fit the patient limb segments. Besides that, an added care must be taken in respect to the position of the joints' center of rotation (especially the shoulder), which may vary while moving the arm. Oppositely, end-effector-based robots are simpler, requiring simpler control algorithms and a shorter setup time (Maciejasz et al., 2014; Lo and Xie, 2012).

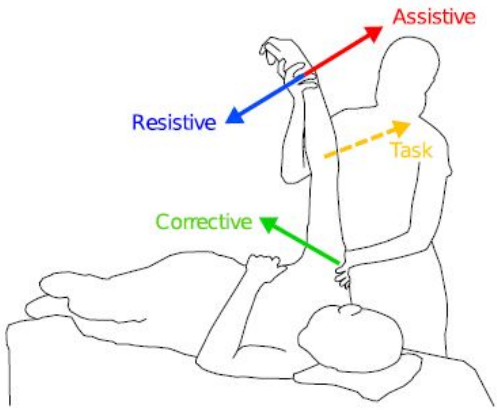

Figure 3.3: Analogy between the main types of control strategies for robotic-aided rehabilitation and a physical therapist work. (Proietti et al., 2016)

On the other hand, given that end-effector-based devices only interface with one joint (at the patient's hand), they make it difficult to control the position and torques on the other joints, allowing multiple combinations of movements at the wrist, elbow and shoulder (inclusively possible incorrect and injury-inducing positions, and uncontrolled load transfer between the joints) to achieve a desired position of the end-effector. On the contrary, exoskeletons can assist each joint of the

limb and allow the control of the position and orientation of their several segments. (Maciejasz et al., 2014; Lo and Xie, 2012)

Table 3.2: Types of assistance provided by robotic devices in rehabilitation.

Active	Device capable of producing movement (of the upper limb) through active actuators (that is, actuators driven by electric motors).
Passive	Device unable to generate movement, having only passive actuators (that is, actuators like brakes or springs, which can only provide resistive force against movements performed in the incorrect direction).

Concerning the most relevant type of assistance provided by robotic devices, these may be classified as active or passive, according to definitions in Table 3.2. In order to move the patient's arm, active devices have one or more actuators, and are appropriate to rehabilitate patients with severe difficulties in exerting force or unable to move the limb. Passive devices have lower-cost, lower-energy consumption, and lighter actuators, and are more suitable for a training dedicated to optimize the patient's strength, or to guide the movement in the correct trajectory (by resisting the patient's movements, when they are not correctly directed) (Maciejasz et al., 2014).

By using one or another type of devices, rehabilitative exercises may also be classified as active or passive - see Table 3.3 (Maciejasz et al., 2014). This distinction between devices and exercises terminology is important to avoid confusion in further reading about the state of the art in robotic-aided rehabilitation.

Table 3.3: Types of rehabilitative exercises.

Active	Exercise during which the patient uses his/her own strength to move the limb, wearing (or not) an active or passive device.
Passive	Exercise during which the patient does not put much effort, since the limb is moved by an active device.

Research to apply robotics in rehabilitation has started many years ago and a lot of novel devices have been invented and foresee promising results. Diverse clinical trials have shown that robotics provides an intense and safe motor rehabilitation (Kwakkel et al., 2008; Lo et al., 2010; Lo and Xie, 2012; Mehrholz et al., 2012; Norouzi-Gheidari et al., 2012; Klamroth-Marganska et al., 2014; Veerbeek et al., 2017). Task-oriented training with robotic devices enhances improvement of motor functions in chronically impaired, especially severe (Klamroth-Marganska et al., 2014),

stroke patients more effectively than conventional therapy. However, this difference in respect to conventional hand-assisted therapy is about 0.78 (Klamroth-Marganska et al., 2014) to 2.17 (Lo et al., 2010) Fugl-Meyer (FM) points, a magnitude not satisfying towards recovering dexterity in daily life activities (Maciejasz et al., 2014).

Aso so, further investigation, development and implementation (in clinical practice) of new technologies for physical therapy of the upper extremity require objective methods to accurately evaluate outcomes of functional recovery and systematically demonstrate advantages of robot-aided treatments (Mazzoleni et al., 2014).

3.3.2 State of the Art

Research into robotics rehabilitation, particularly for post-stroke patients, has been growing rapidly, and the number of therapeutic robots has increased dramatically during the last two decades (Mazzoleni et al., 2014; Proietti et al., 2016).

These robotic devices may be designed for home-based conditions, however, they are mainly used at rehabilitation centers and hospitals due to their unaffordable price and the requirement for supervision/assistance from qualified professionals. Being so, therapists demand for intuitive, easy and fast to setup devices, besides having a reasonable price. (Maciejasz et al., 2014)

In fact, robotic therapy for the upper extremity has begun with end-effector-based devices (Lo and Xie, 2012). Some examples of this type are the MIT-MANUS (Hogan et al., 1992; Krebs et al., 2003), the MIME (Burgar et al., 2000) and the GENTLE/s (Loureiro et al., 2003), which have been extensively tested in clinical environment and contributed to improve the motor ability of robotically-treated patients (Krebs et al., 1999; Lum et al., 2002, 2004, 2006; Coote et al., 2008).

Nowadays, research evolved towards the development of more sophisticated exoskeletons for the upper limb, because they enable the control of multiple joints and offer a larger range of motion to practice rehabilitation exercises when compared to end-effectors (Lo and Xie, 2012). Currently, there are a lot of new devices of such type, but there is a lack of detailed information about their effects in rehabilitation and few have been tested clinically (Proietti et al., 2016). Some examples are detailed in Table 3.4, but more exoskeletons exist and are reviewed in Maciejasz et al. (2014), Proietti et al. (2016), or Lo and Xie (2012). Interestingly, some of these robots, like ARAMIS or EXO-UL7, have two arms, allowing bilateral schemes of rehabilitation training (like mirror therapy) (Kim et al., 2013).

Table 3.4: Examples of exoskeletons used in upper limb rehabilitation. Act./Pass. DoF - Number of active/passive Degrees of Freedom.

Exoskeleton name	Act. DoF	Pass. DoF	Elements	Nationality	year	Other information
ARAMIS (Pignolo et al., 2012, 2016)	6	0	two-arms exoskeleton with fixation in shoulder, forearm and handle	Italy	2009	Clinical testing: Pignolo et al. (2012)
ArmeoPower © (by Hocoma) (Riener et al., 2011)	6	0	fixation in arm, forearm and handle	Switzerland	2011	The first commercialized exoskeleton for rehabilitation of the arm; based on ARMinIII robot
IntelliArm (Park et al., 2008; Ren et al., 2013)	8	2	fixation in arm, forearm and handle	USA	2007	
EXO-UL7 (Simkins et al., 2013)	7	0	two-arms exoskeleton with fixation in arm, forearm and handle	USA	2011	based on CADEN-7 (Perry and Rosen, 2006)
MEDARM (Ball et al., 2007)	6	0	fixation in arm and forearm	Canada	2007	
MGA (Carignan et al., 2009)	5	1	fixation in arm and handle	USA	2005	
ABLE (Garrec et al., 2008)	4	0	fixation in arm and handle	France	2008	Clinical testing: Crocher et al. (2012)
RehabExos (Vertechy et al., 2009)	4	1	fixation in arm, forearm and handle	Italy	2009	
RUPERT IV (Balasubramanian et al., 2008)	5	0	fixation in shoulder, arm, forearm and handle	USA	2005	
ALEx (Pirondini et al., 2014, 2016)	4	2	fixation in arm, forearm and handle	Italy	2013	Clinical testing: ongoing; ClinicalTrials.gov identifier: NCT02770300

Different strategies are known to control movements of the joints of robots. According to Maciejasz et al. (2014) and Proietti et al. (2016), terminology associated to the main types of control strategies is presented in Table 3.5. These approaches are usually combined in physical therapy exercises, similarly to the work which is performed by a patient-assisting therapist (Figure 3.3). More specific, "low-level" [9] (Maciejasz et al., 2014) strategies are considered by each robot developer. See the typical subtypes of assistive control strategies in Table 3.6.

Table 3.5: Types of control strategies for robotic devices in rehabilitation.

Assistance	The limb weight (gravity and friction) is supported by the device, and the robot also helps the patient to complete the desired movement, by providing forces if necessary.
Correction	The device only forces the arm to have a defined interjoint coordination, whenever the patient executes the movement incorrectly. This means the device does not act if the limb stops moving (the robot doesn't complete the task for the patient).
Resistance	The device offers opposite forces to motion. This strategy may also be called "*challenge-based control*" (Maciejasz et al., 2014), since the patient is challenged by the robot to perform some movement with more difficulty, requiring more attention and effort, and promoting the patient capacity to react to perturbations correcting the movement.

Note that, while assistive control acts on both tangential and orthogonal directions respective to the trajectory of the patient's limb movement, corrective control only acts on orthogonal direction. This is the reason why corrective control, in opposition to assistive control, is not able to guide the arm to the target in order to complete the task. (Proietti et al., 2016)

In resistive control, the challenge offered to the patient is often an increased force induced by the robot over the patient limb trajectory (to cause him/her to make larger errors and adapt) and/or a constrain of the unaffected limb (constraint-induced robotic rehabilitation). The challenge may include, in some devices, the presentation to the patient of an amplified value of his/her real performance error. This methods are implemented to promote a faster improvement. (Maciejasz et al., 2014; Krakauer, 2006; Proietti et al., 2016)

Most exoskeletons have a combination of assistance and correction control strategies (Proietti et al., 2016; Maciejasz et al., 2014). ALEx, for example, has a partially-assistive control, also know as "assistance-as-needed (see details in Section 3.3.2.1).

At the acute and early phases of physical therapy, the patient's movements need to be assisted so that mistakes are minimal and the patient feels motivated to continue training (passive or triggered passive control). It is, nevertheless, crucial to progress in the treatment and, thus, the robot

[9] A "sub-strategy" to control specific parameters, like force, position, impedance or admitance, developed when implementing one of the main global types of control strategies.

must be able to adapt its behaviour. When the patient starts recovering his/her motor ability, the control of the movement must be shared between robot and patient, as necessary (partially assistive control). (Proietti et al., 2016)

Table 3.6: "Low-level" subtypes of assistive control strategies. Some devices include a combination of these types.

Passive[10] Control	Deviations of the trajectory followed by the limb, in relation to a reference trajectory[11], are corrected by position control (classically, using a proportional-integral-derivative, PID, feedback controller, or with more complex algorithms, like the recent *sliding mode control with exponential reaching law, SMERL (Rahman et al., 2010)*), with high controller gains. This method is commonly applied at early phase of rehabilitation, because usually the patient weakly moves the injured limb, so the robot performs most of the movement along the desired trajectory.
Triggered Passive Control	The exoskeleton assists the patient when he/she triggers its help (by choosing one target to reach) through a brain-machine interface (BMI). This BMI estimates the patient intention to move the limb towards the target, modulates the due speed, acceleration and jerk, and triggers the exoskeleton to move - then, it is controlled passively along the determined trajectory. This control is adequate to patients with hemiplegia.
Partially Assistive Control	Also called "*assistance-as-needed*", this strategy provides partial assistance: the patient is allowed to control the movement, being only supported by the exoskeleton when the performance is weak. So, in these cases, the controller gains are lower than in passive control, and usually are based on impedance or admittance control approaches: in *impedance control*, the limb position is measured (position feedback) and the controller defines the robot force to be provided (force controller); in *admittance control*, the controller defines the displacement to be performed (position controller), from the force exerted by the patient (force feedback).

[10] Note that "passive", here, has the same meaning as "Passive exercise", defined in Table 3.3. So, a patient wearing a passively controlled exoskeleton does not put much effort to perform the task - the exoskeleton does that for him/her.

[11] The reference trajectory may be recorded during a *teaching phase*, where the therapist guides the patient to perform a desired trajectory with his/her paretic arm, or where the patient uses the unaffected limb to perform the desired movement, wearing, in both cases, the exoskeleton in a transparent mode (in which the robot only compensates for gravity, friction and inertia).

sEMG has already been used, too, firstly to detect the patient intention to move the limb and, then, to obtain the desired reference position determined from a muscle activity model.

Alternatively, optimization algorithms are used to minimize costs (for eg. minimize jerk) in order to define the best trajectory to reach the desired target.

The input signal for the control algorithm of the robotic device is usually one (or a combination of signals) of three types (Maciejasz et al., 2014):

1. **kinematic**: Position, angular/linear velocity and acceleration of the robot joints and/or segments;
2. **dynamic (kinetic)**: Torque or force generated on the robot joints and end-effector (only the latter, in an end-effector-based device) as a function of time;
3. **trigger**: Signal, triggered by a switch/button or, for example, by a threshold value relative to a surface EMG signal (sEMG), used to initiate some operation.

The implemented "low-level" control strategy dictates, in part, the type of signal required, or vice-versa.

The latter type of input signal when used with sEMG allows to identify a contraction of the patient's arm as an intention to execute some movement and, thus, the robot can be controlled to support the action. sEMG signals from the unaffected extremity have already been used in some devices to control actions of the paretic limb.

Interestingly, some robots have also implemented contactless methods (with motion capture systems) for detecting movement.

3.3.2.1 ALEx RS - Arm Light Exoskeleton Rehab Station

One element of this thesis is the Arm Light Exoskeleton (ALEx), a robotic device to support rehabilitation of the upper limb (see Figure 3.4).

Figure 3.4: The Arm Light Exoskeleton Rehab Station - ALEx RS.

ALEx is mechanically compliant to the human upper extremity. The center of rotation of its shoulder is dislocated from a normal position so that the human limb can perfectly align with the robotic arm, and the limb joints' axes overlap the exoskeleton joints' axes. [12]

This exoskeleton can cover 90% of the human arm natural workspace, without singularities, and has six DoF (range of motion for each DoF is provided in Table 3.7.):

- shoulder abduction/adduction (SH-Abd-Ad), rotation (SH-Rot) and flexion/extension (SH-Flx-Ext), as well as elbow flexion/extension (EL-Flx-Ext) are sensorized and actuated;
- forearm prono-supination (FO-Pro-Sup) and wrist flexion/extension (WR-Flx-Ext) are sensorized and passive.

At the EE (end-effector), it is possible to generate, at maximum:

- a continuous interaction force of 50N;
- a peak force of 100N;
- a continuous torque of 40Nm;
- a peak torque of 80Nm;
- a joint speed of 500°/s.

[12] Kinetek, Wearable Robotics

Table 3.7: Range of motion for each degree of freedom (in ^{o}). SH-Abd = shoulder abduction; SH-Rot = shoulder rotation SH-Flx = shoulder flexion; EL-Flx = elbow flexion; FO-Pro = fore-arm prono-supination; WR-Flx = wrist flexion. For each DoF, 0^{o} corresponds to a configuration where the upper arm and trunk are parallel, while the elbow joint is perpendicular, i.e, 90^{o} flexed relatively to the upper arm.

SH-Abd-Ad	[0,100]
SH-Rot	[-40,60]
SH-Flx-Ext	[10,155]
EL-Flx-Ext	[0,160]
FO-Pro-Sup	[-90,90]
WR-Flx-Ext	[-50,50]

The robot can be used in three modalities (terminology used by Pirondini et al. (2016)):

- **Passive**[13]: the robot only performs measurements of the subject arm movements;
- **Assistive**[14]: the subject arm is guided by the robot while he/she performs a movement;
- **"Assisted-when-needed"**[15]: the subject arm is guided by the robot to a defined position if he/she takes 3 seconds or more to initiate the movement.

In the three modalities, ALEx control algorithm generates the necessary compensation for: gravity (weight of the exoskeleton segments); friction between the robot components; masses and inertia of its moving parts (exoskeleton segments and motors).

ALEx can be operated in two modes:

- **Force mode**[16]: forces are provided to the EE, or joint torques to each joint;
- **Position mode**[17]: trajectories are provided to the EE (EE control) or to the joints (joints control) with the respective stiffness.

[13] Passive, here, means ALEx behaves like a "passive device", as defined in Table 3.2, and does not interferes in the movement, besides compensating for dynamics.

[14] ALEx behaves like an "active device", with assistive control - more specifically, the "low-level" strategy of passive control mentioned in Table 3.6.

[15] Partially Assistive Control - Table 3.6

[16] Equivalent to *impedance control* "low-level" approach - see Table 3.6

[17] Equivalent to *admittance control* "low-level" approach - see Table 3.6

3.4 Personalization of Robot-aided Motor Therapy

Improved outcomes of robot-aided motor therapy have been envisioned if the therapeutic training would be tailored to each patient. (Fuhrer and Keith, 1998; Krakauer, 2006) Nevertheless, designing the appropriate customized exercises and the respective robotic assistance is still challenging and how to do it is an open debate. Therefore, currently, the evaluation of the patients' progress and decision to adjust therapy accordingly is done by a physiotherapist (Panarese et al., 2012). However, this assessment is usually done just before and after sessions of treatment, using scores of clinical scales, like Fugl-Meyer, for example. On the other hand, measures continuously recorded by robotic devices can be used as immediate feedback on the patients' progress (Panarese et al., 2012).

In fact, apart from reliable measurement, robotic devices of today allow the patients to repeatedly train general or task-oriented movements or sub-movements (like planar or 3D reaching movements in one or more directions) (Marchal-Crespo and Reinkensmeyer, 2009), and provide variable assistance or resistance (as detailed in Section 3.3.2). When this training is centered in exercising specifically the impaired movements of each patient, the treatment is expected to be more effective and efficient, given that motor learning is optimized if the difficulty of the exercises matches the degree of motor ability (Guadagnoli and Lee, 2004). Additionally, this type of training is more intense (because the therapy is focused on a set of movements and the patient can practice them several times), which increases the level of motor improvement (Kwakkel et al., 1997, 1999; Krebs et al., 2003).

3.4.1 State of the Art

Following the explained perspective, various researchers have been working in designing methods to personalize both the robotic assistance and the rehabilitation training protocol (Krebs et al., 2003; Koenig et al., 2011; Novak et al., 2011; Panarese et al., 2012; Papaleo et al., 2013; Metzger et al., 2014).

Particularly, Panarese et al. (2012) developed a statistical algorithm which estimates motor improvement of stroke patients during upper limb robotic-assisted therapy based on kinematic measures of easiness (average speed), accuracy (distance to a straight path) and smoothness (number of peaks in the speed profile).

In turn, Krebs et al. (2003) proposed an adaptive algorithm to control the robotic-assistance (during training of upper limb movements) using kinematic (speed, or time) or muscle activity (EMG signals) thresholds.

Papaleo et al. (2013) also designed an approach to modulate the level of robotic-assistance (in 3D rehabilitative movements with the upper extremity) in accordance to the patient's performance. However, these investigators evaluated performance using kinematic (measures of accuracy, smoothness and inter-joint coordination) and kinetic (forces exerted by the patient) parameters of the patient's behaviour. Similarly, Metzger et al. (2014) adapted the task difficulty of

robotic hand rehabilitation of post-stroke patients, based on the assessment of the ROM (range of motion) of 2 DoFs of the hand and on the assessment of grasping stiffness.

Other groups of research combined kinematic metrics with psychophysiological measurements. For example, Koenig et al. (2011) studied control methods in robotic-aided gait therapy for post-stroke patients. These authors proposed a metric combining the patient heart rate (to quantify physical effort) and the weighted sum of the interaction torques between the robot and the patient, to select one of two strategies of the gait therapy: voluntary or forced, the last one with speed adaptation. On the other hand, Novak et al. (2011) investigated the usefulness of psychophysiological measurements like heart rate, skin conductance, respiration, and skin temperature, solely or in combination with task performance metrics and biomechanics, to adapt the level of difficulty of upper limb motor tasks during rehabilitation. They have demonstrated that a combination of both types of measurements provides more accurate results in selecting the correct level of difficulty, than using solely psychophysiological or only kinematic measurements.

Despite the good results obtained in the above-mentioned studies, customization of rehabilitation is yet an emerging field and lacks validation concerning its effectiveness over the conventional treatment.

3.4.1.1 The NEUROPROBEs project - pilot study

The Neuroprobes' project is in the framework of robotic-treatment customization. In fact, the first goal of the project is to test safeness and clinical effectiveness of ALEx in assisting post-stroke patients during robotic-rehabilitation. Second, this project aims at designing a personalized robot-based protocol of motor therapy for the upper limb based on the statistical model proposed by Panarese et al. (2012). Finally, the third main aim is to characterize the neurobiomechanical state of stroke patients and its progress during the treatment, and use such information to improve the personalization protocol.

In the context of NeuroPRoBES project and, more specifically, its first goal, a pilot study was already conducted in healthy subjects which evaluated the effects of wearing ALEx while performing point-to-point reaching movements. These evaluation included the analysis of joint and end-effector kinematics, muscle synergies and motoneural activity in the spinal cord of healthy subjects, during active and passive exercises (Pirondini et al., 2016). Different tests were performed during 3 days:

- 1^{st} day: free reaching movements and movements with the exoskeleton in passive modality - allowed the investigators to compare the subjects behaviour with and without the exoskeleton, i.e, to determine if the exoskeleton influenced the subjects muscle activity and coordination;

- 2^{nd} day: reaching movements with the exoskeleton in passive and assistive (position mode

at the EE[18]) modalities - allowed to evaluate if the assistive modality of the robot influenced the subjects behaviour (once again, their muscle activity and coordination);

- 3^{rd} day: reaching movements wearing the exoskeleton in passive modality and, then, in the assistive modality[19] with two control sub-strategies (joint control and EE control - sub-strategies of position mode - see Section 3.3.2.1) - allowed the investigators to compare the two methods of control.

The main results obtained with this pilot evaluation were the following:

- Normal movements are not modifyed by wearing ALEx (based on analysis of end-effector kinematics), although muscle activation patterns and movement coordination are changed to some extent (Pirondini et al., 2014);
- Reaching movements have similar dynamics, similar patterns of muscles recruitment (although with weaker activity in assistive modality) and similar joints' angular excursions both in passive and assistive modalities, when wearing ALEx. However, free movements and movements wearing the exoskeleton differ a little, to be highlighted that wearing ALEx improves the movement accuracy.
- Analysis of muscle synergies allowed to verify that synergies activation over the movement time was different while executing free movements or performing movements wearing ALEx in passive or active modalities, showing that using the exoskeleton influences the muscle coordination in a positive way (the use of the exoskeleton lead to an enhanced distribution of contributions of different muscle groups to perform the reaching movements).
- Both joint and EE control strategies induced similar motor activity and, thus, preserved motor coordination of the passive modality, specially the joint control.

This preliminary results of NeuroPRoBES project endorse the application of ALEx in rehabilitation of post-stroke patients to support physical therapy of the upper extremity.

Regarding the second main aim of Neuroprobes project, an adapted version of Panarese et al. (2012) algorithm was developed and implemented in ALEx to personalize the rehabilitation training of each patient. Indeed, the model proposed by Panarese et al. (2012) was developed for planar movements and tests were performed offline (i.e. after the training session that was part of the experiments). Then, this model was adapted for 3D movements and for execution in real-time, so that motor improvement of patients receiving the robotic treatment could be continuously estimated.

[18] Reference trajectories were defined as straight lines between the initial and final points of the reaching movements.
[19] The natural trajectories performed in the passive modality were recorded and used as the reference trajectories in assistive modality.

This estimation is performed for every task (a reaching movement towards one target) presented during the training session. From the progress (over repetitions of the same movement) of motor improvement for all tasks, the algorithm replaces one task by a more difficult one, when a performance plateau is reached (i.e. the algorithm determines the movements that the patient has to train - the ones that the patient shows more difficulty).

Chapter 4

Kinematic assessment of the Upper Limb

Early investigation on robotic-aided motor therapy has made an extensive use of clinical scales to assess motor performance of stroke patients during rehabilitation, and to infer on the contribution of robotic assistance to that motor ability. Nevertheless, over the years, an increased use of kinematic metrics has been registered (Santisteban et al., 2016), mainly because some studies (Alt Murphy et al., 2013; Bensmail et al., 2010) have shown that sensibility of these metrics is enhanced when compared to clinical scales and, this way, allow more fine-grained measurements of changes in motor ability of patients. In addition, kinematics is often used in combination with the FMUE (Fugl-Meyer scale for the Upper Extremity) (Santisteban et al., 2016).

Therefore, background concepts about kinematics is provided in this chapter, as well as a review of kinematic metrics reported in the literature to assess movement execution in robot-assisted rehabilitation of the upper limb following stroke.

4.1 Background concepts

Kinematics, a component of Biomechanics, describes the movements of bodies using graphical or numeric representations of position, velocity, acceleration, disregarding the applied forces on those bodies. (Binder et al., 2009b)

Specifically, the study of geometrical and temporal features (kinematics) of movements of the human body segments provides important information on the individual motor control, movement smoothness and accuracy, and other.

The human upper extremity, in particular, is a multi-joint, multi-DoF system, as represented in Figures 4.1 and 4.2. The arm is able to execute a broad range of goal-directed actions. For each of these actions, several paths may be taken and different velocity profiles are possible for each path, with more or less expenditure of energy and time, resulting in numerous possible trajectories. Nevertheless, real arm movement trajectories in healthy persons seem to be stereotypical, having

invariant kinematic features: for example, it has been suggested that point-to-point reaching tasks[1] follow approximately straight paths with bell-shaped tangential velocity profiles (Binder et al., 2009a). Notwithstanding, care must be taken with the approximation to straightness, according to results of Wisneski and Johnson (2007) work, which demonstrate that arm trajectories of healthy subjects are more curvilinear than theoretically suggested. This detail must also be considered when assessing modifications in movement execution induced by stroke.

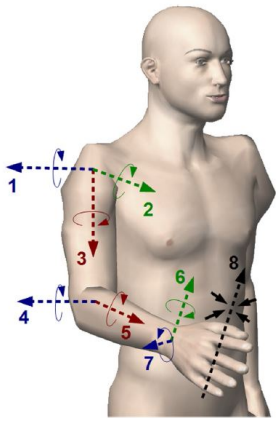

Figure 4.1: Some of the the upper limb degrees of freedom (DoF). 1: arm flexion/extension; 2: arm adduction/abduction; 3: arm internal (medial) / external (lateral) rotation; 4: elbow flexion/extension; 5: forearm pronation/supination; 6: wrist flexion/extension; 7: wrist adduction (ulnar deviation) / abduction (radial deviation); 8: hand grasp/release. (Maciejasz et al., 2014)

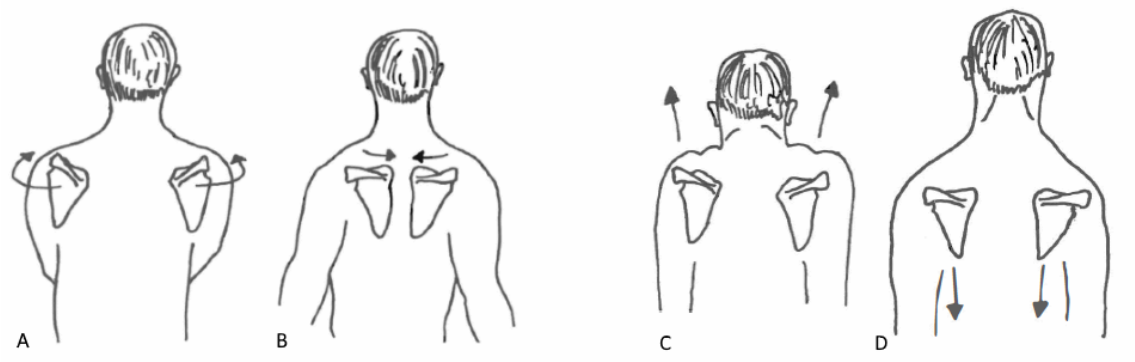

Figure 4.2: Additional degrees of freedom (DoF) of the upper limb, associated to the shoulder (more specifically, the sternoclavicular joint). A - shoulder protraction; B - shoulder retraction; C - shoulder elevation; D - shoulder depression (Kingston, 2005)

Even though, given the stereotypical behavior of nondisabled persons, abnormalities in patterns of kinematic parameters can be monitored in post-stroke patients and used for recovery evaluation (Binder et al., 2009a; Krakauer, 2005).

[1]Reaching movement between two points in the space.

In fact, reduced motor ability following stroke is identified in several features of movement, mainly related to paresis of the arm, increased muscle tone and absence of somatosensation (Lang et al., 2013). Due to paresis, patients move the arm more slowly, less accurately and less efficiently. An abnormal muscle tone is reflected in jagged movements: an increased tonicity causes resistive forces against the movement direction, making the movement less smooth. In addition, loss of somatosensation interferes with the ability to correct movements. (Nordin et al., 2014)

4.2 Review of Kinematic metrics to assess Motor Performance in Upper Limb Robotic-aided Rehabilitation

As mentioned in the beginning of this chapter, most of past investigation assessing motor performance during rehabilitative programs typically use nominal or ordinal scales Krakauer (2005). For example, most of the studies reviewed in Hesse et al. (2003) used only the Fugl–Meyer motor score (which measures the DoFs that a patient is able to control - van Kordelaar et al. (2013)) to evaluate the motor function of the impaired upper extremity at the end of the robotic treatment.

Other similar scales are also used, like the Wolf Motor Test, the Motor Activity Log or the Chedoke-McMaster Stroke Assessment Measure, as mentioned by Krakauer (2005) and Roh et al. (2013), for instance.

Even more recent studies make extensive use of these scales, such as the assessment of the exoskeleton ARAMIS (Pignolo et al., 2012), or the evaluation of the robot ARMin Klamroth-Marganska et al. (2014), and others (Milot et al., 2013).

However, Kinematics has gained importance as a reliable method to assess effectiveness of rehabilitation therapies, mainly because previous studies (Alt Murphy et al., 2013; Bensmail et al., 2010) have shown that sensibility of these metrics is enhanced when compared to clinical scales and, this way, allow more fine-grained measurements of changes in motor ability of stroke patients. In addition, other studies (Sivan et al., 2011) suggest that kinematic measurements are suitable for all phases of stroke rehabilitation.

Specially in the context of robotic-aided rehabilitation, kinematic measurements are facilitated, because robots typically include movement sensors to acquire position, velocity and orientation of the end-effector and/or joints, in a reliable way (Huang and Krakauer, 2009).

As so, more recently, an immense variety of kinematic metrics is used in robot-based rehabilitation studies. Particularly for point-to-point reaching movements, different authors have proposed distinct metrics to quantify movement execution features like efficiency, efficacy, accuracy, easiness and smoothness - see the most used ones in Table 4.1. (Nordin et al., 2014)

Movement accuracy is usually measured in respect to a straight path, that is, the straight line between the initial point of the movement and the reaching point. Metrics of accuracy include: the mean distance to the theoretical path (straigh line), which is computed by averaging the distance between each point of the path and the respective point of the theoretical path (Panarese et al.,

Table 4.1: Example of kinematic metrics to assess different features of movement execution.

Movement features	**Kinematic metrics**
Accuracy	Mean distance from theoretical path, Euclidean distance between target and end-point
Temporal efficiency	Task completion time (movement duration)
Spatial efficiency	Path legth, Ratio of affected path length and unaffected path length
Efficacy	Percentage of successful tasks, Target unreached
Easiness	Mean velocity, Peak velocity
Smothness	Increase in mean acceleration, Ratio of mean acceleration with peak acceleration, Number of peaks in the speed profile, Spectral Arc-Length

2012; Coscia et al., 2014; Colombo et al., 2005); or the euclidean distance between the target location and the point at which the patient stops moving (Daly et al., 2005).

For any of those metrics, a low value corresponds to a good accuracy. This feature has been significantly correlated with severity of impairment following stroke (Cirstea and Levin, 2000) and, thus, it is expected to improve with motor recovery (Panarese et al., 2012).

Temporal efficiency is measured in respect to the optimal time taken to complete some movement/task, being defined as the elapsed time from the beginning to the end of that movement (Zollo et al., 2011). As the patient recovers his/her motor abilities, this time is expected to become shorter (Frisoli et al., 2012; Lum et al., 2004).

Spatial efficiency, in turn, is measured relatively to the optimal path to reach the target. Investigators suggested that an optimal path is the shortest one, and longer paths presuppose a greater energy expenditure (Colombo et al., 2008). Therefore, spatial efficiency is commonly measured with the path length, which has been shown to decrease in chronic stroke patients receiving unimanual rehabilitation (Colombo et al., 2008; Coderre et al., 2010; Beer et al., 2008). In bimanual studies, like Semrau et al. (2013), the ratio between the path length where the patient actively moved and the path length guided by the robot was used.

Efficacy in movement execution is defined as the ability to accomplish a task. For example, in robotic-assisted training of reaching movements, this feature can be measured with the percentage of completed tasks (Panarese et al., 2012) or, inversely, the number of targets which the patients was not able to reach (Coderre et al., 2010). Although this feature is expected to improve with motor ability, solely it is not able to evidence if such improvement occurs as a result of true recovery or compensation (Nordin et al., 2014).

Easiness is defined as the ability to execute the movement using the least effort possible (Nordin et al., 2014). This feature is typically associated to the movement velocity. Colombo et al. (2005), for example, reported that mean velocity significantly increases in chronic patients receiving a robotic-treatment, and also in subacute patients (Colombo et al., 2008). Similarly, other studies with different protocols of rehabilitation also found a significant improvement in mean velocity (Mazzoleni et al., 2013; Panarese et al., 2012).

In turn, an increase in peak velocity with rehabilitation is reported in Zollo et al. (2011) and, moreover, this metric has been correlated with scores of clinical scales like FMUE (Bosecker et al., 2010).

Finally, lack of smoothness is characterized by the occurrence of short sub-movements, due to sudden, increased acceleration and deceleration (Rohrer et al., 2002). Consequently, the speed profile includes several positive and negative peaks and, thus, the number of peaks has been used before to measure this movement feature (Panarese et al., 2012). Differently, Mazzoleni et al. (2011) verified that mean acceleration increases for smoother, planar reaching movements, in chronic patients. Later, they reported significant increase in the ratio between mean acceleration and peak acceleration for subacute stroke patients, but not significant for chronic patients (Mazzoleni et al., 2013).

More recently, a new metric has been developed to quantify smoothness: the Spectral Arc-Length. This metric corresponds to the negative arc length of the Fourier spectrum magnitude of the speed profile (Balasubramanian et al., 2012) - see Equation 4.1.

$$\eta_{sal} \triangleq -\int_0^{\omega_c} \sqrt{\left(\frac{1}{\omega_c}\right)^2 + \left(\frac{d\hat{V}(\omega)}{d\omega}\right)^2}\, d\omega \tag{4.1}$$

$$\hat{V}(\omega) \triangleq \frac{V(\omega)}{V(0)}$$

where $V(\omega)$ is the Fourier magnitude spectrum of the movement velocity, and $[0, \omega_c]$ is the frequency band occupied by the given movement. $\omega_c = 40\pi rad/s$ (which corresponds to 20Hz) covers the normal and abnormal aspects of human movements such as tremor (Balasubramanian et al., 2012).

Chapter 5

Muscle Activity of the Upper Limb

Motor recovery following stroke must be assessed beyond its final result (task accomplishment and kinematic performance). According to the definition of true recovery provided in section 3.1 of the Motor Rehabilitation Chapter, a kinematic description of movement must be completed with an analysis of neuromuscular activity, because it provides additional information on the neurophysiological state of the patient, allowing to infer about the restitution, or not, of movement patterns previous to lesion (healthy patterns).

Thus, features of single muscle activity (following electromyography), muscle coordination (muscle synergies analysis) and estimated motoneural activity of the spinal cord (spinal maps) can be investigated to search for biomarkers of true motor recovery. Thus, theoretical concepts and previous work reported in the literature concerning these analyses are presented in this chapter.

5.1 Electromyographic Analysis

The electromyographic signal (EMG) measures the electric potential generated by muscle cells when these cells are electrically or neurologically activated (Reaz et al., 2006). It represents the local electric current which results from ions crossing the membranes of muscle fibers and which diffuses to surrounding tissues (Wang et al., 2013). Electromyography is the technique used for detecting and analyzing this electrical signals measured from skeletal muscles. (Jamal, 2012)

Each neuron innervates a group of muscle fibers, constituting a "Motor Unit", the functional unit of muscles (Wang et al., 2013). When a stimulus is sent to a motor unit, a "Motor Unit Action Potential" (MUAP) is generated. Until the muscle force is no longer needed, the CNS continues to send the stimulus, originating a train of MUAPs. At the measurement place, the EMG signal results from the superposition of MUAPs trains of nearby motor units which were activated. (Jamal, 2012)

This bioelectrical signal has become an important tool for diagnosing neuromuscular diseases and disorders of the CNS, specially concerning the motor control and movement coordination (Jamal, 2012), providing useful data for quantitatively evaluate outcomes of rehabilitation programs.

EMGs are pre-processed before being further analyzed:

1. to retain only the movement informative content (remove frequency components originated by muscle fibers firing rate, electric/thermal noise, etc.), being filtered,
2. to make the range of amplitudes comparable between muscles, being each signal independently normalized,
3. to extract the envelope of the signal, being rectified or integrated over a time interval.

Filters with different characteristics have been used by distinct scientist, such as filters with FIR (finite-impulse response) and Butterworth response, of 3th, 4th, 7th order, and filtering frequencies of 15/20/50 Hz for the lower cut-off frequency, and 400/450/500 Hz for the upper cut-off frequency. (Grasso et al., 2004; Cheung et al., 2009; Tropea et al., 2013; Pirondini et al., 2016) The normalization procedure is also variable across studies: EMG signals may be normalized to have unit variance (Tropea et al., 2013), normalized by the MVC (maximum voluntary contraction) (Pirondini et al., 2016), or by the maximum of the muscle recordings (d'Avella and Bizzi, 2005; Frère and Hug, 2012). The signal envelope may be obtained by half-wave rectification, full-wave rectification, half/full-wave rectification followed by integration over 25ms, 100ms, 200ms, or other time interval. (Ivanenko et al., 2006; Tropea et al., 2013; Pirondini et al., 2016)

Details of filtering and normalization procedures, as those explained above, must be adapted to the experiment, being this the main reason for the variability of methods used in previous studies.

The pre-processed EMG amplitude is usually analyzed preliminarily using simple measures as the mean activity or the RMS (root-mean square) value (Equation 5.1), to quickly detect trends of muscle activation, compare levels of weakness/strength, and compare muscle activity across conditions (eg. Pirondini et al. (2016)).

$$RMS = \sqrt{\frac{1}{N}\sum_{n=1}^{N} EMG(n)^2} \tag{5.1}$$

In the context of stroke and motor rehabilitation of the upper limb, several muscles of the arm, shoulder and trunk are important. Muscles that were analyzed to develop this thesis are presented in Figure 5.1 and their function is described in Table 5.1.

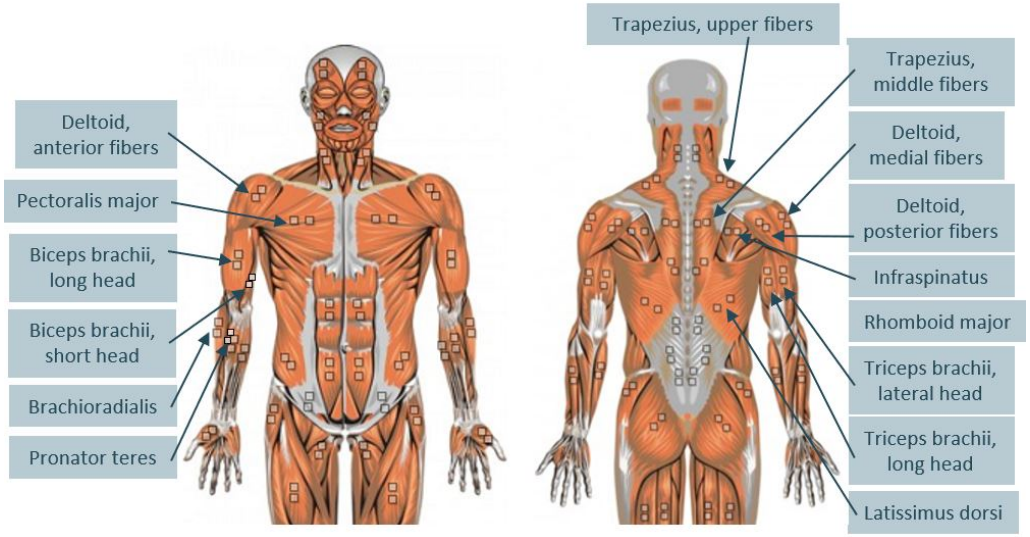

Figure 5.1: Location of muscles of the arm, shoulder and trunk that were analyzed to develop this thesis.

5.2 Analysis of Muscle Synergies

Motor coordination is the result of combining different muscles to perform a goal-oriented action in a smooth and efficient way. The kinematic (like direction and speed) and dynamic (forces) variables of the intended task are achieved with the muscle selection and control performed by the CNS. (Fetz, 1993) Muscles are recruited with specific electric patterns (neural commands sent from the CNS to the muscles), which are hypothetically identifiable in the EMG signals (Kamen and Gabriel, 2010). For each activated muscle, the stimulus intensity varies along time, increasing when the movement direction (as well as the speed and force) is required in the direction of the muscle contraction. (Thach, 1978; Binder et al., 2009d)

Although it seems that muscle patterns are dependent on the above-mentioned kinematic and kinetic variables, their origin in the CNS is believed to follow simplifying rules which define stereotypical profiles of muscle co-activation: the muscle synergies (Tresch et al., 1999; Torres-Oviedo and Ting, 2007; Kargo and Giszter, 2008).

In summary, a muscle synergy is a standardized recruitment of a group of muscles to perform part of some movement, during a time window, therefore, having a structure (a set of weighting coefficients) and being activated by the CNS in different instants (time activation coefficients). (Binder et al., 2009d)

In detail, the synergy structure indicates which muscles are co-activated and the proportion of activation intensity between them (muscle weights profile). While executing some movement, different synergies are combined by modulation of the structure of each synergy in intensity along the movement time (time activation profile of the synergy) (Binder et al., 2009d) - see Figure 5.2.

Table 5.1: Function of relevant muscles in the context of stroke, considered for the present thesis (Kingston, 2005).

Muscle	**Function**
Trapezius	upper fibers - shoulder elevation and forward rotation; middle/lower fibers - shoulder retraction.
Deltoid	middle fibers and whole muscle - shoulder abduction; anterior fibers - flexion and medial rotation of the shoulder; posterior fibers - extension and lateral rotation of the shoulder.
Pectoralis major	adduction, medial rotation and flexion of the shoulder.
Latissimus dorsi	extension, adduction and medial rotation of the shoulder.
Infraspinatus	lateral rotation of the shoulder.
Rhomboid major	Retraction, with slightly elevation, and backward rotation of the shoulder.
Biceps brachii	(long and short heads) elbow flexion, supination of the forearm and hand, and assistance in shoulder flexion
Brachioradialis	elbow flexion, and assistance in pronation, supination of the forearm.
Triceps brachii	(long, lateral and medial heads) elbow extension.
Pronator teres	pronation of the forearm, and assistance in elbow flexion.

In fact, the upper limb musculoskeletal system has redundant ways to generate an action because of its large number of DoFs and, thus, large number of possibilities for muscles combinations. So, synergies are thought to be a simplifying mechanism of:

- first, mapping movement parameters into muscle patterns, just like an implementation of inverse kinematics and inverse dynamics (Binder et al., 2009d).

- and, second, reducing the number of DoFs to be controled, i.e., instead of controlling a big number of muscles separate and independently, the CNS only controls (selects and modulates) a lower number of synergies and linearly combines them to achieve the movement goal. (Cheung et al., 2009)

The muscles synergies real existence is yet in debate (Tresch and Jarc, 2009; de Rugy et al., 2013) but, since Bernstein (1967) proposed this hypothesis, it has been supported by empirical evidences on the past years experiments (d'Avella et al., 2003; Ivanenko et al., 2004; Torres-Oviedo and Ting, 2007; Ting and Macpherson, 2005; Overduin et al., 2012): similar patterns in the muscle

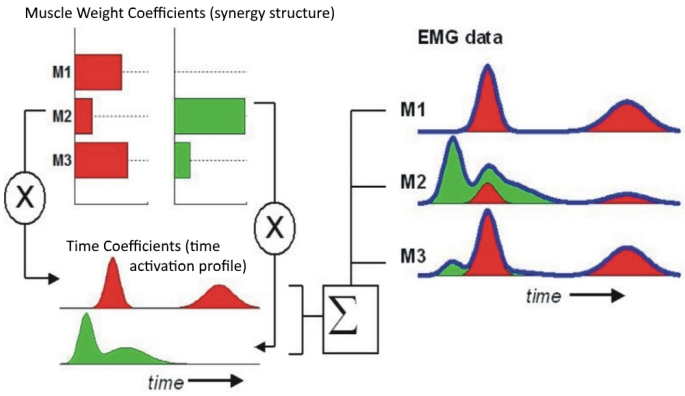

Figure 5.2: Schematic representation of the synergies theory (example with 2 synergies, one green and another red, to command 3 muscles, M1 to M3): recorded EMGs result from the linear combination (thick blue lines) of time-invariant synergies (set of muscles' weighting coefficients - horizontal bars), each being activated by a different time-dependent coefficient (waveforms in the bottom). (Adapted from Cheung et al. (2009).)

activity across individuals, motor activities, and species have lead scientists to propose that muscle synergies reflect a modular organization of movement production by the CNS. As so, it is one of the most adopted theories to study the motor limitations and the motor recovery following stroke, and the effects of rehabilitation. (Cheung et al., 2009; Clark et al., 2010; Salman et al., 2010; Safavynia et al., 2011; Cheung et al., 2012; Tropea et al., 2013; Roh et al., 2013)

After stroke, impaired movements of the upper limb are often expressed in generally increased weakness and atypical patterns of shoulder, elbow and trunk muscles (Krakauer, 2005; Levin et al., 2009; Roh et al., 2013). As mentioned in section 3.1 of the Motor Rehabilitation chapter, hemiparetic patients frequently use less elbow extension and compensate this with the trunk rotation or bending in reaching movements, and/or present difficulties in shoulder flexion/abduction, increasing the shoulder elevation and the elbow flexion to lift the arm (movements in opposite direction to gravity). (Levin et al., 2009; Roh et al., 2013; Coscia et al., 2014). This abnormal coupling between muscles is typically reflected in a reduced number of synergies (Roh et al., 2013). Nevertheless, other types of alterations on muscle synergies (compared to healthy subjects) have been found before, and it must be noted that more than one type of alteration may be present (Roh et al., 2013).

Cheung et al. (2009) concluded that synergies' structure was preserved, but not their activation (time coefficients) in mildly impaired post-stroke patients. However, from a more diverse group of subjects (concerning the level of impairment and age of lesion) (Cheung et al., 2012), they were able to quantitatively demonstrate that synergies structure is preserved, modified by a merging of synergies, or modified by fractionation of synergies, as a function of both severity of functional impairment and time from stroke onset (see Figure 5.3): severely affected patients (regardless of the temporal distance to stroke onset) presented a reduced number of synergies due to synergies

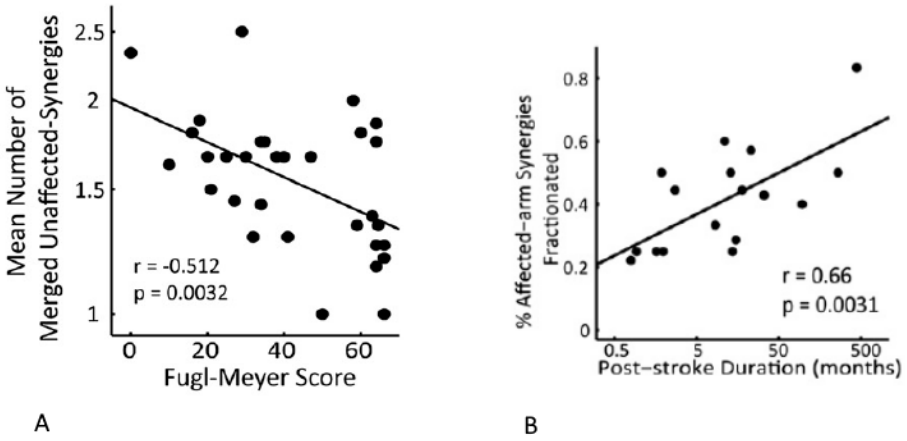

Figure 5.3: Example of correlations found between the synergies structure as result of synergies merging and level of impairment (A), and between the synergies structure as result of synergies fractionation and temporal distance from stroke onset (B), by Cheung et al. (2012).

merging; subjects with mild-to-moderate impairment preserved the number of synergies but presented modifications in the weight coefficients; some synergies of chronic survivors result from the fractionation of healthy synergies.

Additionally, Roh et al. (2013) have observed completely altered synergies' structure, like new synergies, and not a result from merging or fractionation of normal synergies, in chronic survivors.

These conclusions provide clues on muscle coordination of post-stroke patients, but cannot be assumed disregarding the type of movements. Thus, they need to be verified for 3D point-to-point reaching movements as those concerning this work, having been a starting point of this thesis to:

- first, use muscle synergies to characterize the neural state of post-stroke patients along the treatment course with ALEx;

- second, search for features of such muscle synergies that could be correlated with motor performance and, in the future, could be included in the motor improvement algorithm for treatment personalization.

Typically, muscle synergies are obtained from EMG signals using matrix factorization algorithms, like NNMF (non-negative matrix factorization), FA (factor analysis), ICA (independent component analysis), PCA (principal component analysis), and variations of these methods. Factorization algorithms model the observed data (in this case, recorded EMGs) as a linear combination of a small set of basis vectors (synergies). (Tresch et al., 2006) Despite being similar, these algorithms rely on particular assumptions, which are, then, reflected in some differences in the results. However, such differences have been demonstrated not to be significant in several studies with muscle synergies extracted by different algorithms (Tresch et al., 2006; Steele et al., 2015b; Lambert-Shirzad and Van der Loos, 2017). As it will be explained in Chapter 6, an adaptation of the NNMF algorithm was selected to extract the muscle synergies in this work. Therefore, theory on this method is provided in Appendix A.

In fact, matrix factorization methods are dimensionality-reduction algorithms: taking as input a high-dimension dataset, they output a lower-dimension dataset which best approximates the input one, by finding common patterns in the input variables able to algebraically relate one variable to another. This is the reasoning for applying them to EMG data in order to discover the most probable set of muscle synergies used by the CNS. (Tresch et al., 2006)

Notwithstanding, the dimension of the output is not known from the start and it is not determined by the algorithm itself. This number must be provided to the algorithm. As so, the number of muscle synergies needs to be estimated or known from previous studies of the same muscle activity (eg. regarding movements in the same dimensions of space, executed by similar subjects in age and health condition). Although there is an interval of the number of muscle synergies commonly found in healthy subjects to perform point-to-point reaching movements, 4 to 7 synergies (d'Avella et al., 2006; Cheung et al., 2009; Coscia et al., 2014), the exact number may differ for different tasks in a 3D space. Moreover, this number is modified in stroke survivors and differs for each patient, due to the heterogeneity of post-stroke impairments across patients. In spite of several studies on this matter (Roh et al., 2013; Cheung et al., 2012; Clark et al., 2010), the relation between these impairments, as well as the age of the lesion, and the number of synergies is uncertain. (Roh et al., 2013) Therefore, an estimation of the number of synergies is required. Generally, this value is selected as the minimum able to capture the structural variation of the input dataset, so that, by adding one more synergy, it will only add noise to the reconstructed dataset. (d'Avella et al., 2006) However, more specific approaches are followed in different studies, not only to estimate the number of synergies, but also in the other steps of this analysis, as explained next.

A set of steps is commonly found in the literature to analyze muscle synergies. They are enumerated here and adopted variations by different scientists are mentioned:

1. **Synergies Extraction and Determination of the Number of Synergies**:

   Independently of the extraction method (matrix factorization algorithm), different authors have tried distinct approaches to select the correct number of synergies. For example:

   - A searching procedure is frequently followed, where k synergies are repeatedly extracted for several times (for ex., 50 times, like in Pirondini et al. (2016)) using the dimensionality-reduction algorithm and, each time, the set of k synergies found by the algorithm is used to reconstruct the EMGs; an accuracy measure is calculated to evaluate this reconstruction in comparison to the original EMG; the best result of those times is associated to the k value; k is varied from 1 (or other low number) to the number of muscles, repeating the previous steps for each k; finally, the best estimate of the number of synergies is assumed to be the k value for which the best reconstruction accuracy was obtained. Using this method, a threshold may be defined for deciding which is a good value of accuracy (for ex., 95%), or the variation of the slope of the accuracy measure may be analyzed and the number of synergies estimated for the lower variation. This measure of accuracy is frequently the

VAF, variance accounted for (the amount of explained variance retained by the reconstructed dataset) (Frère and Hug, 2012; Pirondini et al., 2016).

- Alternative to the repetition for k synergies and choice for the best result, cross-validation can be performed using datasets of different individuals to obtain the synergies and to assess them (Cheung et al., 2005);

- Another alternative is to determine the eigenvalues of the dataset and use the criterion of $eigenvalue > 1$ to decide if an additional synergy explains significant variance of one initial variable (one EMG signal) (Tropea et al., 2013);

- Alternatively, the number of synergies may be considered the one at which the cumulative variance drops below the 75% of a randomly shuffled dataset (see details in Cheung et al. (2009) or Tropea et al. (2013)).

2. **Matching Synergies**:

   After extraction, muscle synergies are not equally ordered for all datasets, which requires a categorization of each synergy as S1,..., Sn, for each subject, and matching pairs of synergies among different subjects. This procedure may be accomplished using the weight coefficients or the time coefficients.

   Typical methods for this step include a clustering process or the maximization of the dot product between pairs of synergies. The clustering may be achieved, for example, by the minimization of the Minkowski distance. (Cheung et al., 2009)

   When only two sets of synergies are being matched, the dot product maximization is easy to compute. However, when comparing a higher number of set of synergies, the clustering process may be more adequate, although both methods may and, actually, have been applied before (Tropea et al., 2013; Cheung et al., 2009).

3. **Similarity Assessment of Synergies' Structure**:

   The similarity between synergies of the matched pairs can be assessed to evaluate the synergies' structure modifications between groups of comparison (healthy vs. patient, or patient in different moments of the treatment).

   Typical measures of similarity are: the normalized dot product between the synergies' vector of weight coefficients (Pirondini et al., 2016; Tropea et al., 2013), the correlation coefficient between the matched pair (Tresch et al., 2006), and others.

4. **Similarity Assessment of Time Coefficients**:

   Some studies also compare the time activation profiles of muscle synergies. For example, the root mean squared value of the time coefficients (Pirondini et al., 2016) and also the Pearson's correlation coefficient (Tropea et al., 2013) have been used to assess the similarity between synergies activation of the same pairs.

5.3 Analysis of the Motoneural Activity in the Spinal Cord

Muscles are, in general, innervated by more than one segment of the spinal cord. In fact, several myotomal maps (localizing the motoneural pools in the human spinal cord which innervate the body muscles) have been published in the past, based on evidences from different sources: clinical, neuroimaging, autopsy, and electrophysical studies (read Wilbourn and Aminoff (1998) for a review). However, the root innervation of some muscles is not a certainty, being any myotomal chart usually considered a significant approximation of the reality, given that abnormal innervation may occur. (Phillips and Park, 1991; Stewart, 1992)

Notwithstanding, functional MRI of the human spinal cord has been confirming the statements of published charts (Kornelsen and Stroman, 2004; Stroman and Ryner, 2001), so that scientists have been using the muscle activity to estimate the spinal cord activity in cats (Yakovenko et al., 2002), healthy subjects during locomotion with different gaits (Cappellini et al., 2006; Ivanenko et al., 2008), healthy subjects assisted by robots in reaching movements (Pirondini et al., 2016), spinal cord-injured patients (Grasso et al., 2004), among others, based upon such charts.

These authors propose to map recorded EMG activity onto the ipsilateral motoneurons (MN) in the human spinal cord (considering only the approximate location of such MN in the anatomical rostrocaudal axis). In practical, the MN activity of each spinal segment is estimated from the weighted summation of the EMGs of all muscles innervated by that segment (see Equation 5.2). The weight coefficients are usually in accordance with Kendall's chart (Kendall et al., 1993), which indicates the number of sources confirming the connection between the spinal segment and the muscle and, given that number, muscles are weighted: when there is an agreement of five or more sources, the coefficient is 1, and it is 0.5, in case of agreement of three or four sources; the muscles with lower number of sources are neglected. The frequent choice for the Kendall's chart is due to the simplicity of using it as guide and for the comparable results with other charts, at least demonstrated for the lower limb (Ivanenko et al., 2006). For the upper limb, the analysis of the spinal cord activity is yet a novelty and the Kendall's chart was considered in published work (MacLellan et al., 2012; Pirondini et al., 2016).

$$S_j = \frac{\sum_{j=1}^{n_j} k_{ij} \cdot EMG_i}{n_j} \tag{5.2}$$

where S_j is the estimated activity of the jth spinal segment during the execution of some movement, n_j is the number of EMG_i signals corresponding to that segment, recorded during such movement, and k_{ij} is the weighting coefficient for the ith muscle.

Each signal, S_j, reflects the relative magnitude of each spinal segment's activity, during that time interval. It does not provide, however, the absolute amount of activity, since the EMG signals are previously normalized. (Grasso et al., 2004)

Basically, this analysis assumes that, first, rectified-EMGs allow the indirect quantification of the net firing rate of MNs and, second, the total output of the spinal segments is well represented by

the activity of the recorded muscles. The first assumption is based on earlier investigation demonstrating that increases of EMG amplitude are significantly linear with the net firing rate of the motor unit, both in young and elderly subjects. (Day and Hulliger, 2001; Masakado et al., 1994; Zhou and Rymer, 2004) The second assumption has been recently tested with the lumbosacral spinal segments, for movements with the lower limb, and results showed that spinal activity is relatively insensitive to the subset of muscles analyzed. (La Scaleia et al., 2014) Unfortunately, the same has not been validated for the upper limb. Nevertheless, La Scaleia et al. (2014) study was conducted for diverse movements (different types of human gait) and a considerable number of spinal segments. Therefore, until further validation for the arm, the second assumption of this analysis seems quite reasonable to be considered for upper limb studies, as in the present thesis.

For a visual representation of the spinal cord activity along the rostrocaudal axis, the signals S_j, for all j segments, are pooled together and the resulting matrix is represented in a colored map, as in the examples of Figure 5.4. Spinal maps are, therefore, representations of the spatiotemporal distribution of the activity in the spinal cord while executing some movement.

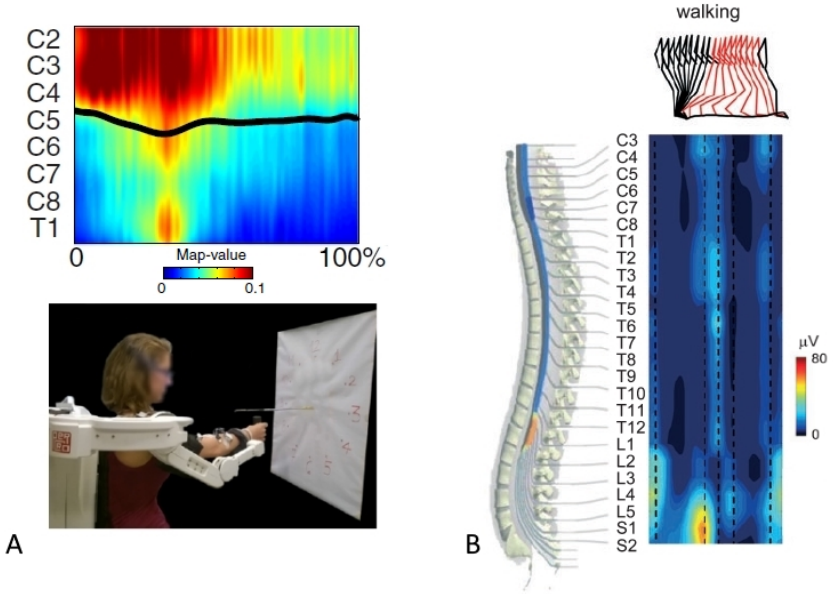

Figure 5.4: Examples of spinal maps extracted (A) for the upper limb, in healthy subjects wearing the exoskeleton in passive mode (i.e. without providing robotic assistance) while executing reaching movements, specifically for targets in the North (targets 1, 2, 11, 12, in the down figure) (Pirondini et al., 2016), and (B) for the lower limb, while walking (Ivanenko et al., 2008). Notice also the representation of the CoA superimposed in the spinal map of (A), in black. The x-axis of the spinal maps correspond to the time interval of the movement (the map results from resampled data of several subjects to have the same lenght, so the axis represents the relative time, from the beggining, 0%, to the end of the movement, 100%). In (A), C2-T1, and in (B), C3-S2 are the considered spinal segments. The color of the map indicates the activity intensity for each instant and spinal zone, provide by each author.

Spinal maps provide a synthetic and simple-to-compute representation of the activity in one upper element of the neuromuscular system, the spinal cord, which is likely to be modified after a stroke given that input for such activity comes from an injured brain cortex. As so, and recalling that spinal cord activity related to upper limb movements is poorly exploited in the literature (although promising results have been obtained in studies with the lower limb), this analysis was considered important for the present thesis.

Chapter 6

Materials and Methods

6.1 Participants

The present work was developed within Neuroprobes project. Accordingly, post-stroke patients are enrolled in the study if they fulfill the following inclusion criteria:

- age more than 18 years old;
- right/left hand dominant;
- cerebral lesion onset between 2-8 weeks (i.e. subacute and acute patients);
- ability to participate to a rehabilitative session of about 30-60 minutes;
- right-hemiplegic with at least 10 deg of motion in the treated joints (shoulder and elbow).

On the contrary, patients are excluded if they:

- have participated in another therapy or study including the use of a robotic device within the 30 days preceding and during this study;
- have previously been enrolled into the study;
- have an active implantable device or wear an active device (e.g., pacemakers, metallic objects in the brain, infusion pumps, etc.);
- have persistent delirium or disturbed vigilance, moderate or severe language comprehension deficits (i.e., incapability of discernment), or a skull breach;
- have a new stroke lesion during the study;
- have reduced mobility due to previous injuries or abnormalities unrelated with the cerebral accident.

Experimental data from four post-stroke patients, that were enrolled in the study and completed the treatment before the end of this work, was used in this work. Clinical data of these patients is reported in Table 6.1.

Table 6.1: Clinical data of the 4 post-stroke patients whose experimental data was used in this thesis.

Subject	**Age (years old)**	**Gender**	**Weight (Kg)**	**Height**	**Time after Injury**	**Hand Dominancy**	**Treatment Group**
ALEX-HUG-001	69	Female	80	155	4 weeks	Right	Group 2
ALEX-HUG-003	34	Female	82	165	2 weeks	Right	Group 2
ALEX-HUG-004	86	Male	66	165	3 weeks	Right	Group 3
ALEX-HUG-006	79	Female	66	160	3 weeks	Right	Group 1

In addition, recordings from eight right-handed healthy persons (7 females and 1 male, age 54.8±13.8, weight 61.6±11.6 kg, and height 167.0±8.5 cm) were used for the control group [1]. The healthy subjects did not present any evidence or known history of skeletal or neurological diseases, and they exhibited intact joint range of motion and muscle strength. Healthy subjects were enrolled in the same age range of the stroke group.

[1] In the following sections of this dissertation, healthy subjects may be referred to as H01, . . . , H08, meaning healthy subject 1, . . . , 8.

6.2 Experimental Setup

In the trial, the patients undergo motor rehabilitation training consisting in four weeks of treatment and four sessions of assessment. In particular, two assessment sessions were administered before the beginning of the treatment (A1 and A2, respectively two weeks and one week before) and two sessions after the end of the treatment (A3 after the last week of treatment, and A4, one-month after, as follow-up) – see Figure 6.1. Each week of treatment includes 3 sessions of arm training that lasts, approximately, 30 minutes of effective training with the robot.

Figure 6.1: Experimental protocol for the post-stroke patients. During each session of treatment (from T1 to T12), stroke patients of group 1, 2 and 3 train the upper limb movements whether being assisted by a physiotherapist, or by the exoskeleton (ALEx) with a conventional robotic treatment, or with a personalized robotic treatment, respectively. During each session of assessment (A1 to A4), a robotic evaluation is done, where the patient (of any group) wears ALEx and performs as many movements with the upper limb as he/she can.

The experimental treatment is proposed in addition to the habitual physical rehabilitative treatment of the patient. Post-stroke patients are enrolled in one of 3 groups of treatment:

1. **Group 1 – Standard physiotherapist-assisted therapy**: during all the sessions of treatment, the patients perform the traditional motor rehabilitation provided by a therapist, where the training exercises are decided and assisted by the clinician;

2. **Robotic-assisted therapy**: the patients train the upper limb movements with the assistance of the exoskeleton (ALEx). In each session of rehabilitation, they execute point-to-point reaching movements towards (and backwards) 8 of 18 possible targets [2] in a 3D space defined by a sphere of 19cm of radius (see Figure 6.2). The movement towards one target starts in the center of the sphere and finishes in that target (forward movement), the opposite movement starts in that target and finishes in the center of the sphere (backward movement). The

[2] A "target" refers to a "reaching point" of the training task of the robotic treatment, located in one of the 18 positions in the sphere of Figure 6.2 and, in this text, it will be numerically identified accordingly (eg. T1 refers to the reaching point 1).

patients perform as many movements as they can, wearing the robot in assisted-as-needed mode, i.e. when the subject is not able to reach the target, the robot moves the arm of the patient towards it. The subject visualizes the task (a red ball signals the target that they must reach) on a monitor placed in front of him/her.

2.1 **Group 2 – Conventional treatment**: the 8 targets are selected by the therapist for each session; the selection is based on the clinician analysis of the patient status and his/her conclusion about the patient (in)ability to reach those targets;

2.2 **Group 3 – Personalized treatment**: the 8 targets are selected automatically by the customization algorithm in the control system of the exoskeleton.[3]

During each session of assessment, a robotic evaluation is done, in which the patient (of any group of treatment) executes point-to-point reaching movements towards (and backwards) all the 18 targets of the sphere, repeating them as many times as possible, wearing the robot in assisted-as-needed mode.

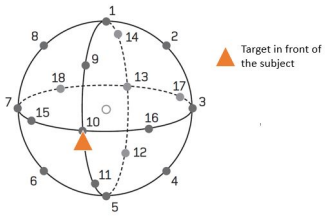

Figure 6.2: 18 targets equally distributed on a sphere with 19 cm radius constituting the reaching points of the tasks of the robotic treatment.

Healthy participants execute at least 3 repetitions of the same 3D point-to-point-reaching movements as the post-stroke group, towards (and backwards) the 18 targets in passive mode, i.e. they wear the exoskeleton only to record their kinematics.

The study was approved by the Commission *cantonale d'ethique de la recherché* (CCER) de Geneve, Switzerland and by the Comitato Etico Area Vasta Nord Ovest in Pisa, Italy, and the recordings were carried out in agreement with the Declaration of Helsinki and Good Clinical Practice norms. The participants were informed of the procedure and they signed an informed consent, which included the consent to the use of all data collected during the experiment in scientific publications.

[3]The personalization algorithm is an adapted version for 3D movements of the model proposed by Panarese et al. (2012), which takes as parameters the mean tangential velocity of the handle, the spectral arc-length of the handle velocity, and the frequency of the robotic assistance. By monitoring these metrics in real-time during the rehabilitation training, the algorithm assesses the level of motor improvement of the patient for all movements performed towards the different targets presented during the training session, and replaces some target by a more difficult one once a performance plateau is detected. Inclusion/exclusion of some target (in the set of 8 targets) is done within the same session, and from one session to the other.

6.3 Movement Kinematics and Muscular Activity Recording

Kinematic data and muscular activity were recorded during the execution of the movements by subjects of both control and stroke groups.

The position and velocity of the end-effector (held by the subject's hand) were acquired by the exoskeleton at a sampling rate of 1000Hz. The state (on/off) of the robotic assistance was also recorded in a binary signal (time points for which the signal is 1 correspond to instants when the movement is being assisted by the robot, i.e. robotic assistance is on, and vice-versa).

As represented in Figure 6.2, for the stroke group, kinematic data is recorded by ALEx during every assessment and treatment sessions of the experimental protocol. Muscular activity (electromyographic signals) is recorded in every session of assessment, and in one day of every week of treatment. The work developed in this thesis was focused on the analysis of recorded data during the assessment sessions.

In particular, it was not possible to record data of patient ALEx-HUG-004 during the Assessment 2, and of patient ALEx-HUG-006 during the Assessment 4. In addition, during the Assessment 3 of ALEx-HUG-003, the patient was not feeling so well and the recordings were interrupted several times.

Each healthy subject participates in a single day of data recording (kinematics and EMG).

The EMGs (electromyographic signals) of 15 muscles of the upper limb (upper trapezius, TRAPS, trapezius medialis, TRAPM, anterior deltoid, DANT, medial deltoid, DMED, posterior deltoid, DPOS, pectoralis major, PECM, latissimus dorsi, LAT, infraspinatus, INFRA, rhomboid major, RHO, biceps brachii long head, BICL, biceps brachii short head, BICS, brachioradialis, BRAD, triceps brachii lateral, TRILA, triceps brachii long head, TRILONG, pronator, PRO) were acquired, for both control and stroke groups, by using superficial Ag-AgCl electrodes (Kendall H124SG, ECG electrodes 30x24 mm) with a Noraxon Desktop DTS wireless system at a sampling rate of 1500Hz, after appropriate skin preparation.

Electrodes were placed according to guidelines of the Surface Electromyography for the Non-Invasive Assessment of Muscles European Community project (SENIAM) (Hermens et al., 2000) and Anatomical guideline (Perotto and Delagi 2005).

The exoskeleton automatically segments the kinematics data by movement and identifies each movement (i.e., indicates the reaching target and the repetition number of that movement [4]).

[4] Forward and backward movements towards/from one target are considered two repetitions of one movement regarding the same target, being a forward movement always followed by a backward movement.

6.4 Data pre-processing

6.4.1 Synchronization of EMG signals with Movement trajectory

15 channels were used in Noraxon to record the EMG signals. An additional channel was used to synchronize these signals with the kinematic data recorded by ALEx: this channel received a trigger signal generated by an Arduino UNO, connected to the exoskeleton, which indicates the starting and ending of any movement, as well as the starting of the robotic assistance in case it is required during the movement. Note that when the robot assists a movement, the end of the movement coincides with the end of the assistance.

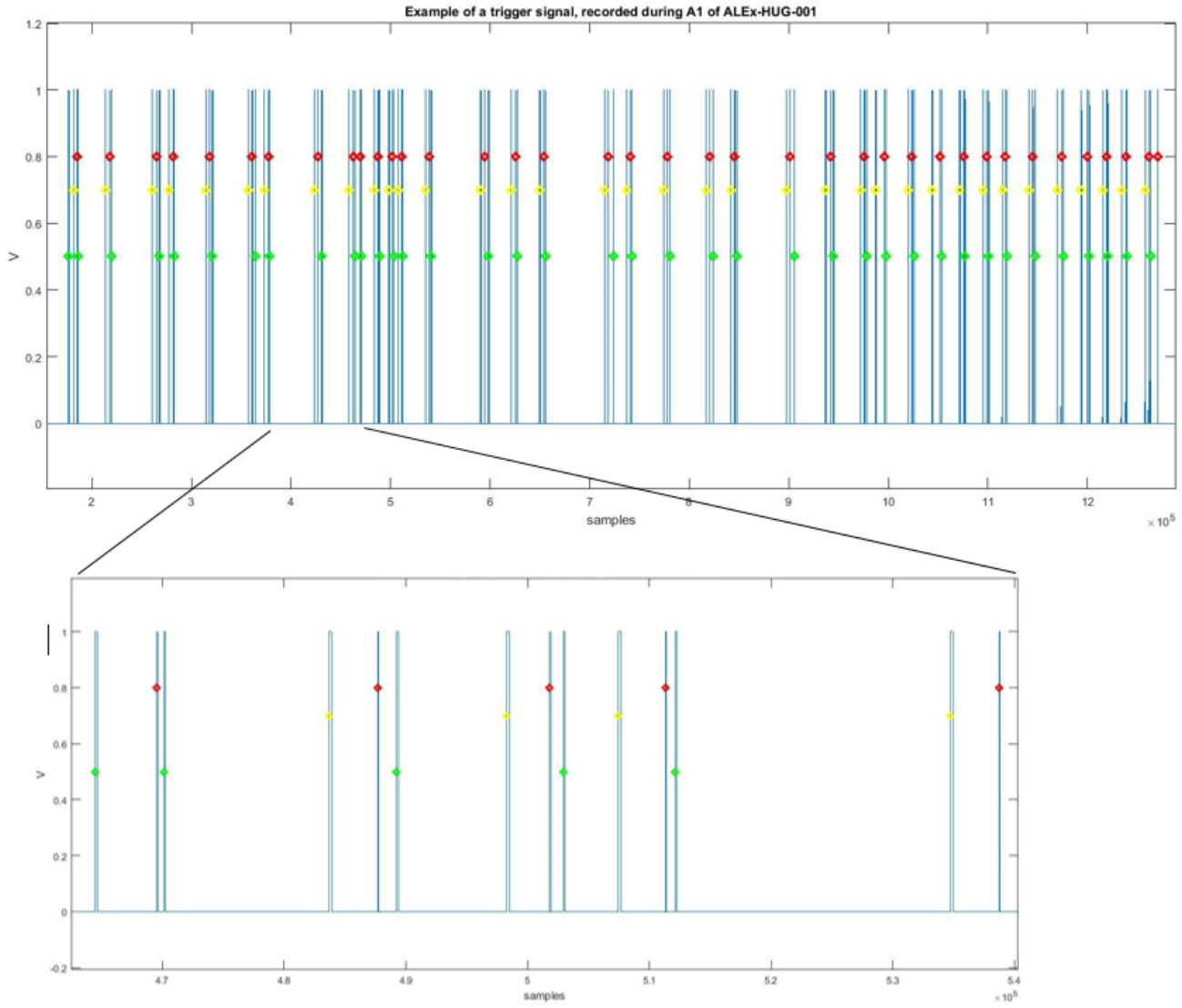

Figure 6.3: Example of a trigger signal (up), and a zoomed part of the signal (down). Different pulse widths refer to different events: green dots indicate the beginning of a movement; yellow dots refer to the beginning of the robotic assistance; and red dots correspond to the end of a movement.

The starting of a movement is registered when the target to be reached by the subject appears in the screen. The instant at which the robot begins assisting one subject (which happens when he/she stops moving for 3s) is registered. The ending of a movement is registered when the target is reached.

This trigger signal is a train of pulses: each pulse represents one of the events explained above, and each event corresponds to a different pulse width (see the illustration in Figure 6.3).

EMG data was, then, partitioned into segments/epochs, each segment regarding one movement (i.e. a task towards/backwards one target), considering the respective initial and final instants identified in the trigger signal by the width of each pulse. The movement corresponding to each EMG segment was also identified by matching it with the corresponding kinematics data.

6.4.2 EMG signals pre-processing

Combinations of methods previously described in the literature, presented in 5.1, were tested to pre-process the raw EMG signals, and the final implementation was chosen so to retain the maximum information accounting for physiologic behavior and to include the minimum of uninformative inter/intra-subject variability. The normalization was done with respect to the complete set of EMG segments (i.e. with all recorded movements), so that movements concerning different targets/directions could be comparable.

Then, the raw EMG signals were:

1. **detrended** (to remove any linear trend of the signal mean),
2. **band-pass filtered** (20-400Hz) using a Butterworth filter response of 4th order (to exclude movement artifacts and the motor units firing rate, frequencies usually under 20Hz, and to remove additional high-frequency noise, over 400Hz),
3. **full-wave rectified** (to obtain the EMGs envelope and, thus, highlight the information regarding the level of muscle activation),
4. **low-pass filtered** (10Hz) using a Butterworth filter response of 4th order (to remove high-frequency components introduced by the previous rectification),
5. and **each EMG channel normalized** by its maximum activity during a complete recording session (i.e., including all movements).

6.5 Scientific analysis plan to formulate the thesis

As explained in Chapter 1, to define the neurobiomechanical state of post-stroke patients during the robot-aided upper limb motor rehabilitation, the present work estimates and quantifies the motor improvement during the treatment using kinematic performance and muscle activity.

To achieve the first goal of this thesis and define the framework for the analysis of patients' data (kinematics and muscle activity), a scientific analysis (see Figure 6.4) was designed to study the variability in movement execution and, mainly, in muscle activity when performing 3D point-to-point reaching movements in different directions. It includes:

I the quantification of effects of the movement condition (reaching point, i.e. targets, and direction, i.e. forward or backward) on single muscle activity, muscle coordination and movement execution, by performing, on datasets related to healthy subjects, an analysis of:

  i spinal maps and electromyographic envelopes (representing single muscle activity),

  ii muscle synergies (a representation of muscle coordination),

  iii smoothness, accuracy, efficiency, and easiness, on the movements' trajectory (a kinematic analysis on movement execution).

II the application of the same methods from i. to iii. to post-stroke patients' data, to quantify effects of the movement condition in this group of subjects.

Finally, to identify which metrics related to kinematics, spinal maps and muscle synergies can be used as biomarkers to quantify motor impairment and recovery, the two groups of subjects are compared, and the correlation between such metrics and FMUE (Fugl-Meyer Scale for the Upper Extremity) is determined.

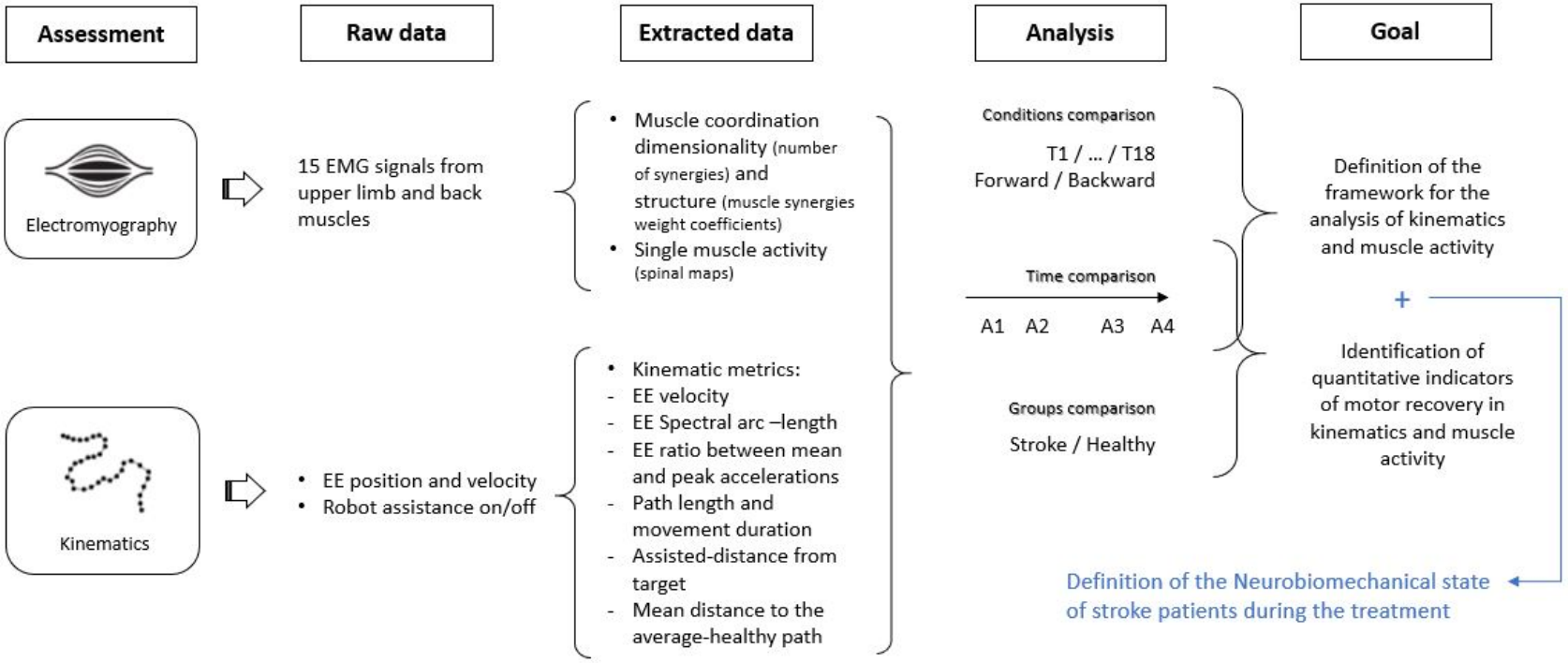

Figure 6.4: Scientific plan designed to analyze the 3D point-to-point reaching movements in different directions, executed by healthy subjects and post-stroke patients, to formulate the thesis on the neurobiomechanical state of stroke patients during the robotic treatment.

6.6 Analysis of the control group (healthy subjects)

6.6.1 Datasets formation

Datasets containing forward/backward movements regarding all targets, and datasets containing movements forward/backward movements regarding one same target (see Table 6.2) were built, for each subject, with the respective epochs of the pre-processed, not resampled EMG signals. Data was organized in this way, because it allows the comparison of the effects of the reaching point (target) and direction (forward/backward) of the movement on single muscle activity, muscle coordination and movement execution. To extract synergies and estimate the spinal cord activity with higher accuracy [5], more than one repetition of each movement was included in the datasets.

Table 6.2: Datasets of EMG signals (identified as D_1 to D_{38}) that were built to assess the influence of the reaching point (target) and direction (forward/backward) of the movement on single muscle activity, muscle coordination and movement execution. The column indicates the target(s) of the movements included in the dataset (eg. T1 denotes target 1), the row indicates the direction.

	[All targets]	**T1**	**T2**	**T...**	**T17**	**T18**
F	D_1	D_3	D_5	$D_{...}$	D_{35}	D_{37}
B	D_2	D_4	D_6	$D_{...}$	D_{36}	D_{38}

6.6.1.1 Exclusion of Movements' Outliers

Each subject executed the movement towards each of the 18 targets (forward and backward), repeating the cycle of those 36 movements for 5 times. However, not all the 5 repetitions of each movement could be used, because:

1. For some subjects, for some targets, the EMG of one of the 5 repetitions was unavailable (i.e., the EMG signals' recording failed) – thus, there were only 4 repetitions in common among all subjects and all targets;

2. The movement execution of each subject was found variable to some extent from one repetition to another of a same movement (i.e., a movement towards a same target) – see the examples in Section 7.1.1 of the Results. This intra-subject (and inter-subject) variability in the movement kinematics (especially the speed and path), mainly due to factors difficult

[5] An accurate extraction of muscle synergies means the EMG signals of each subject could be accurately reconstructed from a set of synergies obtained by averaging, across subjects, the extracted synergies of each subject. The same reasoning can be applied to explicit an accurate estimation of the spinal cord activity.

to control in the experiment [6] , were previously shown to affect at least some synergies underlying the respective muscle activity (Cappellini et al., 2006; Sadaka-Stephan et al., 2015; d'Avella et al., 2008), and, thus, influence the next steps of the analysis.

Therefore, for each subject and each task (i.e. a forward/backward movement in respect to a single target), only 3 repetitions of the movement were used for the analysis of muscle activity and kinematic data. The 3 repetitions were chosen based on the following reasoning:

I Since some features of the movement kinematics influence the extraction of synergies (Cappellini et al., 2006; Sadaka-Stephan et al., 2015; d'Avella et al., 2008), kinematic metrics (path length and movement duration – computed on the movement trajectory recorded by ALEx) were used to compare multiple repetitions of a movement towards the same target.

II The first repetition of a movement executed by some subjects usually reflects the subject adaptation to the task (see Section 7.1.1), and this learning phenomenon is undesirable to be accounted for when defining a set of control synergies (which must represent the healthy human motor coordination).

Considering this reasoning for each subject, the procedure to choose 3 of 4 repetitions was the following:

1. The kinematic metrics (path length and movement duration) were computed for all movements (all repetitions towards all targets).

2. Each repetition of a movement was labeled as outlier, considering separately the path length and the movement duration, if the following two conditions were matched:

   - The metric value corresponding to that given repetition was higher than 75%, or lower than 25% of the percentiles of all repetitions (i.e. all values computed in 1. for the metric)[7] ;
   - The previous condition was also true for a maximum of one additional repetition of the same movement[8].

3. The 2 labels attributed to each repetition (step 2), by using the path length or the movement duration, were combined to decide whether to discard or not a given repetition. This step

[6] These include the residual stiffness of the robot and the unconstrained speed (such as the time to complete the movement) during the experiment. Note that time was not constrained to prevent unrealistic data, because the subjects' behavior was not natural when forced to finish within a time interval.

[7] The 75% and 25% thresholds were empirically selected to balance the inclusion of very different movements with the exclusion of a maximum of one repetition per target, per subject. The selected thresholds were, then, applied to all subjects.

[8] It was considered that, if at least three repetitions of a same movement are outliers among all repetitions of all movements, then, it is possible that such movement is significantly different from the others (i.e., the variability is not due to the experiment), so, the given repetition should not be discarded.

was performed differently to build datasets containing movements towards a single target (a.) and to build datasets containing movements towards all targets (b.) (see examples in Figure 6.5):

a) "Individual targets" datasets
Each repetition labeled as outlier in both metrics was automatically discarded. This resulted in one or zero repetitions of any movement being considered outlier by both metrics simultaneously, and being discarded this way. In the latter case (i.e. zero outliers and, thus, no repetition automatically discarded), repetition 1 was discarded, following the reasoning in II, thus, remaining always 3 repetitions for each movement.

b) "All targets" datasets
For these datasets, one complete cycle of movements towards the 18 targets was considered equivalent to "one repetition". Therefore, discarding a repetition here means to discard all the 18 movements.
The decision to discard or not one complete cycle of movements was based on the number of movements, inside that cycle, which was considered outlier (by both metrics): the 3 cycles containing the less number of outliers were used.

4. The procedure in 3), a. and b., was repeated with forward and backward movements separately

Finally, the EMG signals corresponding to the 3 chosen repetitions for each subject were concatenated to build the datasets of muscle activity. In specific, datasets with All targets (D_1 and D_2, in Table 6.2) included the 3 repetitions of all the 18 targets.

For direct analysis of EMG signals (amplitude analysis) and estimation of the motoneural activity in the spinal cord (spinal maps extraction), it is necessary to have the signals of all subjects with an equal number of time points, so that signals can be averaged and represented in the same relative time (i.e. respect to the movement cycle – beginning to end). Therefore, for those two analyses, EMG signals of each movement repetition included in each dataset were resampled on the minimum number of samples (time points) across all movements executed by all subjects.

For the EMG factorization analysis (muscle synergies extraction), the non-resampled EMGs were used.

To perform the kinematic assessment, movement trajectories of the respective 3 repetitions selected by the exclusion of outliers were associated in datasets for each target and direction.

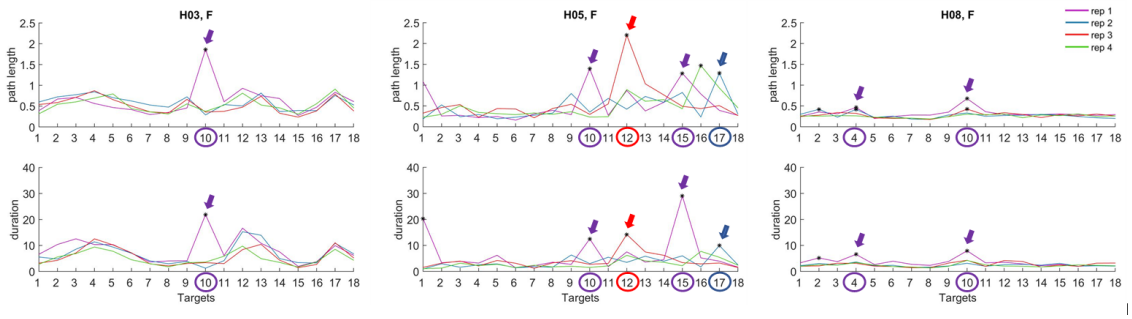

Figure 6.5: Procedure to exclude outliers exemplified with forward (F), i.e. center-to-target, movements of three healthy subjects (H03, H05, H08). The values of path length and movement duration are plotted for each target, for repetitions 1 (purple), 2 (blue), 3 (red) and 4 (green). The * correspond to the outliers identified across the 4 repetitions, independently for each of the two metrics (path length; movement duration). Only repetitions considered an outlier for both metrics (arrows) are discarded, in case of "individual targets" datasets, or counted, in case of "all targets" datasets. In the latter case, the 3 repetitions for which a less number of targets was considered outlier (with both metrics) are chosen to include in the datasets (for example, for H05, repetitions 2, 3 and 4 are chosen, because repetition 1 is considered outlier in movements towards 2 targets, 10 and 15, while the other repetitions are never considered outliers or they are only in the movement towards 1 target).

6.6.2 Task execution – Kinematic Analysis of the Movement

The position and velocity of the robot end-effector were considered to describe the movement of the subject' hand towards any target.

Once the exoskeleton automatically segments and identifies the kinematic data per movement, these datasets did not need any setup or pre-processing, apart from selection of the movements corresponding to the 3 repetitions chosen for each condition (from the exclusion of movement outliers, explained in Section 6.6.1.1).

The execution of 3D reaching movements by healthy subjects was analyzed in terms of kinematic performance. To examine several features of the movement execution, kinematic metrics were computed on the end-effector position and velocity matrices. The selected metrics to analyze each feature are presented in Table 6.3.

In the literature, measures of accuracy are conventionally computed with respect to a straight path, as it happens with metrics like trajectory straightness (Cirstea and Levin, 2000; Kahn et al., 2006) or mean distance from theoretical path (Panarese et al., 2012; Pirondini et al., 2016; Colombo et al., 2005). Oppositely, in this work, the trajectory performed by each healthy subject was verified to have a curvilinear path.Therefore, to measure movement accuracy, it was used a more realistic path: the healthy path (averaged across healthy subjects). Then, mean distance from this path was computed the same way as explained in Chapter 4.

Table 6.3: Selected metrics to examine each feature of the healthy movement execution.

Movement feature	**Kinematic metrics**
Temporal efficiency	Movement Duration
Spatial efficiency	Path Length
Accuracy	Mean Distance from average-Healthy path (MDH)
Smoothness	Spectral Arc-Length (SAL), Ratio of Mean acceleration with Peak acceleration (RMP)
Easiness	Mean velocity

It must be noted that, for this biomechanical analysis, the kinematic metrics can be computed for every single repetition of a movement without any problem of convergence (as it happens with muscle synergies extraction algorithms). Therefore, any target reached by a patient during the assessments can be compared with the respective one of the healthy group and, thus, with kinematics, movements were not organized in groups of targets.

6.6.3 Muscle activity – Amplitude analysis

Pre-processed and resampled EMG signals of all subjects were averaged across subjects to obtain a global representation of the level of muscle activation of the healthy group for each target and direction.

The RMS value of each EMG was computed, as a preliminary analysis, to provide a measure of the signal amplitude and highlight possible differences between movements in the temporal activation of each muscle. Given that EMG for all muscles were previously normalized by the maximum, having the same amplitude range, then, the RMS values were averaged across muscles to provide a global measure of the arm effort while executing the movements.

6.6.4 Muscle coordination – Extraction of muscle synergies

The muscle coordination of the healthy group while executing 3D point-to-point reaching movements was described using muscle synergies.
Synergies were extracted for each dataset and their structure (muscle weight coefficients), as well as the number of synergies, was compared across datasets to quantify the effects of movement

conditions (different targets, and forward/backward movements) on muscle coordination.

6.6.4.1 The Extraction Algorithm

Synergies were extracted for each dataset of each subject, applying the Non-Negative Matrix Factorization (NNMF) method to the EMG signals matrix. The *nnmf* MatLab function was used. This method was selected because it is one of the most used methods to extract muscle synergies in the literature (Pirondini et al., 2016; Coscia et al., 2014; Cheung et al., 2009; Santuz et al., 2017; Steele et al., 2015b; Cheung et al., 2005) and it is the one providing easier interpretable results given its constrain of non-negativity.

The Mult (Multiplicative Update Rules) and ALS (Alternating Least-Squares) algorithms, variations of the NNMF detailed in Appendix A, were combined to improve the synergies extraction. The Mult algorithm was only used to start the convergence (because it is more sensitive to initial values, (Berry et al., 2007)), followed by the ALS algorithm to find the solution:

1. The weight (w) and time (h) coefficients were randomly initialized, and the EMG matrix was given as input to the Mult algorithm, constraining the number of maximum iterations to a very low value (5). The replicates (i.e., the number of times that the *nnmf* function repeats the extraction, for outputting w and h for the lower-error repetition) was set to 50.[9]

2. Then, the computation of weight and time coefficients was repeated cyclically during 100 times, using the ALS algorithm, and the number of maximum iterations was set to a value large enough to allow convergence (500). After each repetition, the output coefficients were used as initial values to the following repetition, except for the first computation, in which the initial values were the output of 1.

This algorithms combination increases the extraction accuracy (about 2%), and reduces the computation time, especially when computing over large datasets (like D_1 and D_2).

6.6.4.2 Estimation of the Number of Synergies

After studying some of the methods detailed in 5.2., a searching procedure was exploited to estimate the correct number of synergies, using the VAF (variance accounted for) as accuracy metric, as in Pirondini et al. (2016); Cheung et al. (2012); Coscia et al. (2014); Clark et al. (2010).

The threshold for a good accuracy was defined as 95%, as in previous investigation (Pirondini et al., 2016; Sadaka-Stephan et al., 2015). This method was selected by its good balance between simplicity and reliability: it is very easy to compute and the results obtained were in fair agreement with the related literature. [10]

[9] This replication is necessary because w and h extracted each time may represent a local extremum of the error surface. (Cheung et al., 2012)

[10] As mentioned in 5.2, the number of muscle synergies during point-to-point reaching movements has been estimated before to range from 4 to 7 in healthy individuals. By using the VAF, the estimated number of synergies (see Chapter 7) is between this range. However, tests on the recorded data using, for example, the cumulative variance instead of the VAF, resulted in a number of synergies ranging from 5 to 8.

The searching procedure was done by extracting 3 to 7 synergies, using the algorithm described in 6.6.4.1, and calculating, for each extraction, the VAF – see Equation 6.1. The number of synergies retained was the minimum leading to a VAF higher than the threshold.

$$VAF = 1 - \frac{\sum_{n=1}^{M}\sum_{t=1}^{T}(D_{original}(n,t) - D_{reconstr}(n,t))^2}{\sum_{n=1}^{M}\sum_{t=1}^{T}(D_{original}(n,t))^2} \tag{6.1}$$

where M=number of muscles,T=number of time-points, $D_{original}$ is the original matrix of EMG signals,and $D_{reconstr}$ is the reconstructed matrix of EMG signals, by multiplcation of the muscle weights and time activation coefficients of each synergy, and sum for all synergies.

6.6.4.3 Quantification of effects of movement conditions on the number of synergies

To quantify the effects of the target and the movement direction on the number of synergies, only the datasets D_3 to D_{38} (i.e. datasets with movements regarding a single target and a single direction) were compared.

As so, for each dataset, the estimated number of synergies of the 8 healthy subjects in that condition were pooled together. This resulted in 36 distributions (corresponding to the 36 conditions), each with 8 values. Then, the statistical difference across conditions was assessed as explained in Section 6.6.4.7.

The results of this and the previous section were considered to determine the number of synergies to be used in the next steps.

6.6.4.4 Synergies Clustering

Muscle synergies extracted from all datasets of all subjects were ordered by their vector of weigh coefficients, maximizing their similarity with a set of reference synergies.

Similarity was assessed by the normalized dot product (DOT) (Pirondini et al., 2016; Cheung et al., 2009; Tropea et al., 2013). The procedure of ordering based on the maximization of similarity was achieved by:

1. computing the DOT between the set of synergies to be ordered and the synergies of the reference set (resulting in a n-by-n matrix of DOT values, being n the number of synergies previously estimated – see Section 7.1.4);

2. matching a pair of synergies having the maximum DOT of all DOTs in the matrix computed in 1.;

3. eliminating from the matrix the matched synergies with the highest DOTs;

4. repeating the steps 2. and 3. until all synergies are matched with one of the reference synergies.

The set of reference synergies was generated with the set of 4 synergies extracted from dataset D_1 of all subjects. First, the synergies of all subjects were categorized into 4 clusters and, then, the synergies of each cluster were averaged.

The chosen clustering method was a hierarchical procedure to minimize the Minkowski distance between the weight coefficient vectors of the synergies within each cluster (Pirondini et al., 2016; Cheung et al., 2009). For that, MatLab statistics-toolbox functions were used: *pdist* (to compute all the Minkowski distances, using the exponent P equal to 3), *linkage* (to compute a tree of hierarchical clusters, based on the matrix of distances, and using the Ward method), and *cluster* (to construct the clusters from the agglomerative hierarchical cluster tree).

6.6.4.5 Quantification of effects of movement conditions on the synergies' structure

To quantify the effects of the reaching point and the movement direction on the synergies' structure, only the datasets D_3 to D_{38} (i.e. datasets with movements regarding a single target and a single direction) were compared.

Thus, for each synergy (S1, S2, S3, S4) and each muscle, the corresponding weight coefficients obtained for the 8 healthy subjects were pooled together, separately for each dataset. These 36 distributions were tested to determine if they were significantly different (see Section 6.6.4.7).

Nevertheless, the conclusion for each synergy is derived from the 15 statistical tests (15 weight coefficients), i.e., one can only conclude the synergy' structure is the same across conditions if, for all the 15 muscle weights, no differences are found across conditions. Therefore, the multi-comparison was done with the Bonferroni correction, to compensate the fact that, with multiple tests (multiple muscle weights), the likelihood of incorrectly rejecting a null hypothesis (equal synergy structure across conditions) increases (i.e. the probability of making a Type I error increases).

6.6.4.6 Quantification of effects of movement conditions on inter-subject similarity of the synergies' structure

The normalized dot product (DOT) between the synergies' vector of weight coefficients was adopted as measure of similarity of the synergies structure. Thus, it was used to assess the robustness of the synergies' structure for each condition and to verify if the movement condition affected this robustness.

As so, for each synergy (S1, S2, S3, S4), the DOT was computed between subjects in the same movement condition, resulting in a distribution of 28 values (combinations of 8 subjects in pairs). Then, the 36 distributions for each synergy were assessed concerning their statistical difference.

6.6.4.7 Statistics

To determine the statistical significance of any difference across movement conditions (targets and directions), the respective data from all subjects (being it the synergies weight coefficients, or the number of synergies, etc.) was pooled together (resulting in a distribution of values for any condition), and the hypothesis that data of all the conditions belong to the same population was tested. A p-value of 0.05 was considered as confidence level.

Therefore, to decide whether to use the 2-Way ANOVA (ANalysis Of Variance) test or the nonparametric Friedman test with 2 factors (being them target and direction), first, two hypothesis were assessed (Rinaldi and Monaco, 2013):

1. The hypothesis of normal distribution for all the conditions was tested by the One-sample Kolmogorov-Smirnov test (using the MatLab function *kstest*).

2. The homogeneity of variance across all the distributions was assessed by the Levene's test (using the MatLab function *vartestn* [11]).

ANOVA is relatively robust with respect to violations of the normality assumption, but it is more sensitive to variance inequality (Kirk, 1982). Thus, even if the conditions were determined not Gaussian distributed, the possibility to assess them using the 2-Way ANOVA was considered, depending on the results of variance homogeneity. This was done because, unlike two-way analysis of variance, Friedman's test does not treat the two factors symmetrically and it does not test for an interaction between them. So, to have the information concerning the interaction between targets and directions, results of the 2-way ANOVA were obtained and, for the above-mentioned situation, they were confirmed by performing also the Friedman test. (Rinaldi and Monaco, 2013)

In addition, a post-doc analysis was performed, using the MatLab *multcompare* function, to determine which pairs of targets and directions were significantly different.

6.6.5 Estimation of Motoneural Activity in the Spinal Cord

For the upper limb muscles considered in the thesis, the reported location of the innervating motoneurons (MN) is in the C2 to T1 segments of the spinal cord. (Kandel et al., 2000; Kendall et al., 1993) Accordingly, the motoneural activity of these spinal segments was estimated by a weighted summation of the EMG signals of all muscles innervated by the respective segment, using the Equation 5.2 introduced in Chapter 5.

Such estimation was computed for each movement condition (target and direction) using the pre-processed, resampled EMG signals averaged across the 3 repetitions included in the respective dataset.

Weight coefficients reported in Kendall chart (Kendall et al., 1993) were assumed for each muscle, as in previous studies with the upper limb (Pirondini et al., 2016; MacLellan et al., 2012). Muscles innervated by spinal segments C2 to T1 are indicated in Table 6.4

[11] The Levene's test is available in 3 options ('LeveneQuadratic', 'LeveneAbsolute' and 'OBrien' for the 'TestType' parameter). The results with the 3 options were considered for the next steps.

Table 6.4: Upper limb muscles innervated by each spinal cord segment. X indicates the spinal cord segment (row) contributing to the activity of the muscle (column). TRAPS – trapezius superior (upper fibers); TRAPM – trapezius medialis (middle fibers); DANT – deltoid anterior; DMED – deltoid medialis; DPOS – deltoid posterior; PEC – pectoralis major; LAT – latissimus dorsi; INFRA – infraspinatus; RHO – rhomboid; BICS –bicep short head; BICL – bicep long head; BRA – brachialis; BRAD – brachioradialis; TRILAT – triceps lateralis; TRILONG – triceps long head; PRO – pronator; C2-C8 - cervical segments 2 to 8 of the spinal cord; T1 - thoracic segment 1 of the spinal cord.

	TRAPS	TRAPM	DANT	DMED	DPOS	PEC	LAT	INFRA	RHO	BICS	BICL	BRAD	TRILAT	TRILONG	PRO
C2	X	X													
C3	X	X													
C4	X	X						X	X						
C5			X	X	X	X		X	X	X	X	X			
C6			X	X	X	X	X	X		X	X	X	X	X	X
C7						X	X						X	X	X
C8							X						X	X	
T1													X	X	

The spatiotemporal distribution of the activity in the spinal cord while executing forward/ backward movements towards each target was represented for each subject and for the average across subjects. To obtain a continuous and smoothed map (illustrating the spatial continuity in the spinal cord), a filled contour plot was used (MatLab function *contourf*), which computes isolines from the matrix of spinal activity in the 8 segments and fills the area between the isolines using a map of constant colors.(Ivanenko et al., 2008)

6.6.5.1 Quantification of effects of movement condition on inter-subject similarity of the spinal maps

To verify the spinal maps similarity across subjects, the two-dimensional (2D) correlation coefficient (see Equation 6.2) was computed (MatLab function *corr2*) between the averaged spinal map and each subject's spinal map, for every movement condition. This measure is the 2D-equivalent of Pearson's correlation coefficient, being adequate to compare two images, like the spinal maps, in which the color is a representation of the signal scale. R ranges from -1 to 1, as the Pearson's coefficient: it is 1 when images are completely identical; 0 if images are completely uncorrelated; and -1 if one image is the negative of the other. (Monaco et al., 2010)

$$R = \frac{\sum_{i=1}^{n}(x_i - \bar{x}).(y_i - \bar{y})}{\sqrt{\sum_{i=1}^{n}(x_i - \bar{x})^2}.\sqrt{\sum_{i=1}^{n}(y_i - \bar{y})^2}} = \frac{cov(x,y)}{\sigma_x.\sigma_y} \tag{6.2}$$

where x_i is the intensity of the ith pixel of the first image, y_i is the intensity of the ith pixel of the second image, and $\bar{x}$ and $\bar{y}$ are the mean intensities of the first and second images, respectively. *cov(x,y)* is the covariance between image x and y, σ_x is the standard deviation of image x and σ_y is

the standard deviation of image y.

The statistical significance of the effects of movement condition on the spinal maps similarity across subjects was tested. The same reasoning explained in Section 6.6.4.1 of the synergies analysis was followed: before any assessment with 2-Way ANOVA or Friedman test, the normality assumption and variance homogeneity were verified.

6.6.5.2 Quantification of effects of movement condition on the shape and magnitude of the spinal maps

To compare the spinal maps across movement conditions, two measures were considered:

1. The covariance between spinal maps of two conditions: this is a measure of the joint variability of two variables (in these case, 2D variables, the spinal maps). Two spinal maps covariate if the increases/decreases of the motoneural activity occur for both maps, in the same spinal zones, with a same magnitude. (Rice, 2006)

2. The 2D correlation coefficient between spinal maps of two conditions: this is a measure of dependence of two variables; explicit in 6.2, it is equivalent to the covariance between maps normalized by the standard deviation of both maps; two spinal maps are correlated if the increases/decreases of the spinal activity occur for both maps, in the same spinal zones, but not necessarily with a same magnitude. (Rice, 2006)

Therefore, covariance was used to assess the similarity of the shape of the spinal maps, and covariance was used to assess the similarity of the level of activity.

To search for trends in the variation of the magnitude and shape of the spinal maps as a function of the reaching point, each target was associated with its distance to 3 references (target 1, T1; target 7, T7; target 13, T13), independently, and the covariance and correlation were computed between the spinal map for that target and the spinal map of each reference. Two distance-metrics were tested: the Euclidean distance and the "one-axis" distance. The former considers the relative position of the target in 3 axes, while the latter one considers the position in 1 axis (the up-down axis, when comparing with reference T1; the left-right axis, with reference T7; the distant-close axis, with reference T13). See the example with target 16 in Figure 6.6 . This procedure was repeated with forward and backward movements, to analyze trends in both directions.

Targets 1, 7 and 13 were taken as references because they are corners in the 3 main axes of the sphere, relative to the subjects position.

The relative shape (correlation) and magnitude (covariance) of the spinal maps as a linear function of the relative position of the target (Euclidean/one-axis distance) was tested: the hypothesis that these variables are not linearly correlated (linear correlation, $\rho = 0$) was assessed (MatLab function *corr*, [ρ, p-value] = *corr*).

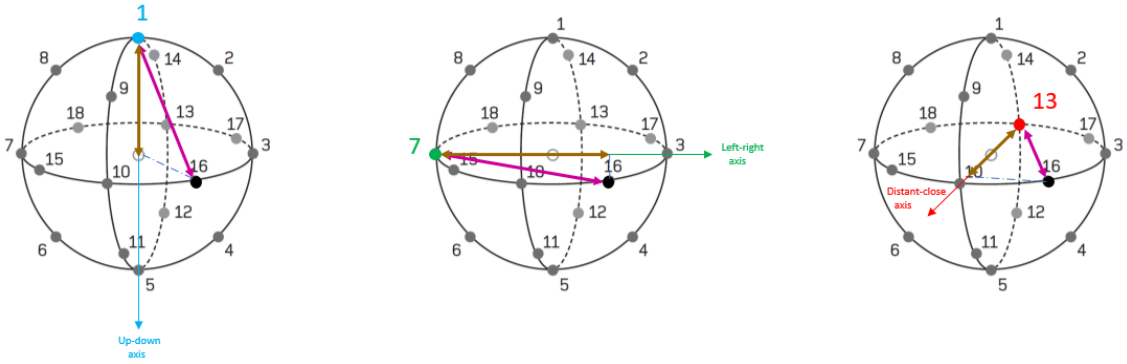

Figure 6.6: Targets 1, 7 and 13 were taken as reference to quantify the variation of the shape and magnitude of the spinal maps as a function of the target position. The Euclidean distance (in pink) and the distance in one axis (in gold) is exemplified with target 16, for the up-down axis (left), the left-right axis (middle), and the distant-close axis (right).

6.6.6 Grouping Targets

Targets were arranged in 4 groups, as shown in Figure 6.7.: group 1 includes targets 1, 2, 8, 9 and 14; group 2 includes targets 4, 5, 6, 11 and 12; group 3 includes targets 7, 18, 13 and 17; and group 4 includes targets 3, 16, 10 and 15. Then, EMG signals of each target dataset were concatenated by group, resulting in new, larger datasets.

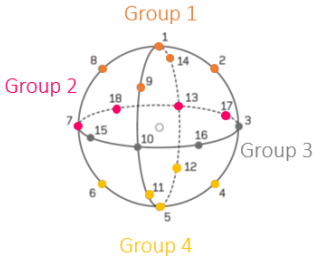

Figure 6.7: Targets arranged in 4 groups: targets included in group 1 are marked in orange; group 2, in pink; group 3, in grey; group 4, in yellow.

Muscle synergies were extracted from the new 4 datasets of each subject and the number of synergies was estimated, following the same methods of Section 6.6.4.

Spinal maps were computed as well for each subject and averaged across subjects for each group of targets. Since spinal maps are linear functions of the EMG signals, basically, the spinal map of the group is the average between the spinal maps corresponding to the targets included in the group.

6.7 Analysis of the stroke group

6.7.1 Datasets formation

Post-stroke patients easily get tired and are not able to repeat the movements as many times as healthy subjects, due to their disability. As so, not as many movement repetitions as in the case of healthy subjects are available to factorize the muscle activity of each individual movement condition.

Therefore, EMG datasets were built in agreement with the latter conclusions of the healthy group, organizing targets in the same way, for every recording session (assessment sessions) of each patient: pre-processed EMGs corresponding to forward movements towards targets 1, 2, 8, 9 and 14 were concatenated in group 1; the ones towards targets 7, 13, 17 and 18 in group 2; the ones towards targets 3, 10, 15 and 16 in group 3; and, finally, targets 4, 5, 6, 11 and 12 in group 4. This was repeated with backward movements.

Although, theoretically, groups are not balanced in number of targets included, in practical, they were balanced, because not all the targets are trained by the patient, especially in the first assessments (being this the reason for the need to define a methodology and data organization to analyze patients' muscular data).

6.7.1.1 Exclusion of bad recordings

During the experiments, the uncoordinated behavior of some patients made it impossible to use some of the EMG recordings. In these acquisitions, the electromyographic signals could not measure the muscle activity due to the superimposition of high voltage noise impossible to be filtered (see Appendix B). These corrupted signals were manually detected and excluded from the analysis, before concatenating the EMGs in datasets.

When, for exceptional cases, more than three repetitions were available for some movement, the first three were selected to proceed with the analysis.

kinematic data corresponding to the selected movement repetitions was organized in separate datasets for each target and direction.

6.7.2 Task execution – Kinematic Analysis of the Movement

The position and velocity of the robot end-effector were considered to describe the movement of the patient's hand towards any target.

Once the exoskeleton automatically segments and identifies the kinematic data per movement, these datasets did not need any setup or pre-processing, apart from exclusion of movements without a correct EMG recording, as explained in the previous section.

The motor ability of post-stroke patients while performing 3D point-to-point reaching movements was assessed by examination of several features of the movement execution similar to

(Panarese et al., 2012). For each of these features, kinematic metrics were computed on the end-effector position and velocity matrices. One metric (in addition to the same computed for healthy subjects) was computed to evaluate the patient's ability to accomplish the task by himself (i.e. his/her independence on the robotic assistance). All of them are presented in Table 6.5.

Table 6.5: Selected metrics to examine each feature of the stroke patients' movement execution.

Movement feature	**Kinematic metrics**
Temporal efficiency	Movement Duration
Spatial efficiency	Path Length
Accuracy	Mean distance to the average-Healthy path (MDH)
Smoothness	Spectral Arc-Length (SAL), Ratio of Mean acceleration with Peak acceleration (RMP)
Easiness	Mean velocity
Task accomplishment	Assisted-distance

The measure of accuracy was computed by taking the mean value of the Euclidean distance to the healthy path (average path across healthy subjects to reach a given target).

The assisted-distance corresponds to the length of the path robotically assisted, if there is robotic assistance.

The other metrics were computed for assisted and non-assisted movements, but considering only the trajectory performed by the patient.

6.7.3 Muscle coordination – Extraction of muscle synergies

Following the same methods as with the healthy group (see Sections 6.6.4.1. and 6.6.4.2), muscle synergies were extracted from EMG datasets.

All patients' synergies were ordered by their vector of weigh coefficients, maximizing their similarity (normalized dot product) with a set of synergies obtained from the healthy subjects: for each group of targets of the patient's datasets, the synergies extracted from all healthy subjects for that same group were averaged across subjects and used as reference.

This procedure was considered even if the estimated number of synergies for the patient was lower or higher than the healthy number (i.e. 4 muscle synergies).

6.7.3.1 Quantification of post-stroke modifications on the synergies structure and number for different movement conditions

The contribution of each synergy to the original EMG data was quantified using a "modified-VAF" (modified version of the Variance Accounted For), i.e. the fraction of the integral of the data reconstructed by that synergy over the integral of the original data (see Equation 6.3).

$$v_n = modified\_VAF_{Sn} = \frac{\sum_{m=1}^{M}\sum_{t=1}^{T}(data_{reconstructed})}{\sum_{m=1}^{M}\sum_{t=1}^{T}(data_{original})} = \frac{\sum_{m=1}^{M}\sum_{t=1}^{T}(H_{Sn} \times W_{Sn})}{\sum_{m=1}^{M}\sum_{t=1}^{T}(data_{original})} \tag{6.3}$$

where S_n is the synergy n, M is the number of muscles, T is the number of time points of the original EMG signals (matrix $data_original$), H_{Sn}) and W_{Sn}) are the time coefficients and the muscle weight coefficients vectors of S_n, respectively; n is the synergy number (1,2,3 or 4).

To compare the contribution of each extracted synergy to the patient's EMG signals with the contribution of the corresponding synergy to the healthy subjects' signals, this measure was obtained for all subjects of both groups and a metric of similarity was defined as presented in Equation 6.4. This metric ($v_{nsimilarity}$) represents the absolute similarity between the contribution of the synergy n for the patient ($v_{npatient}$) and for healthy subjects ($v_{nhealthy}$) and is inherently dependent on the number of synergies[12]. It was computed between the patient and each healthy subject, and averaged across healthy subjects, for every patient's synergy matched with one of the 4 healthy synergies.

$$v_{nsimilarity} = 1 - |v_{nhealthy} - v_{npatient}| \tag{6.4}$$

To compare the structure of each synergy extracted for the patient with the structure of the corresponding synergy extracted for healthy subjects, the Pearson's correlation coefficient (c_n) was used as measure of structure similarity. It was also computed between the patient and each healthy subject, and averaged across subjects, for every patient's synergy matched with one of the 4 healthy synergies.

These measures were obtained for all the EMG datasets (group 1 to 4, forward and backward movements), to verify the modifications on the muscle synergies following stroke for different movement conditions.

[12] For example, if 5 synergies are necessary to account for the patient's $data_{original}$ variability, then, the $modified_{VAF}$ of the patient's 4 synergies corresponding to the 4 healthy synergies will be lower than for healthy subjects, because part of the $data_{original}$ results from the contribution of the 5^{th} synergy.

6.7.4 Estimation of Motoneural Activity in the Spinal Cord

The patients motoneural activity in the C2 to T1 segments of the spinal cord (the reported location for the upper limb innervation (Kandel et al., 2000; Kendall et al., 1993)) was estimated by a weighted summation of the EMGs of the respective innervated muscles (see Table 6.4 in Section 6.6.5). This was done for the 4 groups of targets in both directions of the movement, using the pre-processed, resampled EMGs.

The resulting spinal maps were plotted using the MatLab function *contour*, as explained in Section 6.6.5.

6.7.4.1 Quantification of post-stroke modifications on the shape and magnitude of the spinal maps for different movement conditions

To compare the spinal maps of the patient with the healthy ones, and verify the post-stroke modifications for different movement conditions, the same measures used with the healthy group were adopted: correlation and covariance between the subjects' spinal maps (read the explanation in Section 6.6.5.2).

6.8 The Neurobiomechanical State and Motor Performance of Stroke patients during robot-aided rehabilitation

To assess the progress of the patient neuromuscular state (throughout the treatment) and compare it with the respective evolution of the motor performance, in a more concise way, the two measures of modifications induced by stroke in muscle synergies, were combined in one metric (see Equation 6.5). Basically, for each dataset (each group of targets), the measures of similarity (with healthy persons) in number (v_n) and structure (c_n) of each synergy n (as defined in Section 6.7.3.1) were summed and divided by n (the number of healthy synergies, i.e. 4). This was possible to do because v_n and c_n are in the same order of magnitude (absolute values range from 0 to 1) and, thus, the minimum possible value for their average is -0.5 [13] (complete dissimilarity with the healthy state) and the maximum is 1 (complete similarity with the healthy state).

$$metric_{synergies} = \frac{1}{n}.avg(c_1, v_1) + ... + \frac{1}{n}.avg(c_n, v_n) \tag{6.5}$$

[13] The minimum value occurs with a correlation of -1 and a modified-VAF of 0, being equal to (-1+0)/2=-0.5
Note that it is an assymptote of the metric, because the minimum of the modified-VAF, zero, is never reached (i.e., zero is an assymptote of the modified-VAF), otherwise the respective synergy would not exist.

It was not possible to join the two metrics related to spinal maps because of their very different ranges. Thus, the 2D-correlation and covariance were evaluated separately.

Concerning biomechanics, each kinematic metric was evaluated individually regarding its ability to capture changes in the motor performance of the patient.

The FMUE (Fugl-Meyer for the Upper Extremity) score obtained by the patient in each session of assessment was used to generally indicate his/her motor ability. All metrics were, then, compared with that clinical score, computing the correlation between the two variables.

Additionally, to verify if the improvement trend reflected by the metrics was similar to the improvement trend reported by the FMUE, the correlation between the kinematic metrics variation and the FMUE variation was calculated for the kinematic metrics more correlated with that clinical scale. This variation was taken from one assessment to the following one. The reasoning behind this is based on the estimation of motor improvement by the personalization algorithm: parameters of this algorithm (i.e. the included metrics) must have a clear trend of improvement to allow the convergence of the algorithm to a plateau.

Finally, bootstrap method was applied to measure the uncertainty of the estimated correlation between the metrics and FMUE. This was done due to the reduced number of data representing the stroke population available for the thesis work.

Bootstrapping is a resampling technique which repeatedly chooses random samples from the input data (in this case, the set of metric values and respective FMUE scores) with replacement, and estimates the parameter of interest (the correlation). From these calculation, the confidence interval for the parameter is estimated.

The method was used to resample the patients' data in 1000 different data sets, for which the correlation was estimated. Then, the histogram of the correlation across all bootstrap samples was obtained to verify the distribution of the correlation coefficient, and the standard deviation of the estimated correlation was computed.

The correlation with the FMUE scores and results of bootstrapping were used to validate metrics as good candidates for parameters of the personalization algorithm.

Chapter 7

Results

7.1 Analysis of the control group (healthy subjects)

7.1.1 Movements' outliers

For each subject and each target, from the first to the last repetition, the movement duration tends to decrease; this decrease is higher from the first to the second repetition (-1.8s±6.0s, average across subjects and targets) than between the other repetitions (-0.18±1.9s, from the 2^{nd} to the $3^{r}d$ repetition, -0.53±1.5s, from the 3^{rd} to the 4^{th} repetition). This seems to indicate that, during repetition 1, the subjects are adapting to the experiment. However, to define a set of control synergies (able to generally represent the healthy motor coordination), this learning phenomenon is undesirable and, thus, should not be included in the datasets. Figure 7.1 reports examples of trajectories performed by two healthy subjects towards target 1, where it is possible to see that, in case of H01, all the repetitions of that movement follow a similar path, while, in case of H02, the first repetition was executed with a very complex path and took much longer to reach the target (40s) than the other repetitions (between 2 and 3s).

7.1.2 Task execution – Kinematic Analysis of the Movement

The time taken by healthy subjects to execute the reaching movements is dependent on the target and, in general, they need more time in the forward than in the backward movement. The same can be observed with the length of the path they follow. This indicates that both temporal and spatial efficiency are influenced by the movement condition. Find in Appendix D the illustration of results obtained for the kinematic metrics in healthy subjects.

Concerning the easiness in reaching (mean velocity), it is more consistent across targets and directions, as well as the movement accuracy (mean distance to healthy path), apart from some exceptions like targets 12 and 13.

Moreover, the average path across subjects was found more curvilinear than the typically assumed straight path – see Figure 7.2.

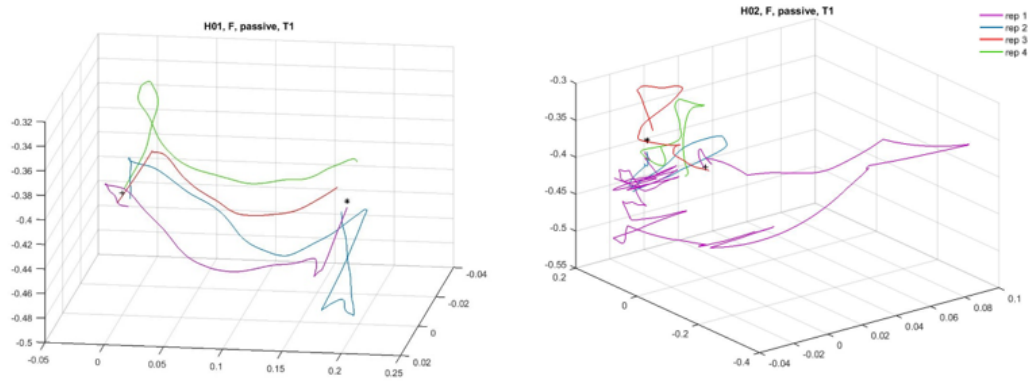

Figure 7.1: Trajectories of the forward movement executed by healthy subjects H01 (left) and H02 (right) towards target 1, during the repetitions 1 (purple), 2 (blue), 3 (red) and 4 (green) of that movement. The path of the 4 repetitions are similar in case of subject H01 (also with similar movement durations: 2s, 3s, 1s, and 1s, respectively), but are very different in case of subject H02 (with movement durations of 40s, 2s, 3s, and 2s, respectively). Note that the axes limits of the 3D plots were selected differently for H01 and H02 to show the best perspective to observe the movement path.

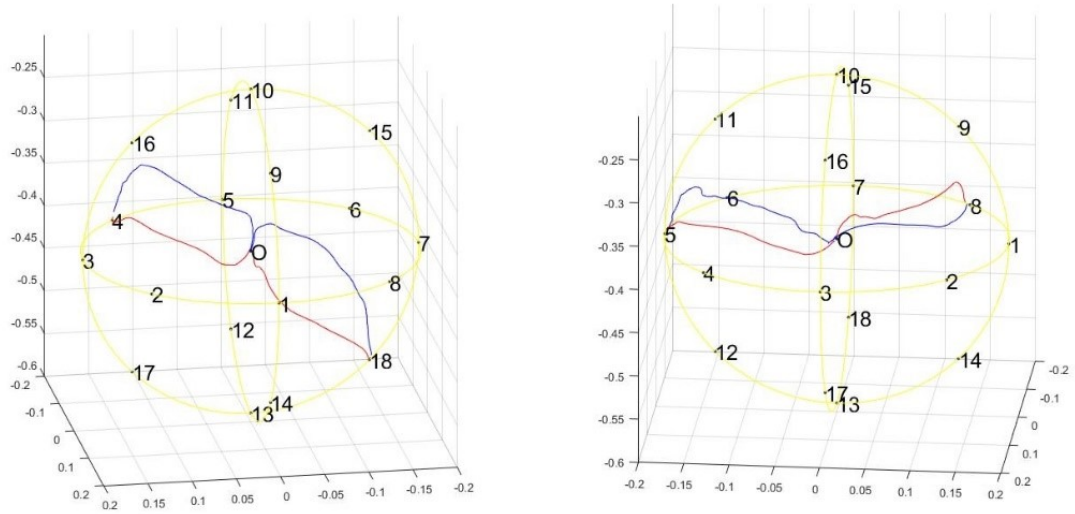

Figure 7.2: Example of the path followed by healthy subjects (in average) to reach targets 5, 8, 4 and 18, forward (in blue) and backward (in red). The sphere is represented in yellow and it is rotated so that a better perspective of the path is observed. ("O" identifies the center of the sphere)

Movement smoothness of the upper limb has been characterized by several different measures in the literature (Nordin et al., 2014). In this work, the Spectral Arc-Length (SAL) and the Ratio between the Mean Acceleration and the Peak Acceleration (RMP) were adopted. Surprisingly, the first (SAL) is more dependent on the target than the RMP. A higher SAL (i.e. a value closer to zero)

corresponds to an increased smoothness, thus, forward movements seem to be less smooth than backward movements, according to this measure. Indeed, a higher RMP also indicates increased smoothness and, generally, this metric is higher for backward movements, nevertheless it does not happen with all targets.

7.1.3 Muscular activity– Amplitude analysis

The averaged muscular activity across healthy subjects is presented in Figure 7.3, for each target and muscle, considering the forward and backward movements separately. The corresponding RMS values for each target is presented in Figure 7.4, for all muscles and averaged across muscles. The average RMS across muscles can be considered a measure of the muscular effort yielded by the subjects to execute the movement towards each target.

Note that x-axis of graphs in Figure 7.3 indicates a relative time (0% to 100%) because the signal of each subject was resampled by the minimum number of samples across subjects (see section 6.4.2 of Chapter Methods) to have signals of all subjects with the same length.

From the EMG envelopes (Figure 7.3), it is visible that muscle activity is more similar across targets and more monotone while executing the backward movement than while executing the forward movement.

In general, in forward direction, the most active muscles for each target show an increasing activity with the proximity to the target. Oppositely, although muscle activity is generally more monotone in backward direction, there is a peak of activity at the beginning of the movement for most targets and muscles, in this direction.

Additionally, activity of all muscles is generally higher during forward movements towards targets at the top of the sphere, like 1, 2, 8, 9, and 14. More specifically, the shoulder elevators (TRAPS, TRAPM) and abductors/rotators (DANT, DMED), as well as the LAT muscle (postural back muscle and rotator of the shoulder) are preferentially recruited in these upper movements. Moreover, the activity of Latissimus muscle and the anterior and medial heads of the Deltoid muscle is also increasing when reaching targets 13, 17, and 18, which are targets more distant from the subject. Another interesting result is the prevalent activity of the PEC (adductor and rotator of the shoulder/arm) in forward movements toward targets in the most-left side of the sphere (6, 7, 8).

Concerning the signals amplitude, no other relevant pattern seems to be highlighted. However, a more objective information can be taken from the RMS values, specially from the average values across muscles (a general representation of the muscular effort yielded by the subjects to execute the movement for each target – in black, Figure 7.4): a patterned variation of the RMS occurs across targets in forward movements – from the bottom to the top of the sphere, as well as from near to distant targets, the RMS value tends to increase.

As expected from the EMG envelopes, in backward movements the RMS does not reveal any particular trend.

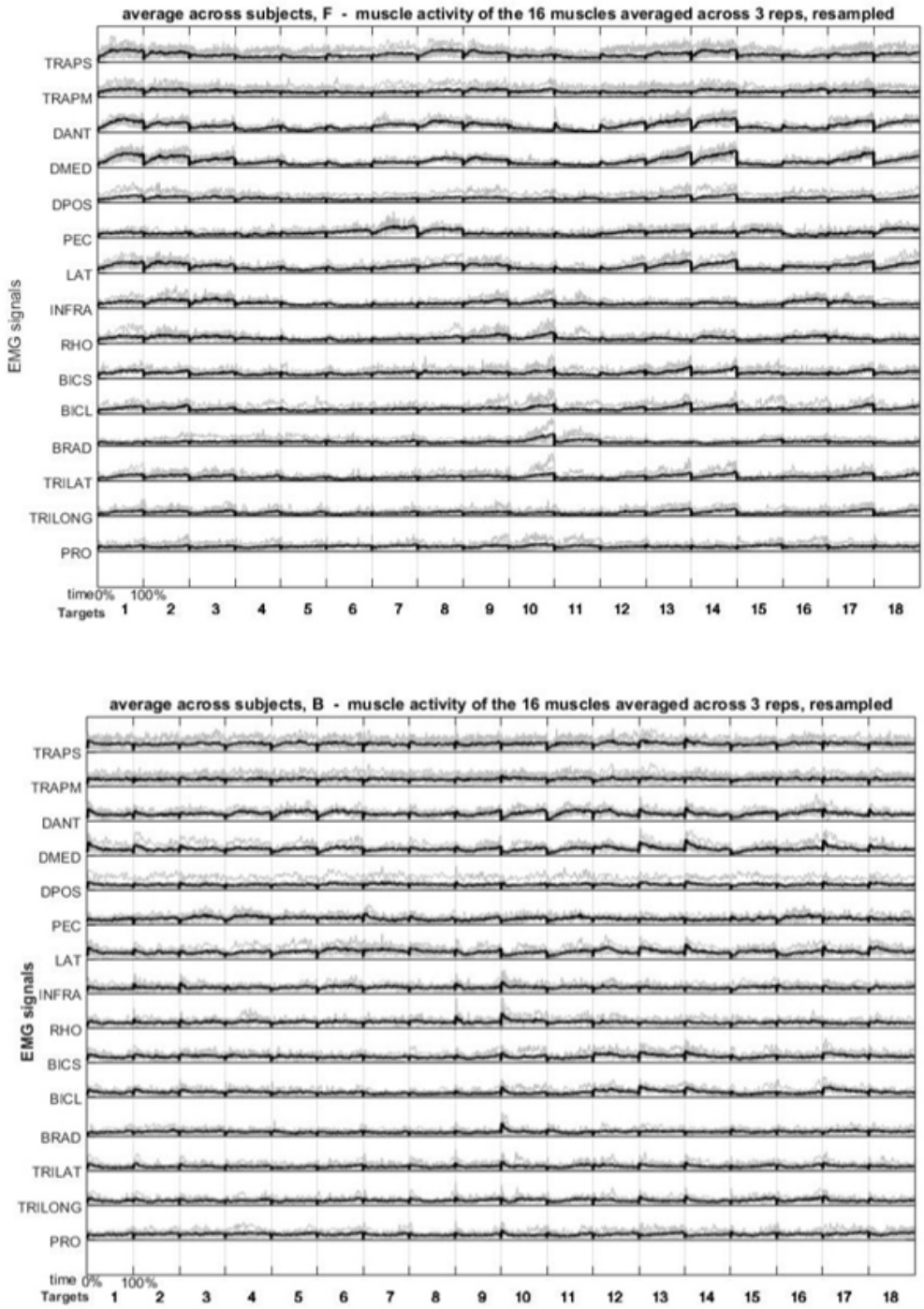

Figure 7.3: EMG envelopes averaged across healthy subjects (in black) while reaching targets 1 to 18, in forward direction (upper graph) and backward direction (lower graph). The envelopes for each subject are represented in grey. The y-axis of each EMG indicates the normalized amplitude of the signal (so, from 0 to 1). In the x-axis, the relative movement time (0% to 100% - beginning to end) is indicated for each movement (i.e. for each target), and the target corresponding to the movement is also indicated (1 to 18).

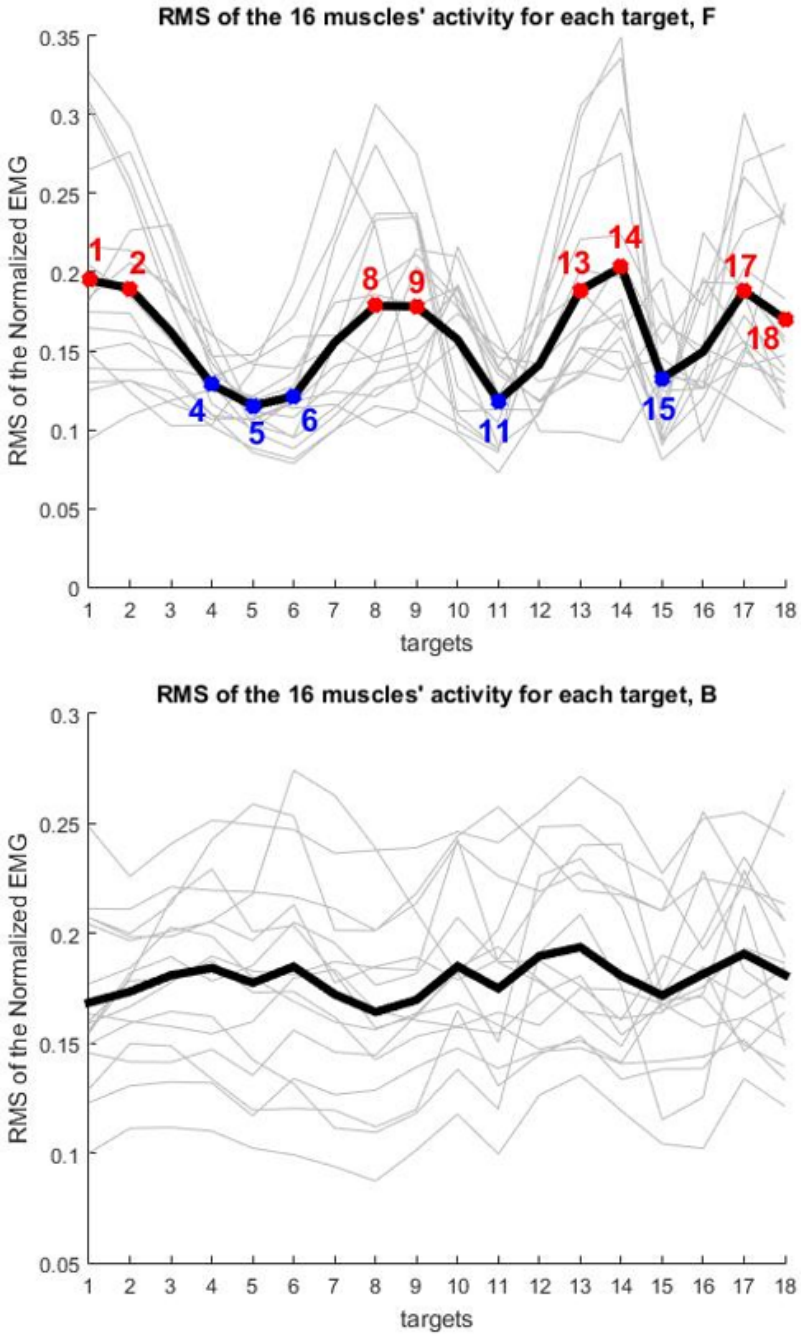

Figure 7.4: Averaged (across subjects) RMS values of the EMG envelope of each muscle (in grey) and averaged across muscles (in black) – global RMS, for targets 1 to 18, in forward (left) and backward direction (right). Given the patterned variation of the RMS across targets, mainly in forward direction, the targets associated to higher RMS values are highlighted in red, and the ones associated to lower RMS values are marked in blue.

7.1.4 Muscle coordination – Extraction of muscle synergies

7.1.4.1 Four Muscle Synergies explain Movements towards/backwards Different Targets

Using a searching procedure to estimate the correct number of synergies explaining the informative variance of each dataset, 4 synergies were found to account for, at least, 95% of the variability of any movement (forward/backward, target 1 to 18) – see Table 7.1. Exceptionally, for target 2, backwards, the average is slightly higher, 4.6 synergies. Nevertheless, in datasets containing all the targets, a higher number of synergies (approximately 6) is necessary to account for the variability included in such data. This last result is a preliminary indication that, although a movement in any condition can be explained by 4 modules of muscle coordination (4 muscle synergies), their structure seems to differ across targets, being shared (or very similar) between some targets.

Note that synergies were extracted for each healthy subject, from 3 to 7, and the number of synergies was estimated for each subject independently (using the $VAF \geq 0.95$ criterion, as explained in section 6.6.4.2). Therefore, results in Table 7.1 are the average (and standard deviation) across healthy subjects. From the low standard deviation values, these results can be considered a good representation of the behavior of the healthy group.

Table 7.1: Estimated number of synergies for datasets D_1 to D_{38}: average $\pm$ standard-deviation, across healthy subjects. Estimation criterion: $VAF \geq 0.95$. T_n stands for target n; F stands for forward movement; B stands for backward movement.

	[All targets]	T1	T2	T3	T4	T5	T6
F	5.5 ± 0.9	3.3 ± 0.5	3.6 ± 0.7	3.9 ± 0.8	4.4 ± 0.7	4.3 ± 0.7	4.1 ± 0.8
B	5.5 ± 1.3	4.3 ± 1.0	4.6 ± 1.1	4.4 ± 0.7	4.0 ± 1.1	3.9 ± 0.8	3.9 ± 0.8

	T7	T8	T9	T10	T11	T12
F	3.8 ± 1.0	3.5 ± 0.5	3.5 ± 0.8	4.3 ± 1.4	4.4 ± 1.1	4.1 ± 0.6
B	4.0 ± 0.5	4.3 ± 1.0	4.5 ± 1.1	4.1 ± 0.8	4.3 ± 0.9	3.5 ± 0.8

	T13	T14	T15	T16	T17	T18
F	3.8 ± 0.9	3.5 ± 0.5	4.4 ± 0.9	4.3 ± 0.9	3.8 ± 0.7	3.9 ± 1.0
B	3.9 ± 0.8	4.1 ± 1.0	4.1 ± 0.8	4.0 ± 0.8	4.1 ± 0.8	4.3 ± 0.9

Although the number of synergies is not Gaussian distributed for any movement condition (p<$1e-7$, One-sample Kolmogorov-Smirnov test), we cannot reject the hypothesis of variance homogeneity ($p = 0.103$, Levene's test). Therefore, distributions of the number of synergies were assessed by the 2-Way ANOVA and results were confirmed by the Friedman test with 2 factors. See results in Table 7.2.

In fact, the two tests agree that we cannot reject the null hypothesis, both for targets and directions, and, thus, differences on the number of synergies across movement conditions are not significant (p>0.05). Moreover, we cannot reject the hypothesis that targets and directions are independent factors (i.e. there is no significant interaction between them, $p = 0.102$). This means that, for example, we can consider forward or backward movements and the above-mentioned result is the same (targets do not affect the number of synergies significantly), and vice-versa.

This confirms that 4 synergies explain well any individual condition of the movement (i.e. one target, one direction), so it was decided to use the set of 4 synergies extracted for each dataset in the next steps of the analysis.

Table 7.2: Statistical difference across movement conditions – results of the 2-Way ANOVA and Friedman test.

direction	**p-value, ANOVA2**	0.050
	p-value, Friedman	0.062
target	**p-value, ANOVA2**	0.887
	p-value, Friedman	0.894
factors interaction	**p-value, ANOVA2**	0.102

7.1.4.2 Muscle Synergies Structure

The Reference Synergies

As explained in Section 6.6.4.4 of Chapter Methods, muscle synergies extracted from all datasets of all subjects were ordered by their vector of weigh coefficients, maximizing their similarity with a set of reference synergies obtained with dataset D1. The weights profile of these synergies is shown in Figure 7.5.

The choice to use as reference the set of 4 synergies extracted from dataset D_1 instead of 6 was done in accordance with the results presented in the previous section (4 synergies explain a movement of any individual condition) and considering that D_1 contains the variability of all the other datasets. This means that, although 4 synergies do not explain all the variability of D_1, they represent the shared organization across all conditions to be compared..

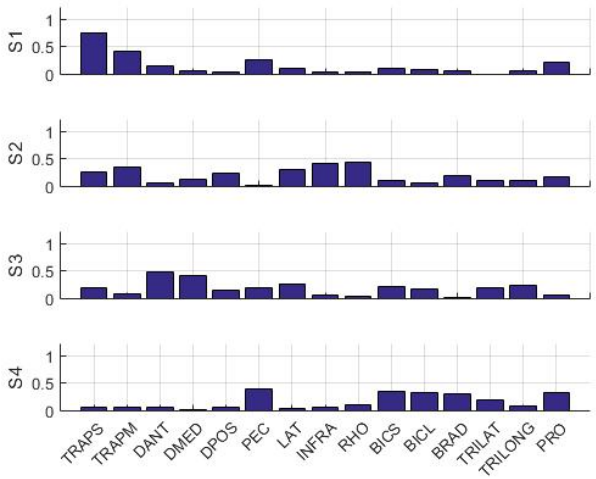

Figure 7.5: Structure of the reference synergies used to order the synergies extracted from all subjects. Each bar represents the weight coefficient of a muscle. S1, S2, S3 and S4 denote synergy 1, 2, 3 and 4, respectively. In the x-axis, the name of the muscles is indicated: TRAPS – trapezius superior; TRAPM – trapezius medialis; DANT – deltoid anterior; DMED – deltoid medialis; DPOS – deltoid posterior; PEC – pectoralis major; LAT – latissimus dorsi; INFRA – infraspinatus; RHO – rhomboid; BICS –bicep short head; BICL – bicep long head; BRA – brachialis; BRAD – brachioradialis; TRILAT – triceps lateralis; TRILONG – triceps long head; PRO – pronator.

Muscles Synergies Structure by Target and Direction

The weights profile of muscle synergies is exemplified in Figure 7.6 using the results regarding Target 1, 5, 10 and 13, forward and backward movements. These targets are reported as example, because they are corners of the main directions (close-distant, and up-down, with respect to the subject) highlighted by results of Section 7.1.3 and of the next sections.

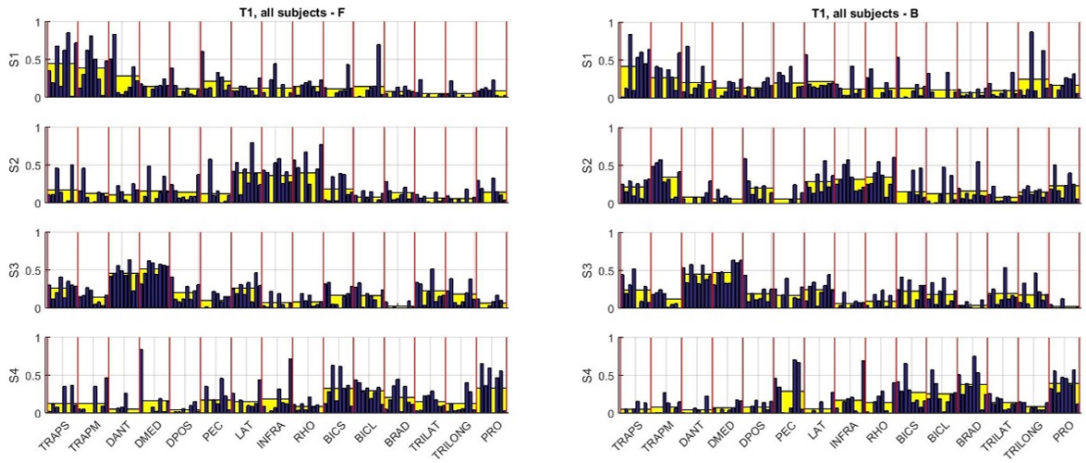

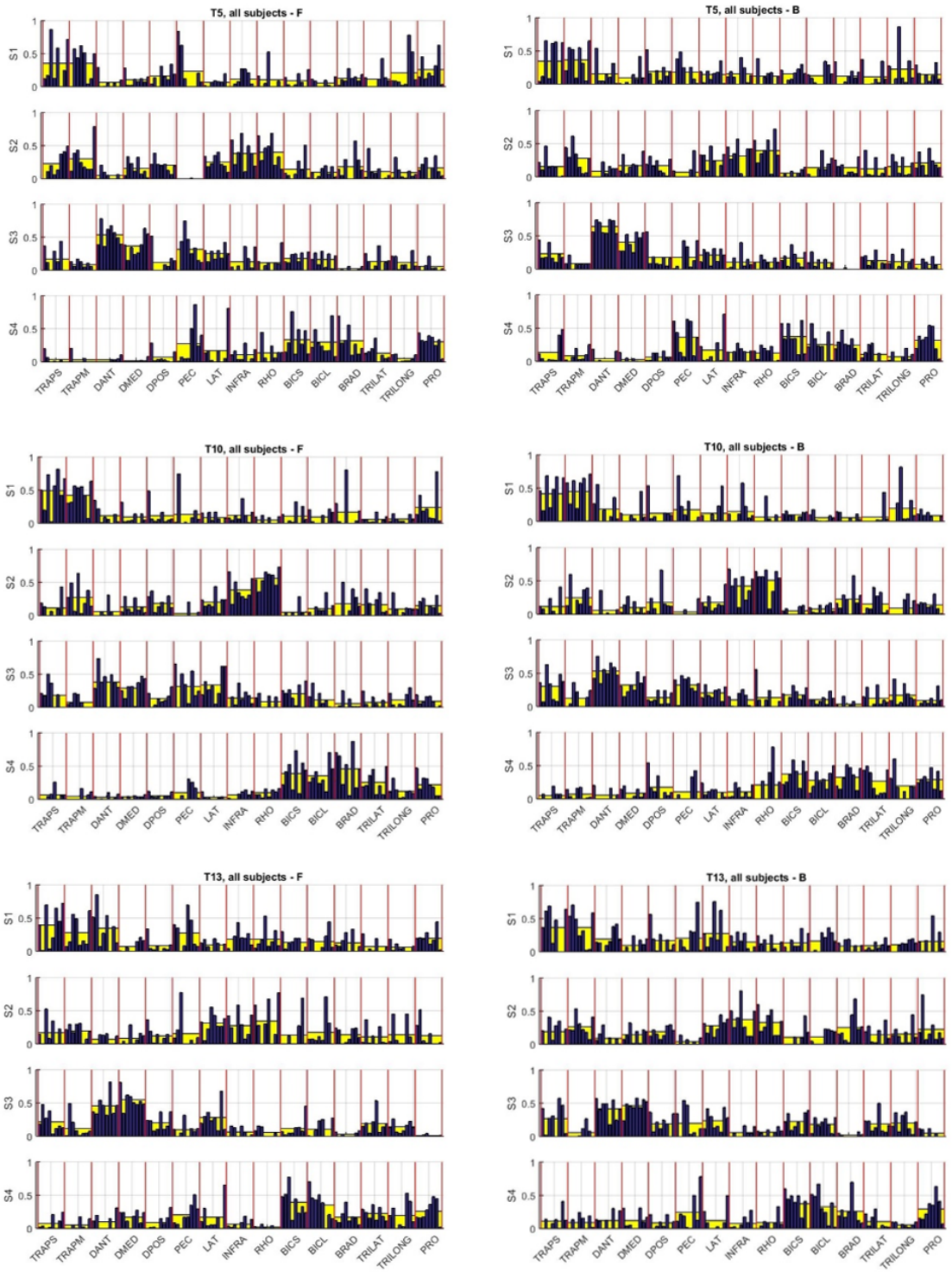

Figure 7.6: Weight coefficients of synergies extracted for forward (left) and backward (right) movements, for targets 1, 5, 10 and 13, respectively from the top to the bottom of the figure. Each blue bar represents the weight coefficient of one muscle, for one of the 8 healthy subjects. Thus, 8 bars are shown for each muscle. The average value across subjects is represented in yellow for each weight coefficient.

Synergies underlying Forward and Backward Movements have a Similar Structure, but it is Modified from Target to target

For all muscles of all synergies, the normality test showed that coefficients are not Gaussian distributed ($p<0.05$). The Levene's test revealed that, for a major part of the weight coefficients of all synergies (38 in 96 – see Figure 7.7), the distributions are not characterized by equal variance. Thus, Friedman test with 2 factors should be used, at least for those cases, to determine if the weight coefficients are significantly different across movement conditions. However, only ANOVA assesses the interaction between factors. Thus, both tests were performed and compared.

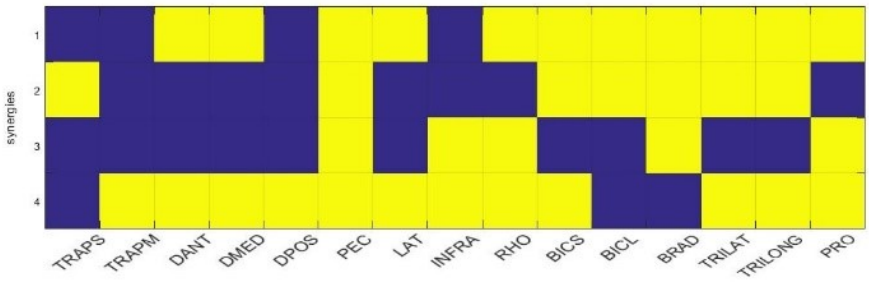

Figure 7.7: Illustration of the results obtained in Levene's test: each cell indicates the result of the test for each weight coefficient (representing one muscle, in the x-axis) of each synergy (1 to 4, indicated in the y-axis). Yellow cells correspond to distributions of weight coefficient values with unequal variance. Blue cells correspond to distributions of weight coefficient values characterized by equal variance.

Results of the 2-Way ANOVA and Friedman tests agreed for all muscle weights. In Figures 7.8 and 7.9, the weight coefficients significantly different ($p<0.05$) are shown for the 2 factors, targets and directions. More specifically, results of the multi-comparison across 18 targets are detailed inside the cell concerning each weight coefficient.

	TRAPS	TRAPM	DANT	DMED	DPOS	PEC	LAT	INFRA	RHO	BICS	BICL	BRAD	TRILAT	TRILONG	PRO
S1															
S2															
S3															
S4															

Figure 7.8: Results of the statistical test to determine the effects of movement direction on the synergies structure. Muscle weight coefficients (columns) of synergies S1 to S4 (rows) which significantly differ ($p<0.05$) between forward and backward movements are highlighted in yellow.

	TRAPS	TRAPM	DANT	DMED	DPOS	PEC	LAT	INFRA	RHO	BICS	BICL	BRAD	TRILAT	TRILONG	PRO
S1				T5-T17; T10-T17; T6-T17; T11-T17; T15-T17; T16-T17						T6-T14					
S2							T1-T10; T10-T6; T10-T8; T10-T16; T10-T18; T12-T18	T3-T13; T3-T14; T3-T18; T13-T2; T13-T16	T10-T13; T10-T6; T10-T12; T10-T15; T10-T18		T3-T13; T13-T2; T13-T4; T13-T14				
S3			T5-T3	T1-T10; T1-T6; T1-T11; T1-T15; T7-T14; T10-T13; T10-T2; T10-T14; T13-T15; T2-T15; T6-T14; T11-T14; T14-T15		T1-T10; T3-T10; T10-T14			T3-T11; T8-T11; T11-T14; T11-T17						T1-T4; T13-T4; T4-T9; T4-T14
S4													T3-T10		

Figure 7.9: Results of the statistical test to determine the effects of the target on the synergies structure. Muscle weight coefficients (columns) of synergies S1 to S4 (rows) which significantly differ ($p<0.05$) across targets are highlighted in yellow. Results of the multi-comparison are specified for each weight coefficient, indicating the pairs of targets which have a significantly different weight coefficient.

Results in Figure 7.8 indicate that synergies' structure is not identical, in case of S1, S2 and S3, but it is very similar, because only one weight coefficient is significantly different between forward and backward movements. Therefore, the movement direction seems to have almost no effects on the profile of muscle weights.

Oppositely, results in Figure 7.9 demonstrate that synergies structure is considerably affected by the target location. Indeed, several weight coefficients (most of them for synergies 1 to 3) are significantly different for a large number of pairs of targets.Moreover, such differences seem to agree with results of Section 7.1.3, occurring in a patterned way in the up-down and close-distant axes. In fact, Figure 7.9 reveals 4 groups of targets for which there are no differences for any weight coefficient between targets within a same group, but, oppositely, there are significantly different weight coefficients between targets of different groups: {T1,T2,T8,T9,T14}; {T4,T5,T6,T11,T12}; {T7,T18,T13,T17}; and {T3,T16,T10,T15}. Exceptionally, in the last group, target 10 is different from one target of its group, but only in four weight coefficients (in red, in Figure 7.9).

Inter-subject similarity of the synergies' structure is affected by the movement condition (target, direction)

The average DOT (normalized dot product) across pairs of subjects is presented for all synergies, targets and directions in Figure 7.10 They reflect the inter-subject variability in muscle coordination in healthy subjects to perform a same task. As one can observe in the figure, the similarity across subjects is lower for S1 and S4.

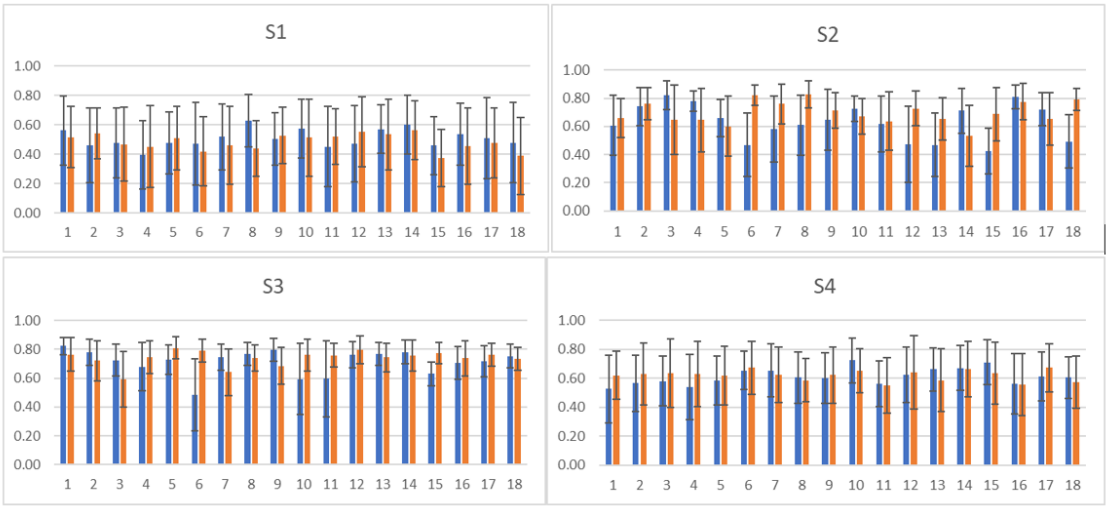

Figure 7.10: Normalized dot product (DOT) between the synergies' structure of pairs of subjects, for synergy 1 (S1), 2 (S2), 3 (S3) and 4 (S4), for each movement condition. The x-axis indicates the target (1 to 18) and the y-axis indicates the average DOT. Blue and orange bars regard forward and backward movements, respectively.

Distributions of DOT values are not Gaussian ($p<1e-7$, One-sample Kolmogorov-Smirnov test), and do not have equal variances ($p<1e-6$, Levene's test). As with weight coefficients, both ANOVA and Friedman tests were performed and compared. Table 7.3 presents the resulting p-values.

Table 7.3: Results of the statistical test to determine the effects of the movement condition on the similarity of the synergies' structure across subjects.

		S1	**S2**	**S3**	**S4**
direction	p-value Friedman	0.153	9.03 e -12	2.44 e -06	0.244
	p-value ANOVA2	0.083	7.39 e -19	1.27 e -11	0.503
Target	p-value Friedman	5.88 e -12	4.11 e -28	7.93 e -13	9.19 e -07
	p-value ANOVA2	2.31 e -1	4.46 e -3	3.30 e -24	1.10 e -07
factors* interaction	p-value ANOVA2	0.190	1.66 e -42	1.94 e -33	0.703

The similarity of S1 across subjects, as well as of S4, is not affected by the direction, but it is significantly affected ($p<0.05$) by the target. The similarity of S2 across subjects, as well as of S3, is significantly affected ($p<0.05$) by both the target and the direction. However, the very low p-value, for S2 and S3, in respect to the interaction between targets and directions indicates that targets and directions are not independent, i.e., the effect of the target on the inter-subject similarity differs if the forward or the backward direction is considered. This means the results of a multi-comparison could not be fairly interpreted and, thus, this step was not considered here.

7.1.4.3 Four Muscle Synergies explain Movements Grouped by Target

The number of synergies estimated for each group of targets is presented in Table 7.4 synergies explain at least 95% of the variability in any of the 4 groups of movements. Given the preservation of the number of synergies when movements are strategically grouped as when they are individually factorized, this result indicates that muscle coordination is similar enough between targets within a same group, supporting the use of these groups of targets to compare healthy subjects' with patients' synergies.

Exceptionally, for group 1, backward direction, the average is slightly higher, 4.6. synergies. In fact, this group includes target 2 and the number of synergies estimated for this target, individually, was also higher (4.6), as reported in Section 7.1.4.1.

Table 7.4: Estimated number of synergies for Groups 1 to 4: average $\pm$ standard-deviation, across healthy subjects. Estimation criterion: VAF ≥ 0.95. G_n stands for group n; F stands for forward movement; B stands for backward movement.

	F	**B**
G1	3.6 ± 0.7	4.6 ± 1.1
G2	3.8 ± 1.0	3.9 ± 0.4
G3	3.9 ± 0.8	4.4 ± 0.7
G4	4.4 ± 0.7	4.4 ± 0.7

The 4 muscle synergies' structure for groups is shown in Figures 7.11 and 7.12., averaged across healthy subjects.

Forward and backward movements are explained by synergies with a very similar structure. However, S4 of group 4 loses, in backward, the contribution of the deltoid posterior highlighted in forward.

One can observe the most important muscles of the first 3 synergies are the same for all groups of targets, apart from slight differences in their coefficients (foreseen by the previous statistical tests): DANT and DMED, in S1; BICS, BICL, BRAD and PRO, in S2; LAT, INFRA and RHO, in S3. The last synergy (S4) is group-specific: TRAPS, TRAPM and DANT are the most important muscles, in group 1; PEC, in group 2; TRILAT and TRILONG (and DPOS, in forwards), in group 4. In particular, for group 3, S4 seems to include the coordinated work of trapezius fibers as in S4 of group 1, but with the contribution of more muscles (deltoid heads, and back muscles).

Note that, after ordering the synergies of all subjects and averaging them across subjects, the 4 synergies were reordered to be represented in figures 7.11 and 7.12 with the 3 most similar in the top, and s4 as last synergy. So, the order is not the same as in figure 7.6, for individual targets.

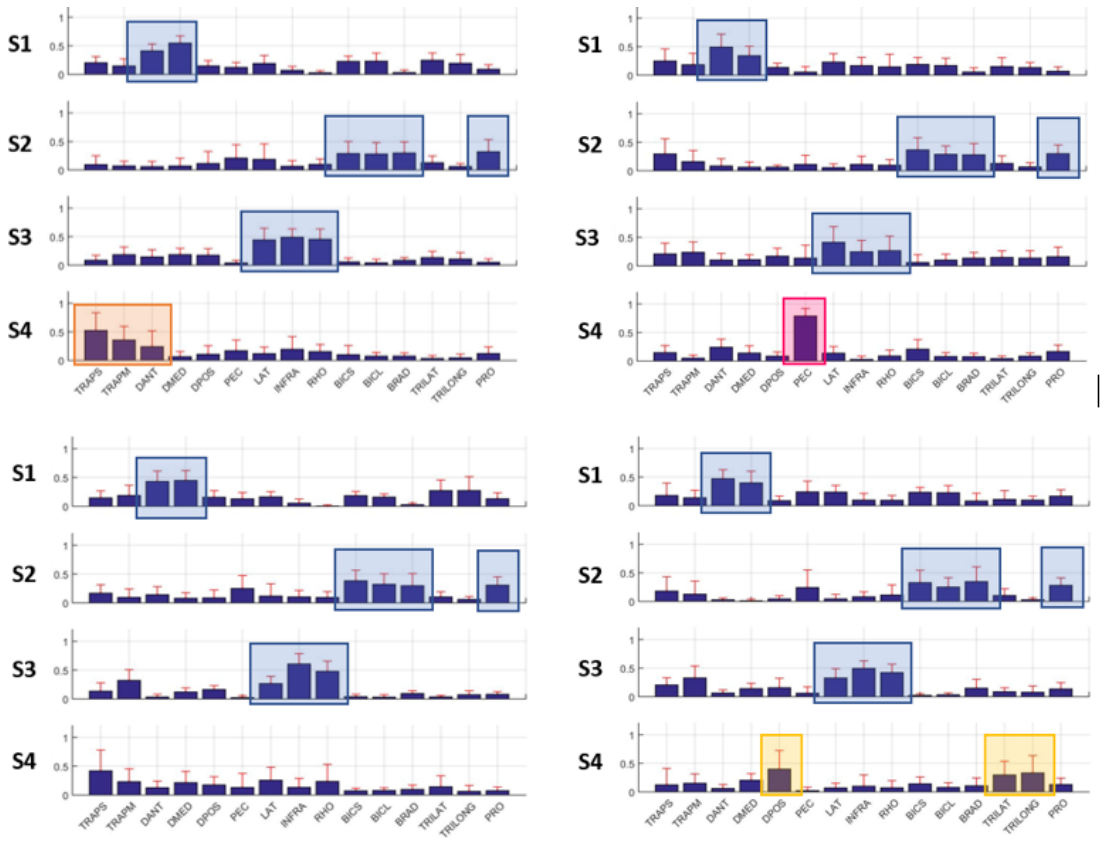

Figure 7.11: Structure of muscles synergies underlying the movements included in group 1 (top-left), 2 (top-right), 3 (bottom-left), and 4 (bottom-right), in forward direction. Weight coefficients are averaged across subjects (standard deviation is also indicated in red). The first three synergies have a similar profile across groups. The last synergy is group-specific (main group of muscles is highlighted in orange, pink and yellow for groups 1, 2 and 4 respectively). In S4 of group 3, a set of several muscles works together (trapezius, deltoid, and back muscles).

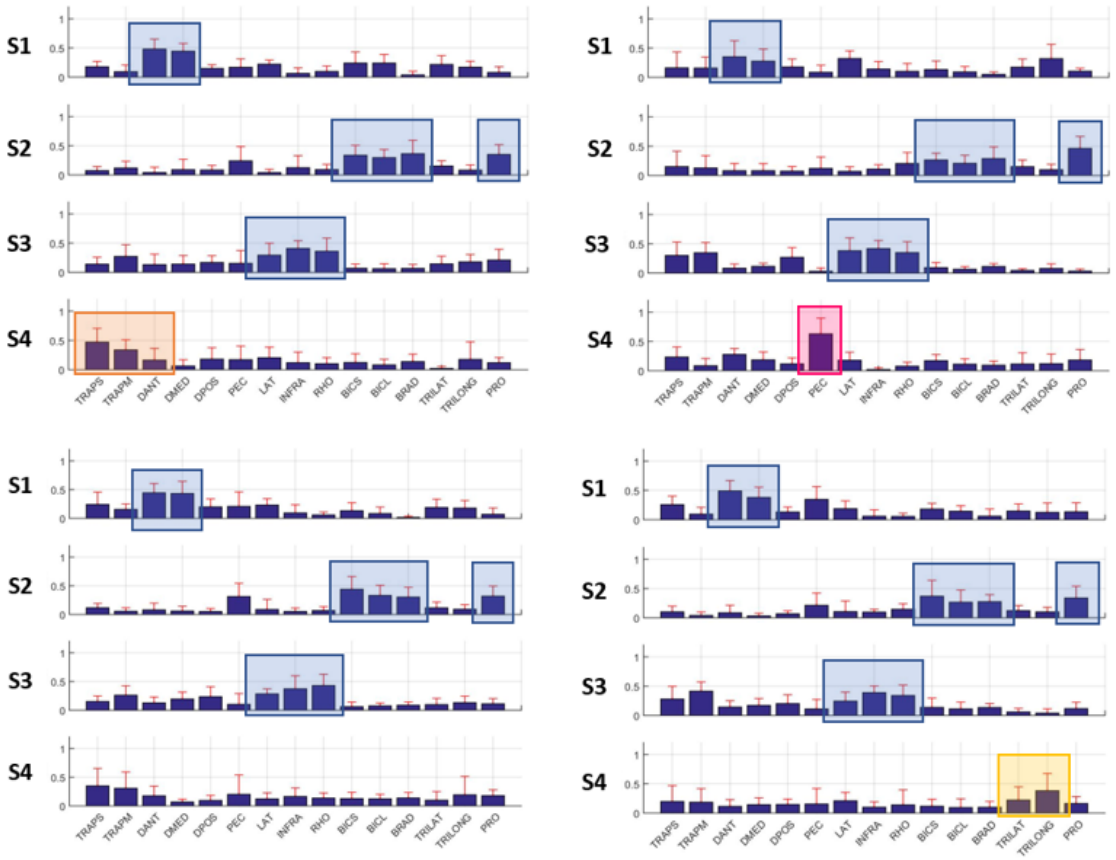

Figure 7.12: Structure of muscles synergies underlying the movements included in group 1 (top-left), 2 (top-right), 3 (bottom-left), and 4 (bottom-right), in backward direction. Weight coefficients are averaged across subjects (standard deviation is also indicated in red). The first three synergies have a similar profile across groups. The last synergy is group-specific (main group of muscles is highlighted in orange, pink and yellow for groups 1, 2 and 4 respectively). In S4 of group 3, a set of several muscles works together (trapezius, deltoid, and back muscles). In S4 of group 4, DPOS is not coordinatively recruited with triceps, as in forward.

7.1.5 Motoneural Activity in the Spinal Cord

Estimated activity in the spinal cord of healthy subjects, between segments C2 to T1 (the ones innervating the upper limb), is represented in Figure 7.13. In forward movements, one can observe how the distribution of this activity is organized along space and time, generally increasing in intensity as subjects go from reaching targets placed at the bottom of the sphere to reaching the ones at the top of the sphere. In the same axis (bottom-top), higher segments of the spinal cord tend to be more active than the lower ones, and the spinal activity increases, in general, from the beginning to the end of the movement.

In backward movements, the spatiotemporal distribution of the motoneural activity seems more regular across almost all targets, being the higher cervical segments more active. Oppositely to forward direction, this activity tends to be more intense in the beginning of the movements.

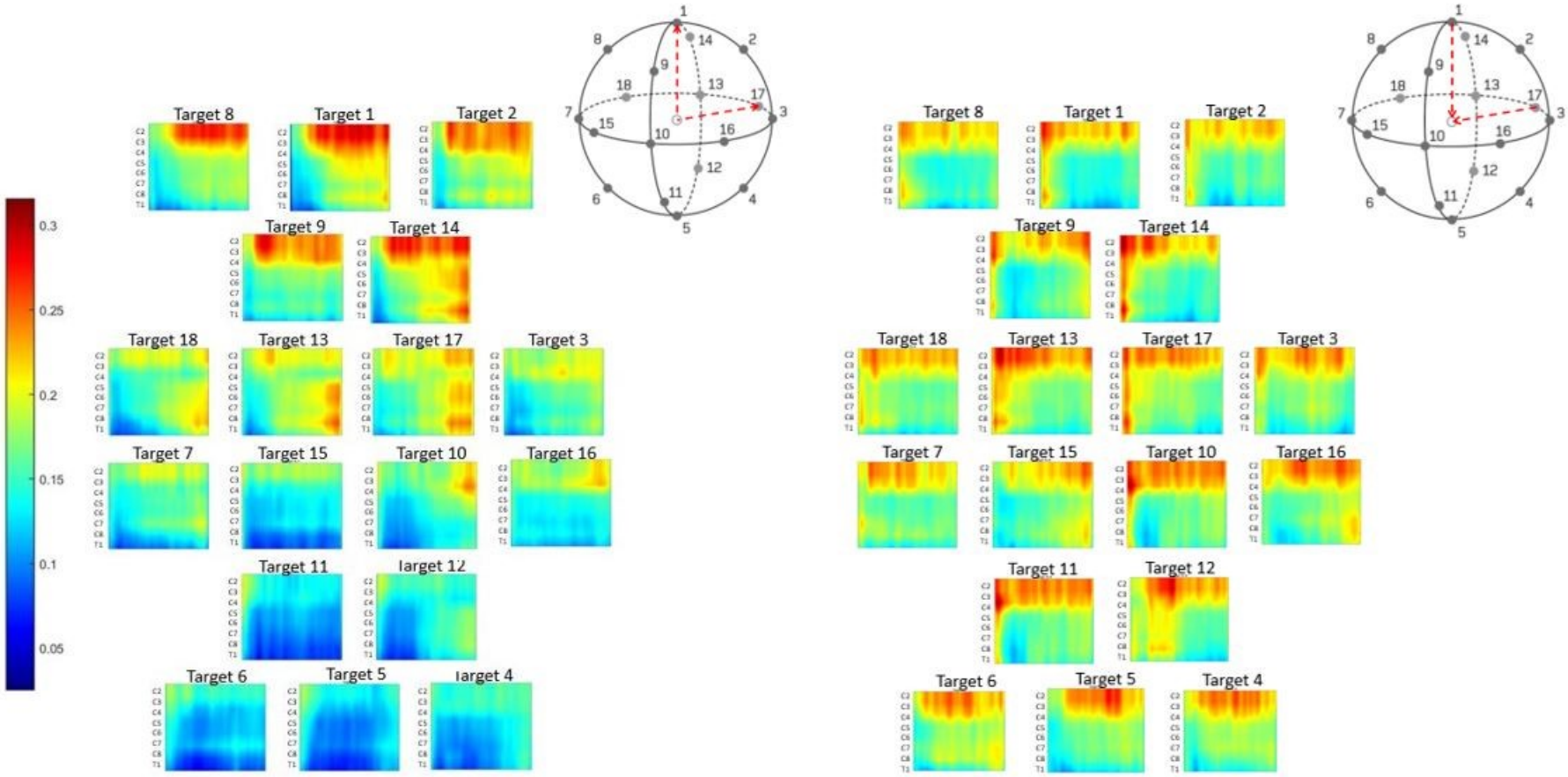

Figure 7.13: Spinal maps (averaged across healthy subjects) obtained for each movement condition: forward (left maps); backward (right maps); targets from 1 to 18. The spinal maps are ordered according to the spatial distribution of the respective targets in the sphere. The color map associated with the value of motoneural activity is presented in the colorbar on the left.

7.1.5.1 Inter-subject Similarity of the Spinal Maps is not affected by the target and movement direction

The 2D correlation coefficient (2-dimensional equivalent of the Pearson's correlation), *r*, between the spinal map averaged across subjects and the spinal map of each subject is presented, for each target and direction, is presented in Table 7.5. The inter-subject similarity of the spinal maps is not significantly affected by the target (p=0.62) nor by the movement direction (p=0.85).

Table 7.5: 2D-Correlation coefficient between the spinal map averaged across subjects and the spinal map of each subject.

	T1	T2	T3	T4	T5	T6
F	0.70 ± 0.20	0.56 ± 0.18	0.52 ± 0.22	0.46 ± 0.19	0.50 ± 0.17	0.47 ± 0.18
B	0.65 ± 0.25	0.49 ± 0.27	0.52 ± 0.24	0.47 ± 0.21	0.54 ± 0.15	0.43 ± 0.28

	T7	T8	T9	T10	T11	T12
F	0.46 ± 0.23	0.61 ± 0.15	0.64 ± 0.18	0.60 ± 0.21	0.62 ± 0.30	0.49 ± 0.26
B	0.45 ± 0.23	0.51 ± 0.18	0.57 ± 0.24	0.56 ± 0.31	0.63 ± 0.29	0.49 ± 0.28

	T13	T14	T15	T16	T17	T18
F	0.51 ± 0.29	0.65 ± 0.17	0.58 ± 0.29	0.59 ± 0.19	0.48 ± 0.27	0.60 ± 0.26
B	0.54 ± 0.24	0.68 ± 0.22	0.53 ± 0.30	0.53 ± 0.18	0.58 ± 0.25	0.54 ± 0.29

7.1.5.2 Estimated spinal cord activity as a linear function of the target distance from the top of the sphere

Both 2D-correlation and covariance (i.e. the similarity in shape and level of activity, respectively) of the spinal map related to each single target with the spinal map of Target 1 (the top of the sphere) linearly decrease with the distance of the target to the top of the sphere. This result was obtained in both movement directions and with both metrics of distance. However, the coefficient of determination (r) is higher for forward movements (Figure 7.14) than for backwards movements (Figure 7.15), and the best determined relations are between correlation and the z-axis distance (Figure 7.14, left), and between covariance and the Euclidean distance (Figure 7.14, right).

In the right-left and close-distant axes, the correlation and covariance are also linearly related with the distance of the target to Target 7 and 13, respectively, but the r is not as high as for the above-mentioned results in forward direction (and some results are not statistical significant) – see Appendix C.

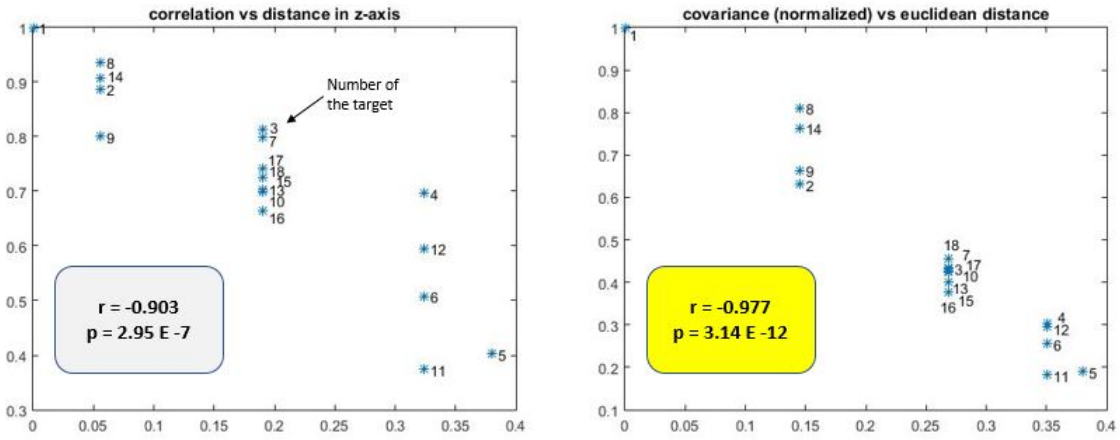

Figure 7.14: Relation between the 2D-correlation and the distance in the z-axis (left), and between covariance and the Euclidean distance (right), for forward movements. In the x-axis is the indicated the distance from the target to Target 1. In the y-axis is indicated the 2D-correlation/covariance between the spinal map for the target and the one for Target 1. r is the coefficient of determination, p is the statistical significance.

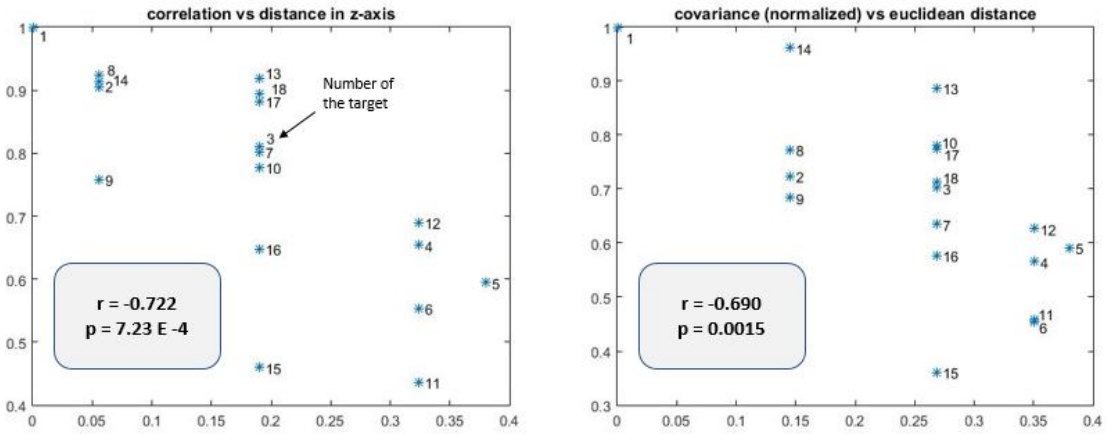

Figure 7.15: Relation between the 2D-correlation and the distance in the z-axis (left), and between covariance and the Euclidean distance (right), for backward movements. In the x-axis is the indicated the distance from the target to Target 1. In the y-axis is indicated the 2D-correlation/covariance between the spinal map for the target and the one for Target 1. r is the coefficient of determination, p is the statistical significance.

7.1.5.3 Spinal Maps for Movements Grouped by Targets

The healthy spinal maps obtained for group 1, 2, 3 and 4 and represented in Figure 7.16. These spinal maps were later used to compare with the ones of patients.

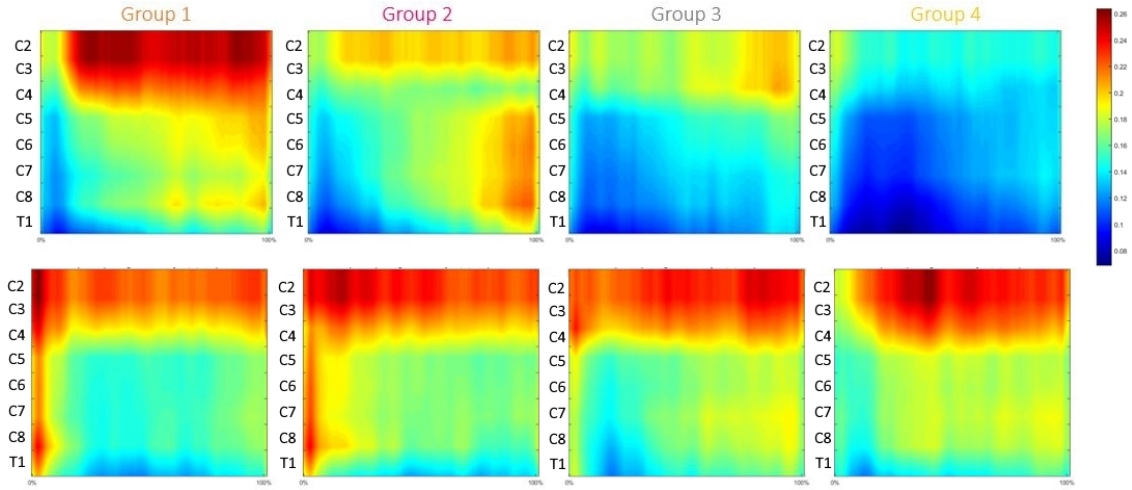

Figure 7.16: Spinal maps obtained after grouping the movements by target, in forward (top) and backward (bottom).

7.2 Analysis of the stroke group

7.2.1 Task execution – Kinematic Analysis of the Movement

Movement features were assessed for every condition (target and direction) by averaging the kinematic metrics' values across repetitions of the same movement. These results are described here for all targets and directions together, to analyze the global performance of the patient, and they are detailed for specific targets/directions when the patient behaves differently to execute movements in that condition. For a matter of concision, given the extension of the results, only global values (i.e. the average across targets and directions) for each metric are presented in the thesis (see Figures H.1 and H.2, in Appendix).

The most remarkable results were obtained when assessing accuracy (with the mean distance to the healthy path, MDH), smoothness (both with the Spectral Arc-Length, SAL, and the Ratio of Mean Acceleration with Peak Acceleration, RMP) and task accomplishment (using the Assisted-Distance).

Patients ALEx-HUG-001, 003 and 004 were able to improve these movement features from the beginning of the experiments until 1 month after the end of the treatment, demonstrating, not only that therapy helped to increase the motor performance of these patients in different aspects (at least in reaching movements), but patients also retained the abilities re-learned.

Patient ALEx-HUG-006 spontaneously recovered these skills (although in a very short range) from assessment 1 to assessment 2. But, when assessed at the end of the treatment (A3), she was assisted by the exoskeleton for several times (more than in A1 and A2) and her kinematic results had worsened in respect to the ones obtained in A1. It must not be forgotten that she was not feeling completely well, during A3, and sometimes the acquisitions were stopped and restarted.

Movements towards targets in the left side of the sphere or more distant from the body, like target 18, 13 and 17, usually do not follow the same trend of improvement as the others. See the example of patient ALEx-HUG-001, in Figure 7.17, with these targets, for which the absolute values of MDH and SAL are not systematically reducing, as with other targets.

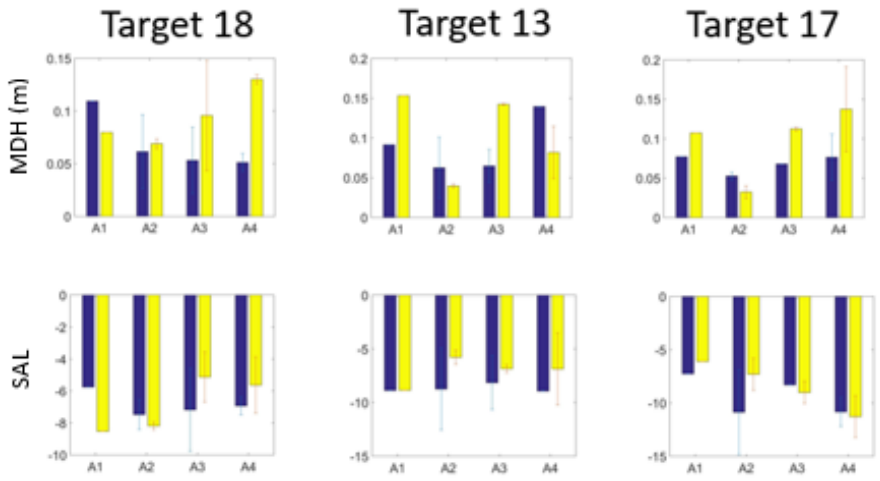

Figure 7.17: Example of results obtained by patient ALEx-HUG-001 in movements towards targets 18, 13 and 17, which do not follow the same trend of improvement as the other targets.

Patients' accuracy is also repeatedly lower in backward than forward movements, at any time of the experiments. This was somehow expected, since one could observe that, typically, patients pay more attention and try harder to execute well the forward movements. And, in addition, all patients have shown to execute backward movements more easily than forward ones, according to the results of mean velocity (slightly higher values in backwards). Thus, it is not the case of a reduced ability when executing backward movements, but more the consequence of a choice/preference. This result must, however, be considered because it influences the global measure of motor performance to be compared with the FMUE.

Patients ALEx-HUG-001, 003 and 004 were able to execute movements in a faster way in assessments 3 and 4 than in assessments 1 and 2 for all targets, demonstrating an increased easiness

in reaching movements after receiving the motor therapy. Oppositely, patient ALEx-HUG-006 could not improve this feature from the beginning to the end of the treatment, always moving more slowly than healthy subjects and the other patients.

Concerning efficiency, patient ALEx-HUG-003 improved both temporal and spatial features (there is a progressive decrease in the movement duration and path length), and her efficiency is consistent across targets. In fact, after the treatment, her mean velocity in reaching movements surpassed the average healthy one and, recalling that her smoothness also progressively increased, these results suggest that training with the exoskeleton had a benefic effect on the patient's motor skills. Also, patients 001 and 004 improved their temporal efficiency, but the path length did not decrease so much as patient 003 after the treatment. However, the behavior of patient 004 is more consistent across targets than patient 001: possibly, patient 001 needed to practice more the movements towards some of the targets in specific, to learn a shorter path.

Finally, the assisted-distance (i.e. the length of the path where the patient required robotic assistance) decreased over the experiments course (even with patient 006, from A1 to A2), supporting the fact that, over the rehabilitation, patients become more skilled in reaching movements and rely less on the assistance of the exoskeleton.

7.2.2 Muscle coordination – Muscle Synergies

The number of muscle synergies estimated for each patient is presented in Table 7.6. Globally, it increases from the beginning (A1) to the end of the experiments (A4) and the patients' motor ability also increases (see the FMUE, Fugl-Meyer for the Upper Extremity, in the table).

Remarkably, in assessment 2 (A2), patient ALEx-HUG-001 spontaneously recovered the 4 synergies for almost all groups of targets. However, her motor ability reported by the FMUE barely changed. In fact, despite the general increase of both FMUE and number of synergies, the trend of this number, during the experiment, is not consistent with the trend of the FMUE score. See other example, patient ALEx-HUG-003, which improved her motor ability from one assessment to the following one, but the number of synergies only increases from A2 to A3.

Interestingly, patient ALEx-HUG-004, which has received the personalized treatment, recovered the 4 muscle synergies for all groups at the third assessment, however, 1 month later (A4), the number of synergies was higher in respect to the healthy one (5 muscle synergies). This was not due to a simple fractionation of synergies (as reported in another study (Cheung et al., 2012)), but due to a new muscular reorganization (as with the chronic patients studied in (Roh et al., 2013)) – see the example with group 2, in Figure 7.18: S2, in assessment 3, was fractionated in S2 and S5, in assessment 4; the contribution of trapezius was considerably reduced, too; and the work of back muscles (LAT, INFRA, RHO) was split in 2 synergies (S3 and S4), being coordinated with the PEC in S3.

Table 7.6: Number of synergies estimated for each patient, group of targets and each assessment. A1, A2, A3 and A4 indicates the assessment session. F denotes forward movements, and B backward movements. G1, G2, G3 and G4 indicates the group of targets. The average number across groups and the FMUE score of the patient is also indicated for each assessment.

	ALEx-HUG-001					**ALEx-HUG-003**			
G1	2	3	3	3	F	2	2	3	3
	2	3	2	4	B	2	2	3	3
G2	3	3	3	4	F	3	2	2	3
	3	4	3	4	B	3	2	3	3
G3	2	4	3	4	F	2	2	3	3
	2	4	3	4	B	3	2	3	3
G4	3	3	3	4	F	2	2	4	3
	2	4	4	3	B	2	2	4	4
average	2.4	3.5	3.0	3.8		2.4	2.0	3.1	3.1
FMUE	47	49	56	55		17	34	46	52
	A1	A2	A3	A4		A1	A2	A3	A4

	ALEx-HUG-004					**ALEx-HUG-006**			
G1	3	–	5	5	F	3	3	3	–
	3	–	4	4	B	3	3	3	–
G2	3	–	4	5	F	3	4	3	–
	3	–	4	5	B	2	4	3	–
G3	3	–	4	5	F	3	3	3	–
	3	–	3	5	B	2	3	3	–
G4	3	–	4	4	F	3	2	2	–
	3	–	5	4	B	3	3	3	–
average	3.0	–	4.1	4.6		2.8	3.1	2.9	–
FMUE	17	–	30	34		24	27	29	–
	A1	A2	A3	A4		A1	A2	A3	A4

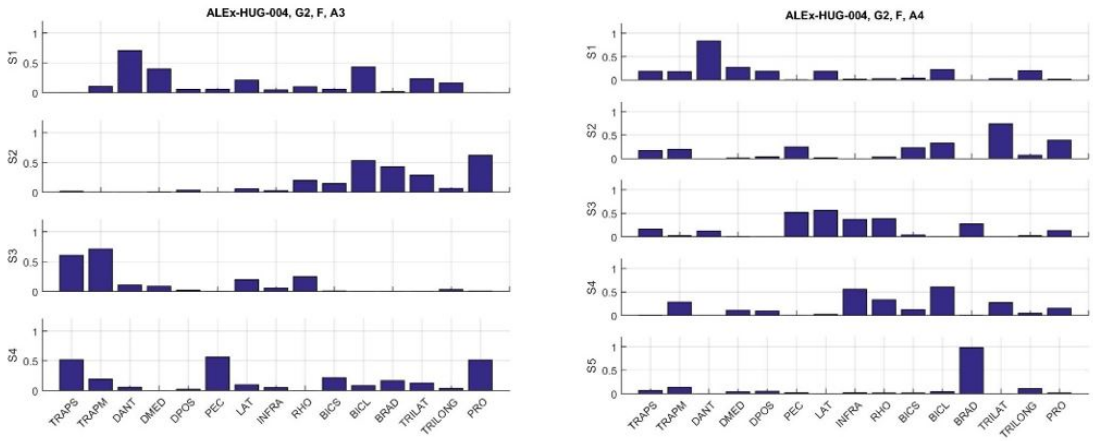

Figure 7.18: Modifications of the synergies structure from assessment 3 (left) to assessment 4 (right), in patient ALEx-HUG-004.

Concerning the similarity of the synergies' structure between the patients and the healthy subjects, the average correlation across the 4 synergies (the 4 most similar to the healthy) is shown for each assessment, group of targets and each patient in Figure E.1 of Appendix E. One can observe that, for all patients, the similarity with healthy is very low (less than 0.5) and, although it generally increases spontaneously from the first to the second assessment, this behavior is not the same for all groups of targets and patients after the treatment (A3 and A4):

- For patients 001 and 003, which received the conventional robotic treatment, the evolution of similarity varies: the correlation between synergies of 001 and healthy synergies generally reduces from A2 to A3, and increases in A4; with 003, it decreases from A2 to A3, but it does not increase in A4;
- For patient 004, which received the personalized treatment, apart from group 2, the similarity increases, but not as much as patient 001;
- The structure of all synergies of patient 006 (which received the standard therapy) is very different from the healthy ones (correlation is less than 0.2).
- Among groups of targets, the similarity with the healthy structure is very poor for group 2, for all patients (see the example with ALEx-HUG-003, in Figure 7.19).

Regarding the importance of each synergy for the patients' data (i.e. the contribution of the synergy to the integral of muscle activity, v_n), it is very similar to the importance of the equivalent synergy for the healthy data (see Appendix E, Figure E.2). For all patients and groups of targets, the $v_{nsimilarity}$ was higher than 0.7. Variations of this value do not have a clear trend with the patient motor improvement.

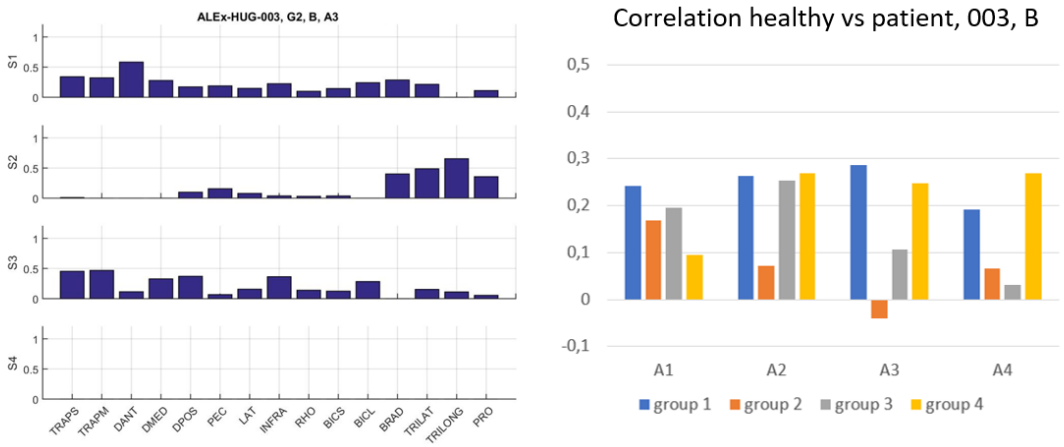

Figure 7.19: Synergies profile of ALEx-HUG-003 in assessment 3, obtained for group 2 (left) and the correlation between all synergies of these patient and the respective healthy ones (right), in backwards. Notice the modified structure of synergies concerning group 2 justifying the negative correlation with the healthy one.

7.2.3 Estimation of Motoneural Activity in the Spinal Cord

Oppositely to healthy subjects, stroke patients did not show any trend in the spatiotemporal distribution of motoneural activity across groups of targets, before the treatment (A1 and A2) and in the follow-up (A4) – See Figure F.1 as example. However, with patients ALEx-HUG-001 and 003, after the treatment (A3), their spinal maps resemble more the healthy ones: there is a progressive reduction of the magnitude of the motoneural activity from group 1 to group 4 (Figure 7.20).

Another interesting result is that motor therapy seems to promote the activity of upper cervical segments of the spinal cord (C2 to C4): in patients treated with the robotic-assisted therapy (001, 003 and 004), activity in these spinal segments increases from A1 to A3; the patient treated with the standard therapy (ALExHUG-006) shows a more intense activity in the lower segments (C7 to T1), even after the treatment (A3), but in A3 cervical segments are also active.

In the follow-up, however, the level of activity of patients 001, 003 and 004 was reduced. See the examples of evolution of spinal maps of patient ALEx-HUG-001 and 006 in Appendix F.

Correlation and covariance between patient and healthy spinal maps of the same group of targets increase from A1 to A3 for patients ALEx-HUG-001 and ALEx-HUG-003, and decrease in A4. For patient 004, the covariance and correlation do not change considerably from A1 to A3 and decrease in A4.

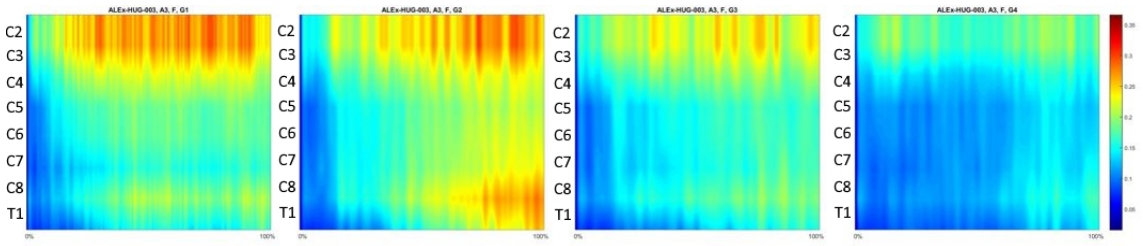

Figure 7.20: Spinal maps of patient Alex-HUG-003 in assessment 3, for groups 1 to 4 (from left to right), forwards. Notice the similar trend as the healthy spinal maps across groups.

Although these measures do not variate according to the trend of the patients' FMUE score (see Table 7.6), it must be highlighted that by the end of the treatment (A3), the spinal maps of these patients are highly correlated with the healthy ones (0.80 ± 0.08, ALEx-HUG-001; 0.85 ± 0.07, ALEx-HUG-003; 0.76 ± 0.11, ALEx-HUG-004).

However, they were not able to retain that similarity one month later, in A4 (0.16 ± 0.30, ALEx-HUG-001; 0.37 ± 0.14, ALEx-HUG-003; 0.12 ± 0.31, ALEx-HUG-004). See details for each group of targets in Appendix G.

As expected from the visual inspection of the spinal maps, the shape and magnitude of the spinal maps of patient 006, before the treatment (A1 and A2), are inversely correlated with the healthy ones, but in A3 the similarity increases due to the activity in the upper segments of the spinal cord. However, no information is available to verify if this patient retains, later, such increase in similarity with healthy.

7.3 The Neurobiomechanical State and Motor Performance of Stroke patients during robot-aided rehabilitation

The neurobiomechanical state of post-stroke patients during the rehabilitation course was defined using the patients' muscular activity and movement kinematics. Measures of similarity between the patient's neuromuscular state and the healthy one were defined based on the muscular coordination (structure of muscle synergies) and the estimated motoneural activity in the spinal cord. In addition, the movement execution was quantified in terms of efficiency, smoothness, accuracy, easiness and dependence on robotic assistance.

In Section 7.2, one could observe that synergies' structure and spinal maps of patients did not progress towards the healthy patterns in the same trend of improvement of their motor skills. This was quantitatively confirmed by the correlation between muscle activity metrics and the FMUE scale.

The synergies' metric, as defined in Section 6.8, poorly correlated with the FMUE scores of

patients: 0.32 ± 0.21. The shape-similarity and magnitude-similarity of the spinal maps also resulted in just 0.25 ± 0.24 and 0.021 ± 0.29 of correlation with this clinical scale, respectively. Given the very low estimated values, bootstrap method was applied to these metrics only to determine the standard error of the correlation when data sets are resampled.

On the other hand, in Section 7.2.1, the kinematic of movement execution reflected the motor improvement of patients in various features of the movement. Patients receiving the robotic treatment improved all features, in general, from the beginning to the end of the treatment, but the best correlated metrics with their clinical scores were the MDH (quantifying accuracy), the RMP (a measure of smoothness), and the assisted-distance (a measure of dependence on the robotic assistance). See the correlation for each metric, and the respective standard deviation obtained by resampling the patients' data (bootstrap method), in Figure 7.21 (left side), together with the histogram (number of occurrences) of correlation obtained in the resampled data.

In addition, the correlation between the variation of the FMUE, over the rehabilitation course, and the variation of these kinematic metrics is higher (graphs on the right side of Figure 7.21). This supports the fact that, more than their absolute value, the variation of these metrics quantifies the progress of the patients' performance.

Results for other kinematic metrics are presented in Appendix I. These metrics did not achieve so good results; thus, graphical representations are provided only for the correlation between these variables and the FMUE, not for the variation of these variables.

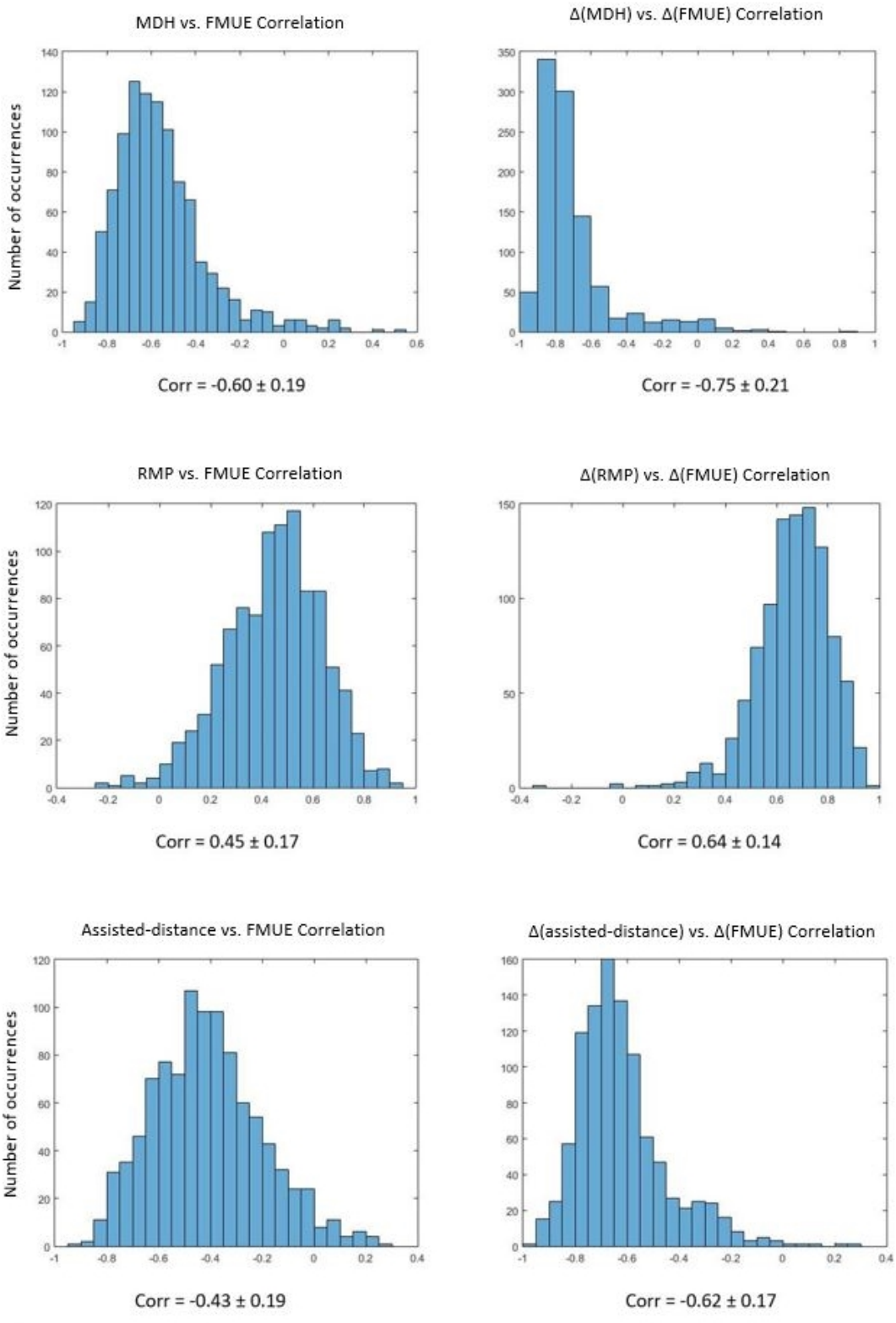

Figure 7.21: Correlation between the clinical scale (FMUE) and metrics of the kinematic assessment (on the left), and between the variation of FMUE and the variation of those metrics (on the right), over the rehabilitation course. The average and standard deviation of the correlation are indicated below the respective histogram of the bootstrap method results. Histograms show the number of occurrences (bootstrap resamples / data sets) which resulted in a value of the correlation indicated in the x-axis. MDH, RMP and Assisted-distance achieved the best results of correlation and the lowest values of standard deviations.

Chapter 8

Discussion

8.1 Analysis of the control group (healthy subjects)

Despite being a narrow sample of the non-disabled human population, the group of healthy subjects was selected to match the range of ages of the stroke patients, and studying these subjects was fundamental to organize the patients' data.

The variation of level of activity of EMG envelops (RMS values) started to provide clues on the main effects of the movement condition in muscular organization, revealing that muscular effort in healthy subjects is particularly intense when reaching more distant targets and near the top of the sphere (i.e. when executing distal and upper movements). These results evidence the effect of gravity on 3D reaching movements.

Then, as expected, the factorization of electromyographic signals confirmed that the activity of 15 muscles can be reduced to a smaller set of variables, the muscle synergies, which describe the coordinated recruitment of a group of muscles. Four muscle synergies were found to account for the variability of muscle activity for every movement condition (every target, in forwards, or backwards). These results agree with other studies of upper limb movements that found 2 to 8 synergies in healthy subjects (Sabatini, 2002; d'Avella et al., 2006; Flanders, 1991).

Indeed, the protocol adopted to record data of healthy subjects did not constrain the movements in terms of speed and motion, thus, subjects presented some differences in movement trajectories. This was mainly verified during the first times that subjects executed the movements, indicating that it is likely due to an adaptation (and learning mechanism) of the subject to use the robot. This could be surpassed in future acquisitions by adding a simple step in the protocol: subjects should be given the opportunity to get familiarized with the exoskeleton and execute one or two times the reaching movements. Only after, the acquisitions should be performed.

Even though, using the available data (acquired without the additional step suggested above), the intra- and inter-subject variability was successfully reduced with the algorithm to exclude movements' outliers, allowing, then, the extraction of similar muscles synergies across subjects

from comparable movements (Figures 7.6 and 7.10).

Therefore, this corroborates the general theory, addressed in Chapter 3, that motor control is modular and movement planning basically consists in organizing these modules to achieve a desired trajectory. In the specific context of 3D point-to-point reaching movements, these modules functionally and generally represent:

1 the shoulder abduction and flexion – synergy S3 (with the weighted coordination of DANT and DMED, and other muscles, depending on the target);

2 the elbow flexion – S4 (essentially with BICS, BICL, BRAD and PRO, but also with TRILAT or PEC, depending on the target);

3 the retraction and medial rotation of the shoulder (to straight the posture) – S2 (with LAT, INFRA and RHO, also with the contribution of TRAPS and TRAPM in several targets).

4 a not very clear function, since the coordinated muscles in S1 are more variable across targets and subjects than with the other synergies.

Particularly concerning S1, the function associated to this muscle synergy was better understood for each target, when they were associated in groups, as discussed later.

Moreover, a very similar muscular organization was found for movements in both directions (forward or backward), when reaching the same target. First, S4 is not affect by this condition (direction), having an identical profile for both movements. Second, only one weight coefficient over 15 muscles was found significantly different ($p<0.05$) between forward and backward movements, for each of the synergies S1, S2 and S3: referring to TRILONG in S1, TRAPS in S2, and DANT in S3. Finally, only the contribution of DANT in S3 is high (a weight coefficient superior to 0.5) for most of the targets and subjects (Figure 7.6). Therefore, one can conclude that effects of movement direction in the synergies' structure may be neglected.

Nevertheless, the same cannot be assumed when comparing movements regarding different targets. Muscle profile of all synergies is affected in several weight coefficients corresponding to muscles with the main function represented by the synergy (for example, LAT, INFRA, and RHO, in S2; DANT and DMED in S3; TRILAT in S4).

Moreover, multi-comparison revealed that such differences in the weight coefficients seem to agree with results of the amplitude analysis (Section 7.1.3), occurring in a patterned way in the up-down and close-distant axes. In fact, results detailed in Figure 7.9 revealed 4 groups of targets for which there are no differences for any weight coefficient between targets within a same group, but, oppositely, there are significantly different weight coefficients between targets of different groups: {T1,T2,T8,T9,T14}; {T4,T5,T6,T11,T12}; {T7,T18,T13,T17}; and {T3,T16,T10,T15}. Exceptionally, in the last group, target 10 is different from one target of its group, but only in four weight coefficients (in red, in Figure 7.9).

This finding suggests that muscle activity is mainly preserved in targets close to 4 main directions. This opens the possibility to consider just 4 main directions for muscle activity analysis with a consequent simplification of the analysis of stroke patients. Having just 4 main directions would allow to increase the number of repetitions for each direction by grouping the repetitions of each target and it would solve the problem of having different movement conditions in each session of assessment and each patient.

In addition to muscle coordination, motoneural activity of the spinal cord was estimated in healthy subjects, between segments C2 and T1 (the ones innervating the upper limb).

As far as it was possible to know, spinal maps of healthy subjects have not been characterized in depth while executing reaching movements in 3-dimensions (Pirondini et al., 2016). This method has been used mainly to study movements with the lower limb (Ivanenko et al., 2008; Monaco et al., 2010). For the thesis, this method was selected because it was expected to be a valuable tool to study muscle organization in the upper limb, as it happened, simplifying the analysis in case of complex movements that require the recording of many muscles.

In fact, spatiotemporal distribution of motoneural activity in the spinal cord demonstrated to be sensitive to the movement condition, like with muscle synergies. Estimated activity in forward movements generally increases from the bottom to the top of the sphere, i.e. the global magnitude of the spinal map increases with the height of the target.

Moreover, a linear relation was found between the distance of the target to the top of the sphere and the respective level of magnitude relatively to the magnitude of the spinal map for Target 1 (the top of the sphere). This relation is very significant ($p < 1 e -11$; $r = -0.98$) if the Euclidean distance is considered to locate the target in respect to Target 1, and the covariance is used to measure the relative magnitude of the spinal map in respect to the one of Target 1.

The same occurred with the shape of the spinal maps (i.e. the relative distribution of motoneural activity along space and time). This shape becomes more similar to the one of spinal map for Target 1 as the distance to that target diminishes. Again, a very significant ($p < 1 e -6$) linear relation ($r = -0.90$) was found between the distance in the z-axis (i.e. top-bottom) and the correlation with the spinal map for Target 1.

In the y-axis (i.e. close-distant axis in respect to the subject), significant variations of the magnitude ($r = -0.63$; $p = 0.005$) and shape ($r = -0.84$; $p = 1.68 e -5$) of the spinal maps were found.

As expected from the visual inspection of the spinal maps, in backward movements, magnitude and shape variate with the location of the target but these results were not as remarkable as with forward movements.

Furthermore, targets 2, 8, 9, and 14 are at the same (Euclidean or z-axis) distance to target 1, as well as targets 3, 7, 10, 15, 16, 17, and 18, and, moreover, targets 4, 6, 11 and 12. Given the results of linear relations with the location and magnitude/shape of the spinal maps, and disregarding the effects of location of target 1 and target 5, the hypothesis to group targets as suggested by the

analysis of muscle synergies was also supported by the analysis of spinal maps.

Therefore, to further test the hypothesis that targets could be grouped, muscle activity of each healthy subject was arranged in new datasets including more than one target (according to the statistical results of synergies' structure and spinal maps): group 1 – {T1, T2, T8, T9, T14}; group 2 – {T4, T5, T6, T11, T12}; group 3 – {T7, T18, T13, T17}; group 4 – {T3, T16, T10, T15}. EMG signals were factorized to extract muscle synergies and weighted-summed to extract spinal maps.

Once again, four muscle synergies were estimated for all groups of targets, both in forward and backward directions. The only exception occurred with group 1, backwards, for which 4.6 synergies (in average across healthy subjects) were estimated. This may be justified by the fact that group 1 includes target 2 and the number of synergies estimated for this target, individually, was also higher, as reported in Section 7.1.4.1.

Given the preservation of the number of synergies when movements are strategically grouped as when they are individually factorized, this result indicates that muscle coordination is similar enough between targets within a same group, supporting the use of these groups of targets to compare with patients' synergies.

Concerning synergies' structure for groups of targets, there are 3 muscle synergies in common among groups (or, at least, with a very similar muscle weights profile), and other 3 synergies differing (S4 of group 1, 2 and 4). The synergy S4 of group 3, however, seems to represent the same function as S4 of group 1, but merged with the contribution of additional muscles. This may be explained by the fact that group 3 is not so homogeneous (concerning the muscular organization) as the others, which was partially foreseen by the statistical differences found for some muscle weights between Target 10 and Targets 3, 15 and 16.

Thus, in total, 6 to 7 different synergies are necessary to reach all the targets of the sphere, which also fairly agrees with the estimated number of synergies when movements regarding all targets are pooled together (Section 7.1.4.1).

More in detail, the profile of S4 (the equivalent of S1 obtained for individual targets) for groups 1, 2 and 4 seems to highlight the necessary muscle functions to move towards the main direction of the movements included in these groups: movements of group 1 are executed in the upper part of the sphere, demanding a coordinated work of trapezius and deltoids to lift the arm to reach higher positions; most targets of group 2 are positioned at the left, distant side of the sphere, demanding medial rotation of the arm/shoulder, function of pectoralis muscle; group 4 is located in the bottom of the sphere, requiring mainly extension of elbow (triceps) and shoulder (posterior deltoid). Profiles of S1, S2 and S3 are equivalent to S3, S4 and S2, respectively, obtained for movements regarding individual targets.

Concerning spinal maps for groups of targets, one could observe that they are a good approximation of the spatiotemporal distribution represented by the spinal map for each target within a same group and, more important, the trend in magnitude and shape along the top-bottom and

close-distant axes, in forwards, was retained by this organization of the targets.

Therefore, it was considered that muscle activity of stroke patients could be organized in the same way (grouping targets) to extract muscle synergies and spinal maps, to compare them with the healthy ones and evaluate the progress of the patients' neuromuscular state.

Regarding the kinematic analysis, it was possible to verify the motor ability of healthy subjects in terms of efficiency, accuracy, smoothness, and easiness.

As expected from the exclusion of movements outliers, time and path length are not uniform across targets and directions. In particular, subjects are more efficient when executing backward movements, which is quite expected because, despite starting in different targets, all backward movements are executed towards the same point, the center of the sphere, and, thus, subjects have the opportunity to practice more times a similar movement (at least when it is closer to the center).

In addition, the smoothness measured by SAL (Spectral Arc-Length) also varied across targets, similarly to the duration and path length. Nevertheless, RMP (Ratio of Mean Acceleration with Peak Acceleration), another measure of smoothness, was not so sensitive as SAL to sudden changes in the movement of healthy subjects and the standard errors are lower. The reduced sensitivity of RMP relative to SAL may imply one of two cases: RMP is less susceptible to noise (i.e. sudden changes in the movement which do not reflect motor ability of the subject but characterize natural movements with the upper limb) than SAL; or SAL provides a wider range to measure smoothness and, consequently, motor performance. The real case was evaluated with the stroke group, since with those subjects it was possible to compare results of both metrics with a clinical scale (FMUE) which characterizes motor performance.

Regarding easiness and movement accuracy, healthy subjects performed similarly across targets. Once more, from the increased speed, one could verify they were capable to execute backward movements more easily than forward ones.

Finally, as hypothesized, the average path across subjects is not a straight line, as theoretically suggested before (Flash and Hogan, 1985; Amirabdollahian et al., 2002), and this correction in a widely used measure of accuracy was expected to obtain good results in capturing motor performance of stroke patients.

8.2 Analysis of the stroke group

Patients who received the robotic-assisted treatment (ALEx-HUG-001, 003 and 004) clearly improved their motor performance, according to their FMUE score, the general increase of the number of synergies from the beginning to the end of the experiments, and their progressively better results in the kinematic assessment.

Nevertheless, the motor improvement of these patients was not clearly reflected by their muscle coordination (the structure of their muscle synergies) nor by the estimated motoneural activity of the spinal cord (spinal maps).

In fact, although the number of synergies tends to 4, as in nondisabled subjects, it seems the muscular organization is highly modified in respect to the healthy one (correlation values are always less than 0.5). These modifications are not systematic, but dependent on the group of targets and the patient.

In specific, the progress of the synergies' structure obtained for group 2 is very distinct from the other groups: these synergies are uncorrelated or inversely correlated with the healthy ones, for all patients. This seems to indicate that patients are not able to use the same muscle coordination as healthy subjects (specially with PEC) to reach targets in the left side of the sphere. In fact, some features of movement execution (like smoothness and accuracy) were found less improved for some of the targets included in these group. Therefore, these results can be used by clinicians to pay specific attention to the posture of future patients enrolled in the study while reaching this group of targets.

From the results with other groups of targets, it is difficult to compare the effects of the two types of robotic-assisted therapy in the neuromuscular state of the patient, because data of few patients is available at the moment, and, for example, the effects of conventional robotic treatment in the synergies' structure was different for patients 001 and 003, indicating that, possibly, more factors (rather than just the type of treatment) influence these results.

The most consistent observation obtained from muscle activity assessment was found in spinal maps: motoneural activity in upper cervical segments of the spinal cord is commonly increased for all patients (inclusively ALEx-HUG-006) after the treatment (A3). However, patients 001, 003 and 004 were not able to retain the same level of activity 1 month later.

Even though, at the follow-up, these patients have maintained or improved their motor skills (such as their accuracy, smoothness and efficiency) and obtained good FMUE scores, which shows that deviations from healthy patterns of muscle activity still allow stroke survivors to re-learn movements of the upper limb.

Patient ALEx-HUG-006, which received the standard therapy, did not improve considerably, according to her FMUE score and the poor results in both the muscle and kinematic assessment.

Particularly concerning the structure of synergies, this is the most different patient from the healthy group. Notwithstanding, in what respects to her motoneural activity, it started with an inverse spatial distribution with respect to the healthy one, but, in assessment 3, upper cervical segments were more active, like other patients and healthy subjects.

Moreover, the fact that data from assessment 4 is missing and, during assessment 3, acquisitions and movement execution by the subject have been constrained by the patient's condition, make it difficult to take reliable conclusions about this patient and, moreover, to fairly compare the conventional therapy with the robotic-assisted one, for now.

Another issue is the fact that all patients to be included in group 1 (like 006) have contact with the exoskeleton only during the assessment sessions. As observed with healthy subjects, it is necessary to execute movements more than one time to be used to the robot and, in addition, patients usually fatigue faster than healthy. Therefore, this may bias the comparison between standard and robotic therapies using muscle and kinematic results obtained from assessment sessions which require the use of the exoskeleton.

A possible solution was to adopt an assessment method that is independent of the rehabilitation therapy: each patient (of any group of treatment) could perform free 3D reaching movements, i.e. without wearing the exoskeleton, and kinematics could be recorded with a motion capture system - mocap (using a set of cameras, and markers placed over the necessary anatomical places in the arm). This method would still allow to compute the same kinematic metrics studied in this thesis, but it would be necessary to determine the 3D position of the target and also to present that target to the patient differently from the current protocol (because this is currently determined by the robot): using virtual reality. The sphere could be presented to the patient wearing virtual reality glasses. This way, the location of the sphere is known relatively to the patient. Matching this data with kinematics recorded by the mocap system, the 3D position of the sphere would be known.

In fact, using virtual reality to present the sphere, instead of the current 2D screen, could also solve another important aspect of the rehabilitation protocol with ALEx: while the reaching movements are three-dimensional, the sphere is two-dimensionally projected; therefore, patients (and also healthy subjects) need to adapt their perception of depth. On the other hand, virtual reality provides a better environment to train arm movements with the normal connection between the human visual and motor systems.

8.3 The Neurobiomechanical State and Motor Performance of Stroke patients during robot-aided rehabilitation

As explained in Section 6.8, the FMUE (Fugl-Meyer for the Upper Extremity) was considered to reflect the global motor ability of the patient in each session of assessment. Therefore, the correlation between this clinical scale and all metrics of kinematics, synergies and spinal maps was determined, to verify which of these could significantly quantify the patient's motor performance. The significance of the estimated correlation was assessed by resampling the patients' data, using the bootstrap method.

Moreover, the motor improvement algorithm of the personalization treatment continuously estimates the patient motor performance and replaces a task by another one more difficult, based on its progress: when the motor performance of the patient in executing the movement towards some target converges to a plateau, this movement is replaced by another one which demands more training. Thus, it is important that the trend of improvement quantified by any metric is correlated with the trend of improvement reported by the FMUE. Therefore, this correlation was also computed to check the ability of each metric to capture changes in motor improvement.

In Section 7.2, one could observe that synergies' structure and spinal maps of patients did not progress towards the healthy patterns in the same trend of improvement of their motor skills. Then, when assessing the synergies' and spinal maps' metrics concerning their ability to capture the patients' level of motor performance, it was expected to obtain a low correlation with the FMUE scale, as it happened.

Indeed, in the literature, a deterministic relation between neuromuscular state following stroke and motor performance has not been validated yet, because different studies have achieved distinct results (Cheung et al., 2009; Coscia et al., 2014; Roh et al., 2013). Thus, the work developed in this thesis with stroke patients was a preliminary study, but imperative to verify the existence of any relation as the above-mentioned, for 3D point-to-point reaching movements, so that parameters of such relation could be included in the personalized treatment.

For the moment, muscle coordination and single muscle activity can only be used as an additional information about the patient condition in respect to healthy subjects. If provided to clinicians that supervise the robotic treatment, the result of these measures can alert them to verify if the patient is executing the tasks with compensatory or more natural movements, if he/she is positioned in the best way and is distributing the effort correctly in the arm and back, to avoid injuries in muscles and joints. Additional data from the remaining 44 patients that will be included in the study will be necessary to establish if and which muscular features as muscle synergies and spinal maps will reflect the patient's motor improvement in order to incorporate them in the personalization algorithm.

On the other hand, from the kinematic assessment of the stroke group, it was possible to demonstrate that metrics of movement smoothness, accuracy and dependence on robotic assis-

tance are able to quantify the motor performance of patients following their FMUE scores. In specific, MDH, RMP and the assisted-distance are good candidates to be parameters of the motor impairment algorithm.

The correlation between MDH and FMUE, as well as between the Assisted-distance and the same scale is negative, because motor performance implies a decrease of these parameters (i.e., a lower distance to the healthy path, and a reduced dependence on the assistance of the exoskeleton). On the contrary, the correlation between the RMP and FMUE is positive, because an increase of RMP means a decrease of peak acceleration in respect to the mean acceleration, i.e. a higher smoothness.

Despite the fact that absolute values of correlation were not higher than 0.75, these results are significative, because, first, standard errors obtained with bootstrap method were not higher than 0.21, and, second, in other similar studies with kinematic robot-based evaluations (Bosecker et al., 2010; Ellis et al., 2008; Yang et al., 2017), reported correlation between assessed metrics and clinical scales are similar or lower than the ones obtained here. Additionally, it must be accounted that clinical scales are always affected by subjectivity to some extent. In particular, FMUE is widely used and highly recommend (Fugl-Meyer et al., 1975) and, during the experiments, the same clinician assessed patients, but intra-rater assessments may change up to 5.2 on 66 points (Singer and Garcia-Vega, 2017).

Moreover, results obtained with the mean distance to the average-healthy path (MDH) show that, in fact, this metric is more realistic than the typically adopted distance to a theoretical, straight path (nMD). Actually, nMD had been previously tested in the context of Neuroprobes' project, but no significant trend of improvement had been observed, in opposition to other studies of planar movements (Cirstea and Levin, 2000; Panarese et al., 2012). The reason for that may rely on a wrong assumption that 3D movements are straight, when, truly, they are more complex, more curvilinear, as verified with the healthy group.

In addition, although both RMP and SAL quantify smoothness, RMP was somewhat more able to follow the motor improvement trend of stroke patients. In fact, also when assessing the healthy group, SAL has shown a higher sensibility to any difference across healthy subjects (explicit in higher standard deviations) and higher variability across targets than RMP. Thus, from the results with stroke patients, this suggests that such increased sensibility may not account for true differences of motor ability, but natural variability across subjects.

Finally, other metrics have been tested, but results were not better than those already described. In particular, this happened with mean velocity. This metric can be used to assess easiness in executing some movement, by observing deviations from healthy values and their evolution along the treatment. For this reason, it was included in the kinematic assessment of stroke patients, so that a more complete evaluation was done. However, it must be noted that, during the experiments, patients were usually encouraged to pay more attention to the trajectory they should follow to reach the target, and not to be too concerned with reaching it quickly. Thus, it was likely that mean velocity would not show a high correlation with the patient FMUE score, as it actually happened.

Chapter 9

Conclusions and Future Perspectives

This thesis contributed to define the neurobiomechanical state of acute/subacute stroke patients during robot-aided motor rehabilitation of the upper limb, with a novel exoskeleton, ALEx Rehab Station.

The work developed towards such definition relied on data collected from 8 healthy subjects and 4 stroke patients, recorded while these persons executed 3D point-to-point reaching movements in different conditions (directions and reaching points).

The first challenge addressed in this work was the fact that each patient only trains some movements in each session of treatment and these are different from session to session and from patient to patient making data analysis among sessions and between patients and healthy group complex.

Muscle synergies and spinal maps allowed to define the structure of muscle activity and highlighted the possibility to organize targets in four groups in both directions (forward and backward), simplifying the analysis of stroke patients' data.

Muscle synergies and spinal maps are representations of a subject's neuromuscular state. Stroke patients were assessed concerning the evolution of their activity towards the healthy state. Results show that even if motor skills are recovered, patients not always reacquire the natural patterns of nondisabled persons (patterns of muscular coordination and motoneural activity in the spinal cord). Notwithstanding, the benefits of recovering such patterns is still an open question concerning their utility for patients to regain their independence and life quality. Additionally, some deviations from healthy patterns may suggest that attention is required to correct maladaptive patients' posture and movement execution during motor rehabilitation, making this a useful information for clinicians. In this thesis, it was possible to detect a consistent case of such usefulness (with targets of group 2), which leads to the conclusion that information provided by muscle synergies and spinal maps can be used as feedback for clinicians, improving the personalization of robotic therapy. To provide a more specific information to clinicians, about the patient's posture when executing some movement, it is necessary, in future work, to identify a relation between the patients' abnormal neural patterns (like the abnormal synergies' profiles) and his/her posture. This would allow, for example, to detect if the patient is using compensatory movements, such

as the exaggerated shoulder protraction (and/or forward rotation of the trunk), during reaching movements, typically observed in stroke patients having a reduced ability to extend the elbow.

Results about kinematics showed a different and more defined trend. Rehabilitation and, in particular the robotic-assisted one, showed benefic effects for stroke patients in more than one feature of movement execution. The patients were able to improve all parameters evaluated: accuracy, smoothness, efficiency, easiness and dependence on robotic assistance (i.e. their ability to accomplish some task with the arm). Thanks to their correlation with the FMUE scores, a widely used clinical scale and reference for the level of motor ability, three kinematic metrics, among those tested, seem significantly able to capture changes of motor performance:

1 The Mean Distance to the average-Healthy path (MDH), which measures movement accuracy;

2 Ratio of Mean Acceleration with Peak Acceleration (RMP), which quantifies smoothness;

3 and the Assisted-Distance, which is a quantity of the patient's dependence on the robotic assistance.

As so, they could contribute to estimate the patient motor impairment in the personalization algorithm. The robustness of these conclusions was estimated using a resampling method (bootstrapping) on the data of the few available patients.

While kinematics describes aspects of the biomechanical state of stroke subjects and it can be used for the personalized algorithm, muscle activity still requires further investigations. To this concern, the framework analysis developed in this work can be applied to the remaining 40 healthy participants and 44 stroke patients planned in Neuroprobes project. It is expected that these additional data will provide evidences for the inclusion of muscle activity features in the personalization algorithm.

References

Alt Murphy, M., Willén, C., and Sunnerhagen, K. S. (2013). Responsiveness of upper extremity kinematic measures and clinical improvement during the first three months after stroke. *Neurorehabilitation and neural repair*, 27(9):844–853.

Amirabdollahian, F., Loureiro, R., and Harwin, W. (2002). Minimum jerk trajectory control for rehabilitation and haptic applications. In *Robotics and Automation, 2002. Proceedings. ICRA'02. IEEE International Conference on*, volume 4, pages 3380–3385. IEEE.

Balasubramanian, S., Melendez-Calderon, A., and Burdet, E. (2012). A robust and sensitive metric for quantifying movement smoothness. *IEEE transactions on biomedical engineering*, 59(8):2126–2136.

Balasubramanian, S., Wei, R., Perez, M., Shepard, B., Koeneman, E., Koeneman, J., and He, J. (2008). Rupert: An exoskeleton robot for assisting rehabilitation of arm functions. In *Virtual Rehabilitation, 2008*, pages 163–167. IEEE.

Ball, S. J., Brown, I. E., and Scott, S. H. (2007). Medarm: a rehabilitation robot with 5dof at the shoulder complex. In *Advanced intelligent mechatronics, 2007 IEEE/ASME international conference on*, pages 1–6. IEEE.

Barnes, M. and Good, D. (2013). Neurorehabilitation approaches to facilitate motor recovery. *Neurological Rehabilitation: Handbook of Clinical Neurology*, 110:161.

Basteris, A., Nijenhuis, S. M., Buurke, J. H., Prange, G. B., and Amirabdollahian, F. (2015). Lag-lead based assessment and adaptation of exercise speed for stroke survivors. *Robotics and autonomous systems*, 73:144–154.

Beer, R. F., Naujokas, C., Bachrach, B., and Mayhew, D. (2008). Development and evaluation of a gravity compensated training environment for robotic rehabilitation of post-stroke reaching. In *Biomedical Robotics and Biomechatronics, 2008. BioRob 2008. 2nd IEEE RAS & EMBS International Conference on*, pages 205–210. IEEE.

Bensmail, D., Robertson, J. V., Fermanian, C., and Roby-Brami, A. (2010). Botulinum toxin to treat upper-limb spasticity in hemiparetic patients: analysis of function and kinematics of reaching movements. *Neurorehabilitation and neural repair*, 24(3):273–281.

Bernstein, N. A. (1967). *The co-ordination and regulation of movements*. Pergamon Press Ltd.

Berry, M. W., Browne, M., Langville, A. N., Pauca, V. P., and Plemmons, R. J. (2007). Algorithms and applications for approximate nonnegative matrix factorization. *Computational statistics & data analysis*, 52(1):155–173.

Binder, M. D., Hirokawa, N., and Windhorst, U., editors (2009a). *Encyclopedia of Neuroscience. Arm Trajectory Formation*. Springer Berlin Heidelberg.

Binder, M. D., Hirokawa, N., and Windhorst, U., editors (2009b). *Encyclopedia of Neuroscience. Kinematics*. Springer Berlin Heidelberg.

Binder, M. D., Hirokawa, N., and Windhorst, U., editors (2009c). *Encyclopedia of Neuroscience. Motor Cortex*. Springer Berlin Heidelberg.

Binder, M. D., Hirokawa, N., and Windhorst, U., editors (2009d). *Encyclopedia of Neuroscience. Reaching Movements*. Springer Berlin Heidelberg.

Bosecker, C., Dipietro, L., Volpe, B., and Igo Krebs, H. (2010). Kinematic robot-based evaluation scales and clinical counterparts to measure upper limb motor performance in patients with chronic stroke. *Neurorehabilitation and neural repair*, 24(1):62–69.

Burgar, C. G., Lum, P. S., Shor, P. C., and Van der Loos, H. M. (2000). Development of robots for rehabilitation therapy: The palo alto va/stanford experience. *Journal of rehabilitation research and development*, 37(6):663–674.

Cappellini, G., Ivanenko, Y. P., Poppele, R. E., and Lacquaniti, F. (2006). Motor patterns in human walking and running. *Journal of neurophysiology*, 95(6):3426–3437.

Carignan, C., Tang, J., and Roderick, S. (2009). Development of an exoskeleton haptic interface for virtual task training. In *Intelligent Robots and Systems, 2009. IROS 2009. IEEE/RSJ International Conference on*, pages 3697–3702. IEEE.

Carod-Artal, J., Egido, J. A., González, J. L., and De Seijas, E. V. (2000). Quality of life among stroke survivors evaluated 1 year after stroke experience of a stroke unit. *Stroke*, 31(12):2995–3000.

Chang, W. H. and Kim, Y.-H. (2013). Robot-assisted therapy in stroke rehabilitation. *Journal of stroke*, 15(3):174.

Cheung, V. C., d'Avella, A., Tresch, M. C., and Bizzi, E. (2005). Central and sensory contributions to the activation and organization of muscle synergies during natural motor behaviors. *Journal of Neuroscience*, 25(27):6419–6434.

Cheung, V. C., Piron, L., Agostini, M., Silvoni, S., Turolla, A., and Bizzi, E. (2009). Stability of muscle synergies for voluntary actions after cortical stroke in humans. *Proceedings of the National Academy of Sciences*, 106(46):19563–19568.

Cheung, V. C., Turolla, A., Agostini, M., Silvoni, S., Bennis, C., Kasi, P., Paganoni, S., Bonato, P., and Bizzi, E. (2012). Muscle synergy patterns as physiological markers of motor cortical damage. *Proceedings of the National Academy of Sciences*, 109(36):14652–14656.

Cirstea, M. and Levin, M. F. (2000). Compensatory strategies for reaching in stroke. *Brain*, 123(5):940–953.

Clark, D. J., Ting, L. H., Zajac, F. E., Neptune, R. R., and Kautz, S. A. (2010). Merging of healthy motor modules predicts reduced locomotor performance and muscle coordination complexity post-stroke. *Journal of neurophysiology*, 103(2):844–857.

Clarke, P., Marshall, V., Black, S. E., and Colantonio, A. (2002). Well-being after stroke in canadian seniors. *Stroke*, 33(4):1016–1021.

Coderre, A. M., Zeid, A. A., Dukelow, S. P., Demmer, M. J., Moore, K. D., Demers, M. J., Bretzke, H., Herter, T. M., Glasgow, J. I., Norman, K. E., et al. (2010). Assessment of upper-limb sensorimotor function of subacute stroke patients using visually guided reaching. *Neurorehabilitation and neural repair*, 24(6):528–541.

Colombo, R., Pisano, F., Micera, S., Mazzone, A., Delconte, C., Carrozza, M., Dario, P., and Minuco, G. (2008). Assessing mechanisms of recovery during robot-aided neurorehabilitation of the upper limb. *Neurorehabilitation and neural repair*, 22(1):50–63.

Colombo, R., Pisano, F., Micera, S., Mazzone, A., Delconte, C., Carrozza, M. C., Dario, P., and Minuco, G. (2005). Robotic techniques for upper limb evaluation and rehabilitation of stroke patients. *IEEE transactions on neural systems and rehabilitation engineering*, 13(3):311–324.

Coote, S., Murphy, B., Harwin, W., and Stokes, E. (2008). The effect of the gentle/s robot-mediated therapy system on arm function after stroke. *Clinical rehabilitation*, 22(5):395–405.

Coscia, M., Cheung, V. C., Tropea, P., Koenig, A., Monaco, V., Bennis, C., Micera, S., and Bonato, P. (2014). The effect of arm weight support on upper limb muscle synergies during reaching movements. *Journal of neuroengineering and rehabilitation*, 11(1):22.

Crocher, V., Sahbani, A., Robertson, J., Roby-Brami, A., and Morel, G. (2012). Constraining upper limb synergies of hemiparetic patients using a robotic exoskeleton in the perspective of neuro-rehabilitation. *IEEE Transactions on Neural Systems and Rehabilitation Engineering*, 20(3):247–257.

Daly, J. J., Hogan, N., Perepezko, E. M., Krebs, H. I., et al. (2005). Response to upper-limb robotics and functional neuromuscular stimulation following stroke. *Journal of rehabilitation research and development*, 42(6):723.

d'Avella, A. and Bizzi, E. (2005). Shared and specific muscle synergies in natural motor behaviors. *Proceedings of the National Academy of Sciences of the United States of America*, 102(8):3076–3081.

d'Avella, A., Fernandez, L., Portone, A., and Lacquaniti, F. (2008). Modulation of phasic and tonic muscle synergies with reaching direction and speed. *Journal of neurophysiology*, 100(3):1433–1454.

d'Avella, A., Portone, A., Fernandez, L., and Lacquaniti, F. (2006). Control of fast-reaching movements by muscle synergy combinations. *Journal of Neuroscience*, 26(30):7791–7810.

d'Avella, A., Saltiel, P., and Bizzi, E. (2003). Combinations of muscle synergies in the construction of a natural motor behavior. *Nature neuroscience*, 6(3):300.

Day, S. J. and Hulliger, M. (2001). Experimental simulation of cat electromyogram: evidence for algebraic summation of motor-unit action-potential trains. *Journal of Neurophysiology*, 86(5):2144–2158.

de Rugy, A., Loeb, G. E., and Carroll, T. J. (2013). Are muscle synergies useful for neural control? *Frontiers in computational neuroscience*, 7.

Di Pino, G., Pellegrino, G., Assenza, G., Capone, F., Ferreri, F., Formica, D., Ranieri, F., Tombini, M., Ziemann, U., Rothwell, J. C., et al. (2014). Modulation of brain plasticity in stroke: a novel model for neurorehabilitation. *Nature Reviews Neurology*, 10(10):597–608.

Donnan, G. A., Fisher, M., Macleod, M., and Davis, S. M. (2008). Stroke. *The Lancet*, 371:1612–1623.

Dorland, W. A. N. (2011). *Dorland's Illustrated Medical Dictionary32: Dorland's Illustrated Medical Dictionary*. Elsevier Health Sciences.

Dromerick, A., Lang, C., Birkenmeier, R., Wagner, J., Miller, J., Videen, T., Powers, W., Wolf, S., and Edwards, D. (2009). Very early constraint-induced movement during stroke rehabilitation (vectors) a single-center rct. *Neurology*, 73(3):195–201.

Ellis, M. D., Sukal, T., DeMott, T., and Dewald, J. P. (2008). Augmenting clinical evaluation of hemiparetic arm movement with a laboratory-based quantitative measurement of kinematics as a function of limb loading. *Neurorehabilitation and neural repair*, 22(4):321–329.

Erik Ween, J. (2008). Functional imaging of stroke recovery: an ecological review from a neural network perspective with an emphasis on motor systems. *Journal of Neuroimaging*, 18(3):227–236.

Esquenazi, A. and Packel, A. (2012). Robotic-assisted gait training and restoration. *American journal of physical medicine & rehabilitation*, 91(11):S217–S231.

Fetz, E. E. (1993). Cortical mechanisms controlling limb movement. *Current opinion in neurobiology*, 3(6):932–939.

Feydy, A., Carlier, R., Roby-Brami, A., Bussel, B., Cazalis, F., Pierot, L., Burnod, Y., and Maier, M. (2002). Longitudinal study of motor recovery after stroke. *Stroke*, 33(6):1610–1617.

Fisher, C. M. (1958). Intermittent cerebral ischemia. *Cerebral vascular disease. New York: Grune & Stratton*, pages 81–97.

Flanders, M. (1991). Temporal patterns of muscle activation for arm movements in three-dimensional space. *Journal of Neuroscience*, 11(9):2680–2693.

Flash, T. and Hogan, N. (1985). The coordination of arm movements: an experimentally confirmed mathematical model. *Journal of neuroscience*, 5(7):1688–1703.

Frère, J. and Hug, F. (2012). Between-subject variability of muscle synergies during a complex motor skill. *Frontiers in computational Neuroscience*, 6.

Frisoli, A., Sotgiu, E., Procopio, C., Bergamasco, M., Chisari, C., Lamola, G., and Rossi, B. (2012). Training and assessment of upper limb motor function with a robotic exoskeleton after stroke. In *Biomedical Robotics and Biomechatronics (BioRob), 2012 4th IEEE RAS & EMBS International Conference on*, pages 1782–1787. IEEE.

Fugl-Meyer, A. R., Jääskö, L., Leyman, I., Olsson, S., and Steglind, S. (1975). The post-stroke hemiplegic patient. 1. a method for evaluation of physical performance. *Scandinavian journal of rehabilitation medicine*, 7(1):13–31.

Fuhrer, M. J. and Keith, R. A. (1998). Facilitating patient learning during medical rehabilitation: A research agenda1. *American journal of physical medicine & rehabilitation*, 77(6):557–561.

Ganguly, K., Byl, N. N., and Abrams, G. M. (2013). Neurorehabilitation: Motor recovery after stroke as an example. *Annals of neurology*, 74(3):373–381.

Garrec, P., Friconneau, J., Measson, Y., and Perrot, Y. (2008). Able, an innovative transparent exoskeleton for the upper-limb. In *Intelligent Robots and Systems, 2008. IROS 2008. IEEE/RSJ International Conference on*, pages 1483–1488. IEEE.

Graham, J. V., Eustace, C., Brock, K., Swain, E., and Irwin-Carruthers, S. (2009). The bobath concept in contemporary clinical practice. *Topics in stroke rehabilitation*, 16(1):57–68.

Grasso, R., Ivanenko, Y. P., Zago, M., Molinari, M., Scivoletto, G., Castellano, V., Macellari, V., and Lacquaniti, F. (2004). Distributed plasticity of locomotor pattern generators in spinal cord injured patients. *Brain*, 127(5):1019–1034.

Guadagnoli, M. A. and Lee, T. D. (2004). Challenge point: a framework for conceptualizing the effects of various practice conditions in motor learning. *Journal of motor behavior*, 36(2):212–224.

Guglielmelli, E., Johnson, M. J., and Shibata, T. (2009). Guest editorial special issue on rehabilitation robotics. *IEEE Transactions on Robotics*, 25(3):477–480.

Hakimelahi, R. and González, R. G. (2009). Neuroimaging of ischemic stroke with ct and mri: advancing towards physiology-based diagnosis and therapy. *Expert review of cardiovascular therapy*, 7(1):29–48.

Hall, M. J., Levant, S., and DeFrances, C. J. (2012). Hospitalization for stroke in us hospitals, 1989–2009. *Diabetes*, 18(23):23.

Hatem, S. M., Saussez, G., della Faille, M., Prist, V., Zhang, X., Dispa, D., and Bleyenheuft, Y. (2016). Rehabilitation of motor function after stroke: A multiple systematic review focused on techniques to stimulate upper extremity recovery. *Frontiers in human neuroscience*, 10.

Hermens, H. J., Freriks, B., Disselhorst-Klug, C., and Rau, G. (2000). Development of recommendations for semg sensors and sensor placement procedures. *Journal of electromyography and Kinesiology*, 10(5):361–374.

Hesse, S., Schmidt, H., Werner, C., and Bardeleben, A. (2003). Upper and lower extremity robotic devices for rehabilitation and for studying motor control. *Current opinion in neurology*, 16(6):705–710.

Hogan, N., Krebs, H. I., Charnnarong, J., Srikrishna, P., and Sharon, A. (1992). Mit-manus: a workstation for manual therapy and training. i. In *Robot and Human Communication, 1992. Proceedings., IEEE International Workshop on*, pages 161–165. IEEE.

Huang, V. S. and Krakauer, J. W. (2009). Robotic neurorehabilitation: a computational motor learning perspective. *Journal of neuroengineering and rehabilitation*, 6(1):5.

Ivanenko, Y., Cappellini, G., Poppele, R., and Lacquaniti, F. (2008). Spatiotemporal organization of α-motoneuron activity in the human spinal cord during different gaits and gait transitions. *European Journal of Neuroscience*, 27(12):3351–3368.

Ivanenko, Y. P., Poppele, R. E., and Lacquaniti, F. (2004). Five basic muscle activation patterns account for muscle activity during human locomotion. *The Journal of physiology*, 556(1):267–282.

Ivanenko, Y. P., Poppele, R. E., and Lacquaniti, F. (2006). Spinal cord maps of spatiotemporal alpha-motoneuron activation in humans walking at different speeds. *Journal of neurophysiology*, 95(2):602–618.

Jamal, M. Z. (2012). *Signal acquisition using surface EMG and circuit design considerations for robotic prosthesis*. INTECH Open Access Publisher.

Kahn, L. E., Zygman, M. L., Rymer, W. Z., and Reinkensmeyer, D. J. (2006). Robot-assisted reaching exercise promotes arm movement recovery in chronic hemiparetic stroke: a randomized controlled pilot study. *Journal of neuroengineering and rehabilitation*, 3(1):12.

Kamen, G. and Gabriel, D. (2010). *Essentials of electromyography*. Human kinetics.

Kandel, E. R., Schwartz, J. H., Jessell, T. M., Siegelbaum, S. A., Hudspeth, A. J., et al. (2000). *Principles of neural science*, volume 4. McGraw-hill New York.

Kargo, W. J. and Giszter, S. F. (2008). Individual premotor drive pulses, not time-varying synergies, are the units of adjustment for limb trajectories constructed in spinal cord. *Journal of Neuroscience*, 28(10):2409–2425.

Kendall, F., McCreary, E., and Provance, P. (1993). Lower extremity strength tests. *Muscles: testing and function, 4th edn. Williams and Wilkins, Baltimore*, pages 220–221.

Kim, H., Miller, L. M., Fedulow, I., Simkins, M., Abrams, G. M., Byl, N., and Rosen, J. (2013). Kinematic data analysis for post-stroke patients following bilateral versus unilateral rehabilitation with an upper limb wearable robotic system. *IEEE Transactions on Neural Systems and Rehabilitation Engineering*, 21(2):153–164.

Kingston, B. (2005). *Understanding muscles: a practical guide to muscle function*. Nelson Thornes.

Kirk, R. E. (1982). *Experimental design*. Wiley Online Library.

Kitago, T. and Krakauer, J. W. (2013). Motor learning principles for neurorehabilitation. *Handb Clin Neurol*, 110:93–103.

Klamroth-Marganska, V., Blanco, J., Campen, K., Curt, A., Dietz, V., Ettlin, T., Felder, M., Fellinghauer, B., Guidali, M., Kollmar, A., et al. (2014). Three-dimensional, task-specific robot therapy of the arm after stroke: a multicentre, parallel-group randomised trial. *The Lancet Neurology*, 13(2):159–166.

Koenig, A., Omlin, X., Bergmann, J., Zimmerli, L., Bolliger, M., Müller, F., and Riener, R. (2011). Controlling patient participation during robot-assisted gait training. *Journal of neuroengineering and rehabilitation*, 8(1):14.

Kornelsen, J. and Stroman, P. (2004). fmri of the lumbar spinal cord during a lower limb motor task. *Magnetic resonance in medicine*, 52(2):411–414.

Krakauer, J. W. (2005). Arm function after stroke: from physiology to recovery. In *Seminars in neurology*, volume 25, pages 384–395. Copyright© 2005 by Thieme Medical Publishers, Inc., 333 Seventh Avenue, New York, NY 10001, USA.

Krakauer, J. W. (2006). Motor learning: its relevance to stroke recovery and neurorehabilitation. *Current opinion in neurology*, 19(1):84–90.

Krebs, H., Hogan, N., Volpe, B., Aisen, M., Edelstein, L., and Diels, C. (1999). Overview of clinical trials with mit-manus: a robot-aided neuro-rehabilitation facility. *Technology and Health Care*, 7(6):419–423.

Krebs, H. I., Palazzolo, J. J., Dipietro, L., Ferraro, M., Krol, J., Rannekleiv, K., Volpe, B. T., and Hogan, N. (2003). Rehabilitation robotics: Performance-based progressive robot-assisted therapy. *Autonomous robots*, 15(1):7–20.

Kwakkel, G., Kollen, B., and Twisk, J. (2006). Impact of time on improvement of outcome after stroke. *Stroke*, 37(9):2348–2353.

Kwakkel, G., Kollen, B. J., and Krebs, H. I. (2008). Effects of robot-assisted therapy on upper limb recovery after stroke: a systematic review. *Neurorehabilitation and neural repair*, 22(2):111–121.

Kwakkel, G., Kollen, B. J., van der Grond, J., and Prevo, A. J. (2003). Probability of regaining dexterity in the flaccid upper limb. *Stroke*, 34(9):2181–2186.

Kwakkel, G., Wagenaar, R. C., Koelman, T. W., Lankhorst, G. J., and Koetsier, J. C. (1997). Effects of intensity of rehabilitation after stroke. *Stroke*, 28(8):1550–1556.

Kwakkel, G., Wagenaar, R. C., Twisk, J. W., Lankhorst, G. J., and Koetsier, J. C. (1999). Intensity of leg and arm training after primary middle-cerebral-artery stroke: a randomised trial. *The Lancet*, 354(9174):191–196.

La Scaleia, V., Ivanenko, Y. P., Zelik, K. E., and Lacquaniti, F. (2014). Spinal motor outputs during step-to-step transitions of diverse human gaits. *Frontiers in human neuroscience*, 8.

Lambert-Shirzad, N. and Van der Loos, H. M. (2017). On identifying kinematic and muscle synergies: a comparison of matrix factorization methods using experimental data from the healthy population. *Journal of neurophysiology*, 117(1):290–302.

Lang, C. E., Bland, M. D., Bailey, R. R., Schaefer, S. Y., and Birkenmeier, R. L. (2013). Assessment of upper extremity impairment, function, and activity after stroke: foundations for clinical decision making. *Journal of Hand Therapy*, 26(2):104–115.

Lang, C. E., Lohse, K. R., and Birkenmeier, R. L. (2015). Dose and timing in neurorehabilitation: prescribing motor therapy after stroke. *Current opinion in neurology*, 28(6):549–555.

Lee, D. D. and Seung, H. S. (2001). Algorithms for non-negative matrix factorization. In *Advances in neural information processing systems*, pages 556–562.

Lennon, S. and Ashburn, A. (2000). The bobath concept in stroke rehabilitation: a focus group study of the experienced physiotherapists' perspective. *Disability and rehabilitation*, 22(15):665–674.

Levin, M. F., Kleim, J. A., and Wolf, S. L. (2009). What do motor "recovery" and "compensation" mean in patients following stroke? *Neurorehabilitation and neural repair*, 23(4):313–319.

Liebeskind, D. S. (2017). Hemorrhagic stroke. *Medscape,* `http://emedicine.medscape.com/article/1916662-overview`.

Lipovsek, M., von Wild, K., Mendelow, A., and Truelle, J. (2012). *Functional Rehabilitation in Neurosurgery and Neurotraumatology*. Acta Neurochirurgica Supplement. Springer Vienna.

Lo, A. C., Guarino, P. D., Richards, L. G., Haselkorn, J. K., Wittenberg, G. F., Federman, D. G., Ringer, R. J., Wagner, T. H., Krebs, H. I., Volpe, B. T., et al. (2010). Robot-assisted therapy for long-term upper-limb impairment after stroke. *New England Journal of Medicine*, 362(19):1772–1783.

Lo, H. S. and Xie, S. Q. (2012). Exoskeleton robots for upper-limb rehabilitation: State of the art and future prospects. *Medical engineering & physics*, 34(3):261–268.

Loureiro, R., Amirabdollahian, F., Topping, M., Driessen, B., and Harwin, W. (2003). Upper limb robot mediated stroke therapy—gentle/s approach. *Autonomous Robots*, 15(1):35–51.

Lum, P. S., Burgar, C. G., and Shor, P. C. (2004). Evidence for improved muscle activation patterns after retraining of reaching movements with the mime robotic system in subjects with post-stroke hemiparesis. *IEEE Transactions on Neural Systems and Rehabilitation Engineering*, 12(2):186–194.

Lum, P. S., Burgar, C. G., Shor, P. C., Majmundar, M., and Van der Loos, M. (2002). Robot-assisted movement training compared with conventional therapy techniques for the rehabilitation of upper-limb motor function after stroke. *Archives of physical medicine and rehabilitation*, 83(7):952–959.

Lum, P. S., Burgar, C. G., Van der Loos, M., Shor, P. C., et al. (2006). Mime robotic device for upper-limb neurorehabilitation in subacute stroke subjects: A follow-up study. *Journal of rehabilitation research and development*, 43(5):631.

Maciejasz, P., Eschweiler, J., Gerlach-Hahn, K., Jansen-Troy, A., and Leonhardt, S. (2014). A survey on robotic devices for upper limb rehabilitation. *Journal of neuroengineering and rehabilitation*, 11(1):1.

MacLellan, M. J., Ivanenko, Y. P., Cappellini, G., Labini, F. S., and Lacquaniti, F. (2012). Features of hand-foot crawling behavior in human adults. *Journal of neurophysiology*, 107(1):114–125.

Marchal-Crespo, L. and Reinkensmeyer, D. J. (2009). Review of control strategies for robotic movement training after neurologic injury. *Journal of neuroengineering and rehabilitation*, 6(1):20.

Masakado, Y., Noda, Y., Nagata, M.-a., Kimura, A., Chino, N., and Akaboshi, K. (1994). Macro-emg and motor unit recruitment threshold: differences between the young and the aged. *Neuroscience letters*, 179(1):1–4.

Mazzoleni, S., Posteraro, F., Filippi, M., Forte, F., Micera, S., Dario, P., and Carrozza, M. (2011). Biomechanical assessment of reaching movements in post-stroke patients during a robot-aided rehabilitation. *Applied Bionics and Biomechanics*, 8(1):39–54.

Mazzoleni, S., Sale, P., Tiboni, M., Franceschini, M., Posteraro, F., and Carrozza, M. (2013). Upper limb robot-assisted therapy in chronic and subacute stroke patients: a kinematic analysis. In *Converging Clinical and Engineering Research on Neurorehabilitation*, pages 129–133. Springer.

Mazzoleni, S., Turchetti, G., Palla, I., Posteraro, F., and Dario, P. (2014). Acceptability of robotic technology in neuro-rehabilitation: Preliminary results on chronic stroke patients. *Computer methods and programs in biomedicine*, 116(2):116–122.

Mehrholz, J., Hädrich, A., Platz, T., Kugler, J., and Pohl, M. (2012). Electromechanical and robot-assisted arm training for improving generic activities of daily living, arm function, and arm muscle strength after stroke. *Cochrane Database Syst Rev*, 6(6).

Mendis, S. (2013). Stroke disability and rehabilitation of stroke: World health organization perspective. *International Journal of stroke*, 8(1):3–4.

Metzger, J.-C., Lambercy, O., Califfi, A., Dinacci, D., Petrillo, C., Rossi, P., Conti, F. M., and Gassert, R. (2014). Assessment-driven selection and adaptation of exercise difficulty in robot-assisted therapy: a pilot study with a hand rehabilitation robot. *Journal of neuroengineering and rehabilitation*, 11(1):154.

Milot, M.-H., Spencer, S. J., Chan, V., Allington, J. P., Klein, J., Chou, C., Bobrow, J. E., Cramer, S. C., and Reinkensmeyer, D. J. (2013). A crossover pilot study evaluating the functional outcomes of two different types of robotic movement training in chronic stroke survivors using the arm exoskeleton bones. *Journal of neuroengineering and rehabilitation*, 10(1):112.

Monaco, V., Ghionzoli, A., and Micera, S. (2010). Age-related modifications of muscle synergies and spinal cord activity during locomotion. *Journal of neurophysiology*, 104(4):2092–2102.

NIH (2009). National institute of neurological disorders and stroke: Preventing stroke.

Nijland, R., Kwakkel, G., Bakers, J., and van Wegen, E. (2011). Constraint-induced movement therapy for the upper paretic limb in acute or sub-acute stroke: a systematic review. *International Journal of Stroke*, 6(5):425–433.

Nijland, R. H., van Wegen, E. E., Harmeling-van der Wel, B. C., Kwakkel, G., et al. (2010). Presence of finger extension and shoulder abduction within 72 hours after stroke predicts functional recovery. *stroke*, 41(4):745–750.

Nordin, N., Xie, S. Q., and Wünsche, B. (2014). Assessment of movement quality in robot-assisted upper limb rehabilitation after stroke: a review. *Journal of neuroengineering and rehabilitation*, 11(1):137.

Norouzi-Gheidari, N., Archambault, P. S., and Fung, J. (2012). Effects of robot-assisted therapy on stroke rehabilitation in upper limbs: systematic review and meta-analysis of the literature. *Journal of rehabilitation research and development*, 49(4):479.

Novak, D., Mihelj, M., Ziherl, J., Olensek, A., and Munih, M. (2011). Psychophysiological measurements in a biocooperative feedback loop for upper extremity rehabilitation. *IEEE Transactions on Neural Systems and Rehabilitation Engineering*, 19(4):400–410.

Overduin, S. A., d'Avella, A., Carmena, J. M., and Bizzi, E. (2012). Microstimulation activates a handful of muscle synergies. *Neuron*, 76(6):1071–1077.

Panarese, A., Colombo, R., Sterpi, I., Pisano, F., and Micera, S. (2012). Tracking motor improvement at the subtask level during robot-aided neurorehabilitation of stroke patients. *Neurorehabilitation and neural repair*, 26(7):822–833.

Papaleo, E., Zollo, L., Spedaliere, L., and Guglielmelli, E. (2013). Patient-tailored adaptive robotic system for upper-limb rehabilitation. In *Robotics and Automation (ICRA), 2013 IEEE International Conference on*, pages 3860–3865. IEEE.

Park, H.-S., Ren, Y., and Zhang, L.-Q. (2008). Intelliarm: An exoskeleton for diagnosis and treatment of patients with neurological impairments. In *Biomedical Robotics and Biomechatronics, 2008. BioRob 2008. 2nd IEEE RAS & EMBS International Conference on*, pages 109–114. IEEE.

Perry, J. C. and Rosen, J. (2006). Design of a 7 degree-of-freedom upper-limb powered exoskeleton. In *Biomedical Robotics and Biomechatronics, 2006. BioRob 2006. The First IEEE/RAS-EMBS International Conference on*, pages 805–810. IEEE.

Phillips, L. H. and Park, T. (1991). Electrophysiologic mapping of the segmental anatomy of the muscles of the lower extremity. *Muscle & nerve*, 14(12):1213–1218.

Pignolo, L., Dolce, G., Basta, G., Lucca, L., Serra, S., and Sannita, W. (2012). Upper limb rehabilitation after stroke: Aramis a "robo-mechatronic" innovative approach and prototype. In *Biomedical Robotics and Biomechatronics (BioRob), 2012 4th IEEE RAS & EMBS International Conference on*, pages 1410–1414. IEEE.

Pignolo, L., Lucca, L. L., Basta, G., Serra, S., Pugliese, M. E., Sannita, W. G., and Dolce, G. (2016). A new treatment in the rehabilitation of the paretic upper limb after stroke: the aramis prototype and treatment protocol. *Annali dell'Istituto Superiore di Sanità*, 52(2):301–308.

Pirondini, E., Coscia, M., Marcheschi, S., Roas, G., Salsedo, F., Frisoli, A., Bergamasco, M., and Micera, S. (2014). Evaluation of a new exoskeleton for upper limb post-stroke neurorehabilitation: Preliminary results. In *Replace, Repair, Restore, Relieve–Bridging Clinical and Engineering Solutions in Neurorehabilitation*, pages 637–645. Springer.

Pirondini, E., Coscia, M., Marcheschi, S., Roas, G., Salsedo, F., Frisoli, A., Bergamasco, M., and Micera, S. (2016). Evaluation of the effects of the arm light exoskeleton on movement execution and muscle activities: a pilot study on healthy subjects. *Journal of neuroengineering and rehabilitation*, 13(1):1.

Proietti, T., Crocher, V., Roby-Brami, A., and Jarrassé, N. (2016). Upper-limb robotic exoskeletons for neurorehabilitation: a review on control strategies. *IEEE reviews in biomedical engineering*, 9:4–14.

Rahman, M., Ouimet, T., Saad, M., Kenne, J., and Archambault, P. (2010). Development and control of a wearable robot for rehabilitation of elbow and shoulder joint movements. In *IECON 2010-36th Annual Conference on IEEE Industrial Electronics Society*, pages 1506–1511. IEEE.

Reaz, M. B., Hussain, M., and Mohd-Yasin, F. (2006). Techniques of emg signal analysis: detection, processing, classification and applications. *Biological procedures online*, 8(1):11–35.

Rehme, A. K., Eickhoff, S. B., Rottschy, C., Fink, G. R., and Grefkes, C. (2012). Activation likelihood estimation meta-analysis of motor-related neural activity after stroke. *Neuroimage*, 59(3):2771–2782.

Ren, Y., Kang, S. H., Park, H.-S., Wu, Y.-N., and Zhang, L.-Q. (2013). Developing a multi-joint upper limb exoskeleton robot for diagnosis, therapy, and outcome evaluation in neurorehabilitation. *IEEE Transactions on Neural Systems and Rehabilitation Engineering*, 21(3):490–499.

Reviews, C. (2016). *Human Motor Control: Medicine, Human anatomy*. Cram101.

Rice, J. (2006). *Mathematical statistics and data analysis*. Nelson Education.

Riehle, A. and Vaadia, E. (2004). *Motor cortex in voluntary movements: a distributed system for distributed functions*. CRC Press.

Riener, R., Guidali, M., Keller, U., Duschau-Wicke, A., Klamroth, V., and Nef, T. (2011). Transferring armin to the clinics and industry. *Topics in spinal cord injury rehabilitation*, 17(1):54–59.

Rinaldi, L. A. and Monaco, V. (2013). Spatio-temporal parameters and intralimb coordination patterns describing hemiparetic locomotion at controlled speed. *Journal of neuroengineering and rehabilitation*, 10(1):53.

Rod R. Seeley, Trent D. Stephens, P. T. (2003). *Anatomia & Fisiologia*. Lusociência.

Roh, J., Rymer, W. Z., Perreault, E. J., Yoo, S. B., and Beer, R. F. (2013). Alterations in upper limb muscle synergy structure in chronic stroke survivors. *Journal of neurophysiology*, 109(3):768–781.

Rohrer, B., Fasoli, S., Krebs, H. I., Hughes, R., Volpe, B., Frontera, W. R., Stein, J., and Hogan, N. (2002). Movement smoothness changes during stroke recovery. *Journal of Neuroscience*, 22(18):8297–8304.

Sabatini, A. M. (2002). Identification of neuromuscular synergies in natural upper-arm movements. *Biological cybernetics*, 86(4):253–262.

Sacco, R. L., Kasner, S. E., Broderick, J. P., Caplan, L. R., Culebras, A., Elkind, M. S., George, M. G., Hamdan, A. D., Higashida, R. T., Hoh, B. L., et al. (2013). An updated definition of stroke for the 21st century a statement for healthcare professionals from the american heart association/american stroke association. *Stroke*, 44(7):2064–2089.

Sadaka-Stephan, A., Pirondini, E., Coscia, M., and Micera, S. (2015). Influence of trajectory and speed profile on muscle organization during robot-aided training. In *Rehabilitation Robotics (ICORR), 2015 IEEE International Conference on*, pages 241–246. IEEE.

Safavynia, S., Torres-Oviedo, G., and Ting, L. (2011). Muscle synergies: implications for clinical evaluation and rehabilitation of movement. *Topics in spinal cord injury rehabilitation*, 17(1):16–24.

Salman, B., Vahdat, S., Lambercy, O., Dovat, L., Burdet, E., and Milner, T. (2010). Changes in muscle activation patterns following robot-assisted training of hand function after stroke. In *Intelligent Robots and Systems (IROS), 2010 IEEE/RSJ International Conference on*, pages 5145–5150. IEEE.

Santisteban, L., Térémetz, M., Bleton, J.-P., Baron, J.-C., Maier, M. A., and Lindberg, P. G. (2016). Upper limb outcome measures used in stroke rehabilitation studies: a systematic literature review. *PloS one*, 11(5):e0154792.

Santuz, A., Ekizos, A., Janshen, L., Baltzopoulos, V., and Arampatzis, A. (2017). On the methodological implications of extracting muscle synergies from human locomotion. *International Journal of Neural Systems*, page 1750007.

Semrau, J. A., Herter, T. M., Scott, S. H., and Dukelow, S. P. (2013). Robotic identification of kinesthetic deficits after stroke. *Stroke*, 44(12):3414–3421.

Shourijeh, M. S., Flaxman, T. E., and Benoit, D. L. (2016). An approach for improving repeatability and reliability of non-negative matrix factorization for muscle synergy analysis. *Journal of Electromyography and Kinesiology*, 26:36–43.

Simkins, M., Kim, H., Abrams, G., Byl, N., and Rosen, J. (2013). Robotic unilateral and bilateral upper-limb movement training for stroke survivors afflicted by chronic hemiparesis. In *Rehabilitation Robotics (ICORR), 2013 IEEE International Conference on*, pages 1–6. IEEE.

Singer, B. and Garcia-Vega, J. (2017). The fugl-meyer upper extremity scale. *Journal of physiotherapy*, 63(1):53.

Sivan, M., O'Connor, R. J., Makower, S., Levesley, M., and Bhakta, B. (2011). Systematic review of outcome measures used in the evaluation of robot-assisted upper limb exercise in stroke. *Journal of Rehabilitation Medicine*, 43(3):181–189.

Soekadar, S. R., Birbaumer, N., Slutzky, M. W., and Cohen, L. G. (2014). Brain–machine interfaces in neurorehabilitation of stroke. *Neurobiology of disease*, 83:172–179.

Steele, K. M., Rozumalski, A., and Schwartz, M. H. (2015a). Muscle synergies and complexity of neuromuscular control during gait in cerebral palsy. *Developmental Medicine & Child Neurology*, 57(12):1176–1182.

Steele, K. M., Tresch, M. C., and Perreault, E. J. (2015b). Consequences of biomechanically constrained tasks in the design and interpretation of synergy analyses. *Journal of neurophysiology*, 113(7):2102–2113.

Steward, O. (2000). *Functional Neuroscience*. Springer New York.

Stewart, J. (1992). Electrophysiological mapping of the segmental anatomy of the muscles of the lower extremity. *Muscle & nerve*, 15(8):965–966.

Stroman, P. and Ryner, L. (2001). Functional mri of motor and sensory activation in the human spinal cord. *Magnetic resonance imaging*, 19(1):27–32.

Sullivan, K. J. (2007). On "modified constraint-induced therapy..." page and levine. phys ther. 2007; 87: 872–878. *Physical therapy*, 87(11):1560–1560.

Thach, W. (1978). Correlation of neural discharge with pattern and force of muscular activity, joint position, and direction of intended next movement in motor cortex and cerebellum. *Journal of neurophysiology*, 41(3):654–676.

Ting, L. H. and Macpherson, J. M. (2005). A limited set of muscle synergies for force control during a postural task. *Journal of neurophysiology*, 93(1):609–613.

Torres-Oviedo, G. and Ting, L. H. (2007). Muscle synergies characterizing human postural responses. *Journal of neurophysiology*, 98(4):2144–2156.

Tresch, M. C., Cheung, V. C., and d'Avella, A. (2006). Matrix factorization algorithms for the identification of muscle synergies: evaluation on simulated and experimental data sets. *Journal of neurophysiology*, 95(4):2199–2212.

Tresch, M. C. and Jarc, A. (2009). The case for and against muscle synergies. *Current opinion in neurobiology*, 19(6):601–607.

Tresch, M. C., Saltiel, P., and Bizzi, E. (1999). The construction of movement by the spinal cord. *Nature neuroscience*, 2(2).

Tropea, P., Monaco, V., Coscia, M., Posteraro, F., and Micera, S. (2013). Effects of early and intensive neuro-rehabilitative treatment on muscle synergies in acute post-stroke patients: a pilot study. *Journal of neuroengineering and rehabilitation*, 10(1):103.

van Kordelaar, J., van Wegen, E. E., Nijland, R. H., Daffertshofer, A., and Kwakkel, G. (2013). Understanding adaptive motor control of the paretic upper limb early poststroke: the explicit-stroke program. *Neurorehabilitation and neural repair*, 27(9):854–863.

Van Vliet, P., Lincoln, N., and Foxall, A. (2005). Comparison of bobath based and movement science based treatment for stroke: a randomised controlled trial. *Journal of Neurology, Neurosurgery & Psychiatry*, 76(4):503–508.

Veerbeek, J. M., Langbroek-Amersfoort, A. C., van Wegen, E. E., Meskers, C. G., and Kwakkel, G. (2017). Effects of robot-assisted therapy for the upper limb after stroke: a systematic review and meta-analysis. *Neurorehabilitation and neural repair*, 31(2):107–121.

Veerbeek, J. M., van Wegen, E., van Peppen, R., van der Wees, P. J., Hendriks, E., Rietberg, M., and Kwakkel, G. (2014). What is the evidence for physical therapy poststroke? a systematic review and meta-analysis. *PloS one*, 9(2):e87987.

Vertechy, R., Frisoli, A., Dettori, A., Solazzi, M., and Bergamasco, M. (2009). Development of a new exoskeleton for upper limb rehabilitation. In *Rehabilitation Robotics, 2009. ICORR 2009. IEEE International Conference on*, pages 188–193. IEEE.

Wang, J., Tang, L., and Bronlund, J. E. (2013). Surface emg signal amplification and filtering. *International Journal of Computer Applications*, 82(1).

WHO, W. H. O. (2002). The world health report 2002 - reducing risks, promoting healthy life. URL http://www.who.int/whr/2002/en/, Last checked on September 29th, 2017.

WHO, W. H. O. (2017). The top 10 causes of death. URL http://www.who.int/mediacentre/factsheets/fs310/en/, Last checked on July 28th, 2017.

Wilbourn, A. J. and Aminoff, M. J. (1998). Aaem minimonograph 32: the electrodiagnostic examination in patients with radiculopathies. *Muscle & nerve*, 21(12):1612–1631.

Wisneski, K. J. and Johnson, M. J. (2007). Quantifying kinematics of purposeful movements to real, imagined, or absent functional objects: implications for modelling trajectories for robot-assisted adl tasks. *Journal of NeuroEngineering and Rehabilitation*, 4(1):7.

Wu, W., Wang, D., Wang, T., and Liu, M. (2016). A personalized limb rehabilitation training system for stroke patients. In *Robotics and Biomimetics (ROBIO), 2016 IEEE International Conference on*, pages 1924–1929. IEEE.

Yakovenko, S., Mushahwar, V., VanderHorst, V., Holstege, G., and Prochazka, A. (2002). Spatiotemporal activation of lumbosacral motoneurons in the locomotor step cycle. *Journal of neurophysiology*, 87(3):1542–1553.

Yang, Q., Yang, Y., Luo, J., Li, L., Yan, T., and Song, R. (2017). Kinematic outcome measures using target-reaching arm movement in stroke. *Annals of Biomedical Engineering*, pages 1–10.

Zhou, P. and Rymer, W. Z. (2004). Factors governing the form of the relation between muscle force and the emg: a simulation study. *Journal of neurophysiology*, 92(5):2878–2886.

Zollo, L., Rossini, L., Bravi, M., Magrone, G., Sterzi, S., and Guglielmelli, E. (2011). Quantitative evaluation of upper-limb motor control in robot-aided rehabilitation. *Medical & biological engineering & computing*, 49(10):1131.

Appendix A

Non-Negative Matrix Factorization (NNMF)

Non-Negative Matrix Factorization (NNMF) is a method of linear algebra to decompose multivariate data. Thus, the problem is the following: given a matrix V (being a set of m multivariate t-dimensional data vectors, in the case of muscle activity, being m EMG signals with t time points), find two matrices C and S in which matrix V can be factorized. This is equivalent to Equation A (* $\equiv$ matrix multiplication), because usually the problem has not an exact solution, being only approximated numerically. (Steele et al., 2015a; Shourijeh et al., 2016; Lee and Seung, 2001)

$$V \approx C * S \tag{A.1}$$

In this problem, V, C and S have the particularity of having only non-negative elements, which facilitates the process of discovering. This property (non-negativity) is, on the other hand, inherent to the envelope of muscular activity data, so this method is adequate to analyze EMG signals, during the arm movements, in order to find the combination of activated synergies. In this context, C represents the matrix of m x N_s scaling coefficients (relative activation of synergies) and S represents the N_s x t matrix of muscle synergies, being N_s the number of synergies to be determined. EMG signals are assumed to be possible to reconstruct from more than one synergy. (Steele et al., 2015a; Shourijeh et al., 2016; Lee and Seung, 2001)

Several algorithms have been proposed to find C and S matrices by minimization of the error between matrix V (the original EMG signals) and the approximated reconstructed matrix (signals resulting from the matrices C and S multiplication). Currently, available algorithms can only reach a local optimal solution, not a global one.

The most used, because of their easy implementation and for converging fast enough, are the two numerical algorithms analyzed by Lee and Seung (2001) which allow a locally optimal matrix factorization by multiplicative update rules. Another algorithm was later developed, the ALS (alternating least-squares) algorithm, which converges faster and more consistently (the multiplicative update rules have been shown more sensitive to initial values). (Berry et al., 2007)

So, this subsection describes only these three algorithms.

The two algorithms of Lee and Seung (2001) iteratively update matrices C and S until a cost function is minimized. Thus, they differ in the cost function considered to evaluate the approximation of Equation A. Algorithm 1 aims to minimize the Euclidean distance (Equation A), the algorithm 2 aims to minimize a measure called, by the authors, "divergence" of V from the matrix resulting from C*S (Equation A). (Lee and Seung, 2001)

$$\|V - C*S\|^2 = \sum_{ij}[V_{ij} - (C*S)_{ij}]^2 \tag{A.2}$$

$$D(V\|(C*S)) = \sum_{ij}(V_{ij} * \log\frac{V_{ij}}{(C*S)_{ij}} - V_{ij} + (C*S)_{ij}) \tag{A.3}$$

Matrices C and S are determined, at each iteration, from the multiplication of their current values by a factor, different for algorithms 1 and 2 (Equations A and Equation A, respectively). These factors are the ones which guarantee that the cost does not increase with increasing iterations (but converge to a local minimum). When C and S reach a stationary point of those cost functions, the cost function value becomes invariant. (Lee and Seung, 2001)

$$S_{\alpha\mu} \leftarrow S_{\alpha\mu}\frac{(C^T*V)_{\alpha\mu}}{(C^T*C*S)_{\alpha\mu}} \tag{A.4}$$

$$C_{i\alpha} \leftarrow C_{i\alpha}\frac{(V*S^T)_{i\alpha}}{(C*S*S^T)_{i\alpha}} \tag{A.5}$$

$$S_{\alpha\mu} \leftarrow S_{\alpha\mu}\frac{\sum_i C_{i\alpha}*V_{i\mu}/(C*S)_{i\mu}}{\sum_k C_{k\alpha}} \tag{A.6}$$

$$C_{i\alpha} \leftarrow C_{i\alpha}\frac{\sum_\mu S_{\alpha\mu}*V_{i\mu}/(C*S)_{i\mu}}{\sum_v S_{\alpha v}} \tag{A.7}$$

Concerning the ALS algorithm (Berry et al., 2007), it is based on the fact that, given one matrix, C or S, the other matrix can be found computing the least squares error and minimizing it. As so, as the name itself indicates, a least square computation is followed by another least square computation to alternatively determine the matrices C and S, like in the following pseudocode:

for i = 1:maxiter

(LS) Solve for H in matrix equation $W^T*W*H = W^T*A$.

Set all negative elements in H to 0.

(LS) Solve for W in matrix equation $H*H^T*W^T = H*A^T$.

Set all negative elements in W to 0.

end

The multiplicative update rules have the disadvantage of restricting the path followed by the algorithm: once an element of C or S becomes 0, it must remain 0. So, even if that path for a given zero element is a poor path, the algorithm will continue following it. On the contrary, ALS algorithm is more flexible, thus leading to more consistent results. (Berry et al., 2007)

Appendix B

Example of a corrupted EMG signal

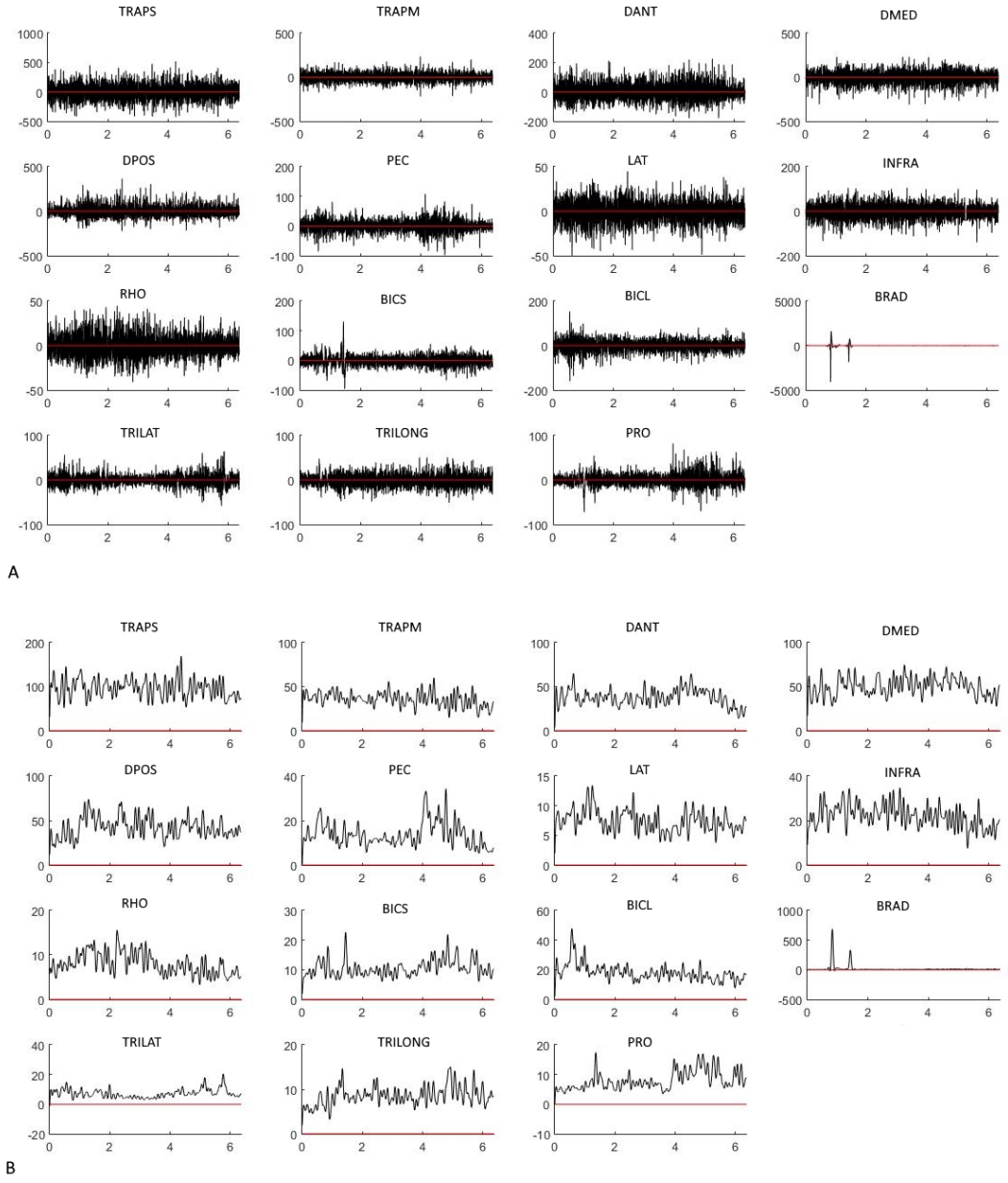

Figure B.1: Example of a bad recording where Brachioradialis EMG is severely corrupted. (A) Raw EMG signals. (B) Pre-processed EMG signals.

Appendix C

Spinal maps and the location of the target - linear relations

Table C.1: Linear relation between the 2D-correlation/covariance and the distance from one target to the respective reference (Target 13 in close-distant axis; Target 7 in left-right axis). r is the coefficient of determination and p is the respective statistical significance.

Forward		**Backward**	
Close-distant axis (y-axis)	Left-right axis (x-axis)	Close-distant axis (y-axis)	Left-right axis (x-axis)
2D-correlation vs. y-distance: $r = -0.84$ $p = 1.68e-5$	2D-correlation vs. Euclidean distance: $r = -0.79$ $p = 9.96e-5$	2D-correlation vs. y-distance: $r = -0.72$ $p = 7.10e-4$	2D-correlation vs. x-distance: $r = -0.49$ $p = 0.039$
Covariance vs. Euclidean distance: $r = -0.63$ $p = 0.005$	Covariance vs. x-distance: $r = -0.40$ $p = 0.096$	Covariance vs. Euclidean distance: $r = -0.68$ $p = 0.002$	Covariance vs. x-distance: $r = -0.07$ $p = 0.096$

Appendix D

Kinematic results of healthy subjects

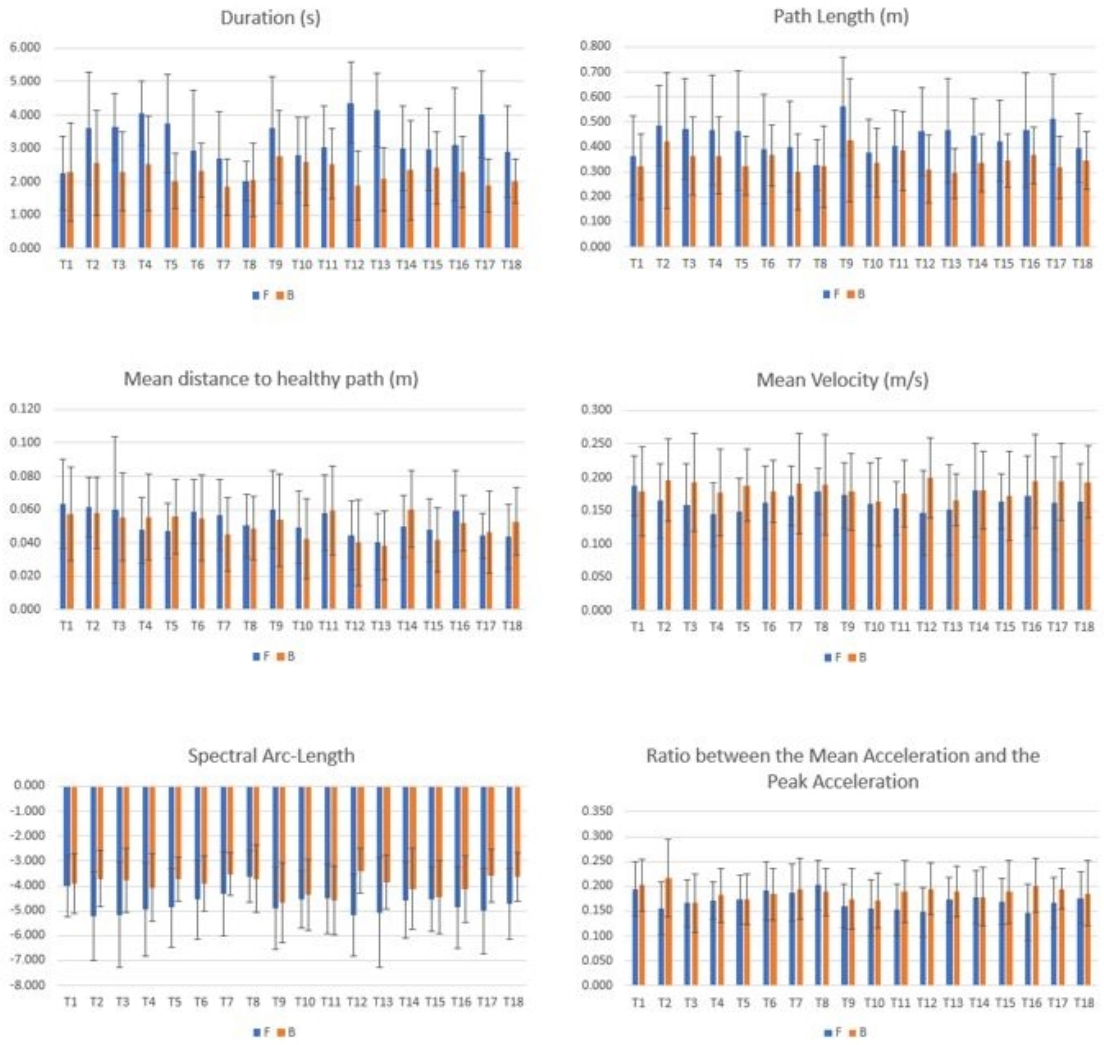

Figure D.1: Kinematic metric results obtained in healthy subjects. Average and standard deviation is indicated across subjects.

Appendix E

Muscle synergies' measures - results of stroke patients

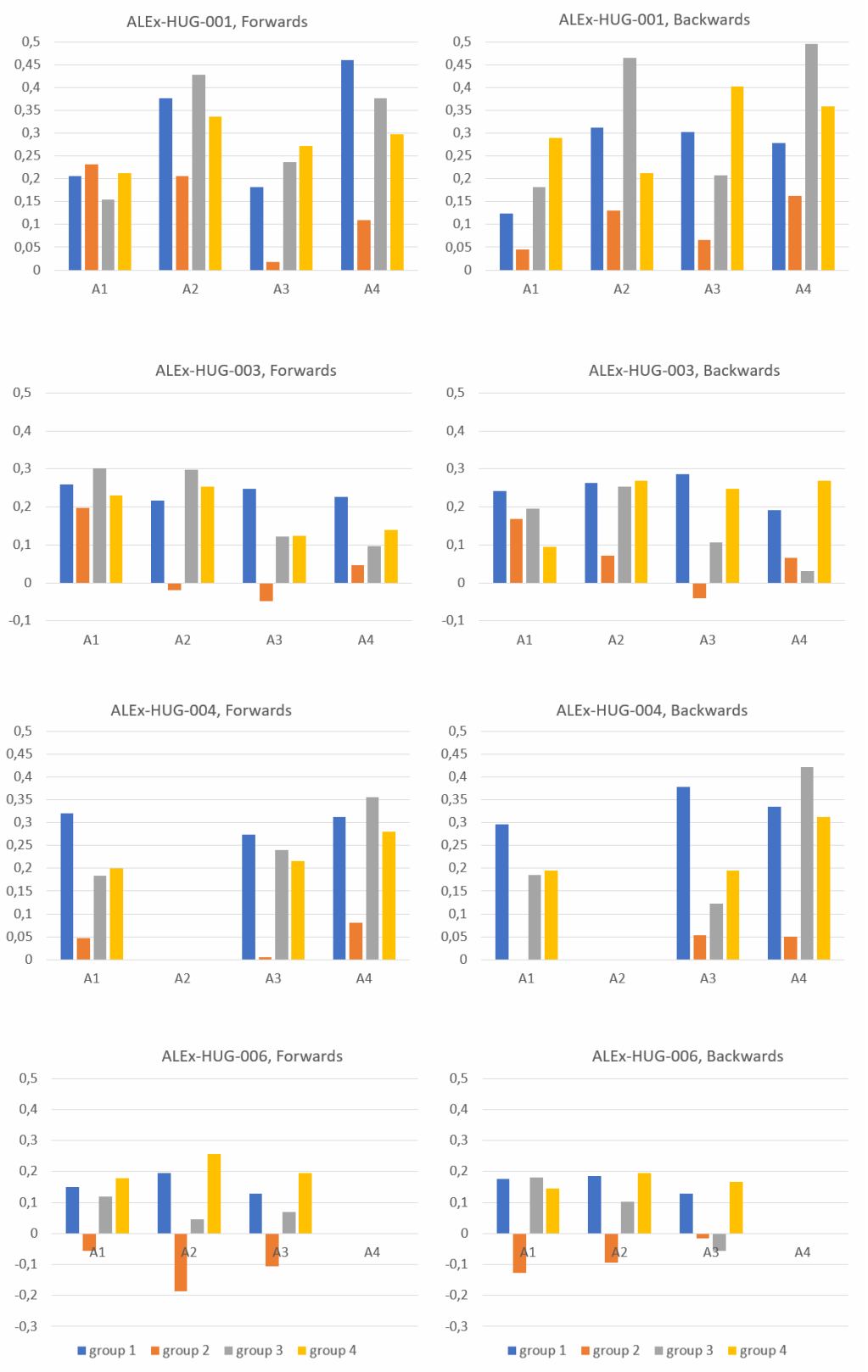

Figure E.1: Correlation between the structure of the patients' synergies and the healthy synergies (average across 4 synergies), for each group of targets (group 1, 2, 3 and 4), assessment and patient.

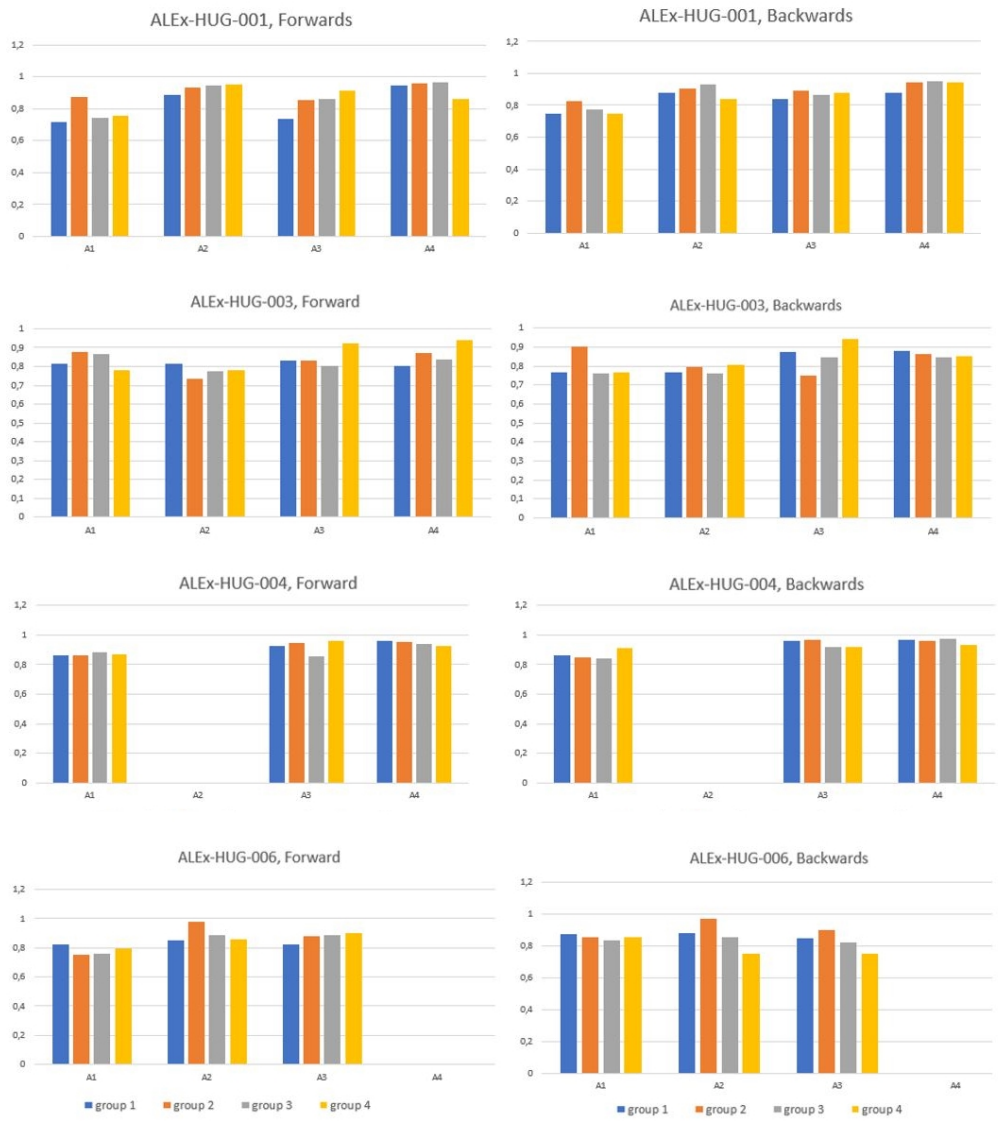

Figure E.2: "Modified-VAF" similarity ($v_{nsimilarity}$, see Section 6.7.3.1) for each group of targets in each assessment session of patients 001, 003, 004 and 006.

Appendix F

Spinal maps of stroke patients - examples

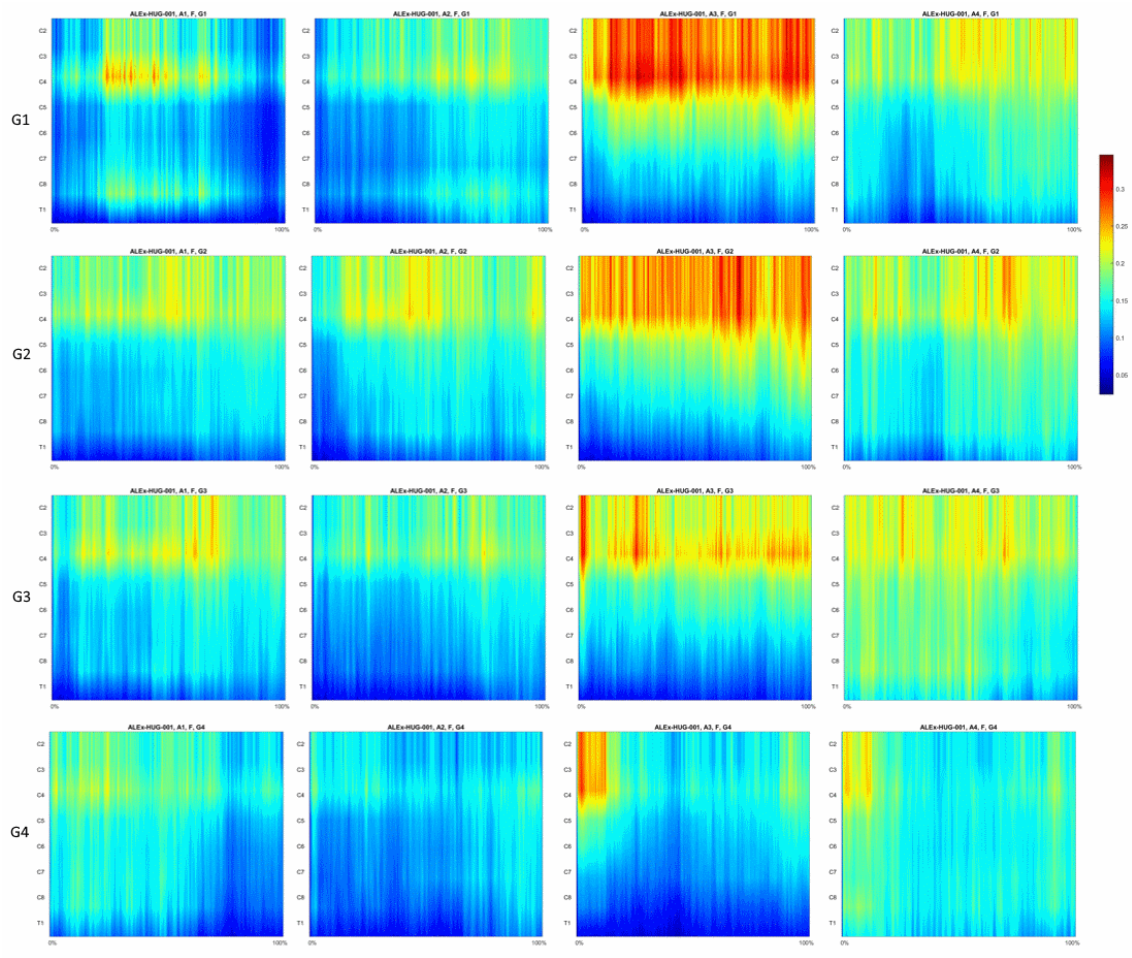

Figure F.1: Spinal maps of patient ALEx-HUG-001, for forward movements. Each row corresponds to one group of targets (G1, G2, G3 and G4). Each column corresponds to one assessment (A1 to A4, from left to right).

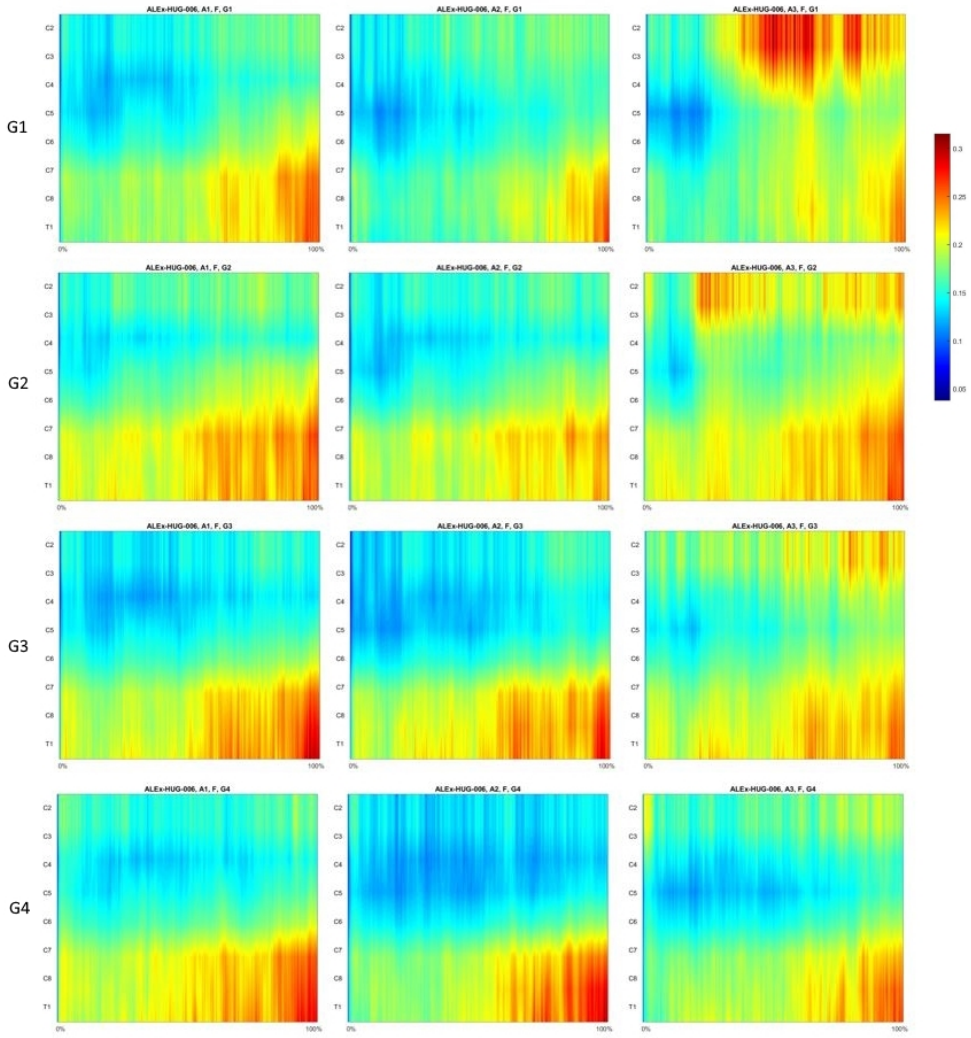

Figure F.2: Spinal maps of patient ALEx-HUG-006, for forward movements. Each row corresponds to one group of targets (G1, G2, G3 and G4). Each column corresponds to one assessment (A1 to A3, from left to right).

Appendix G

Spinal maps' measures - results of stroke patients

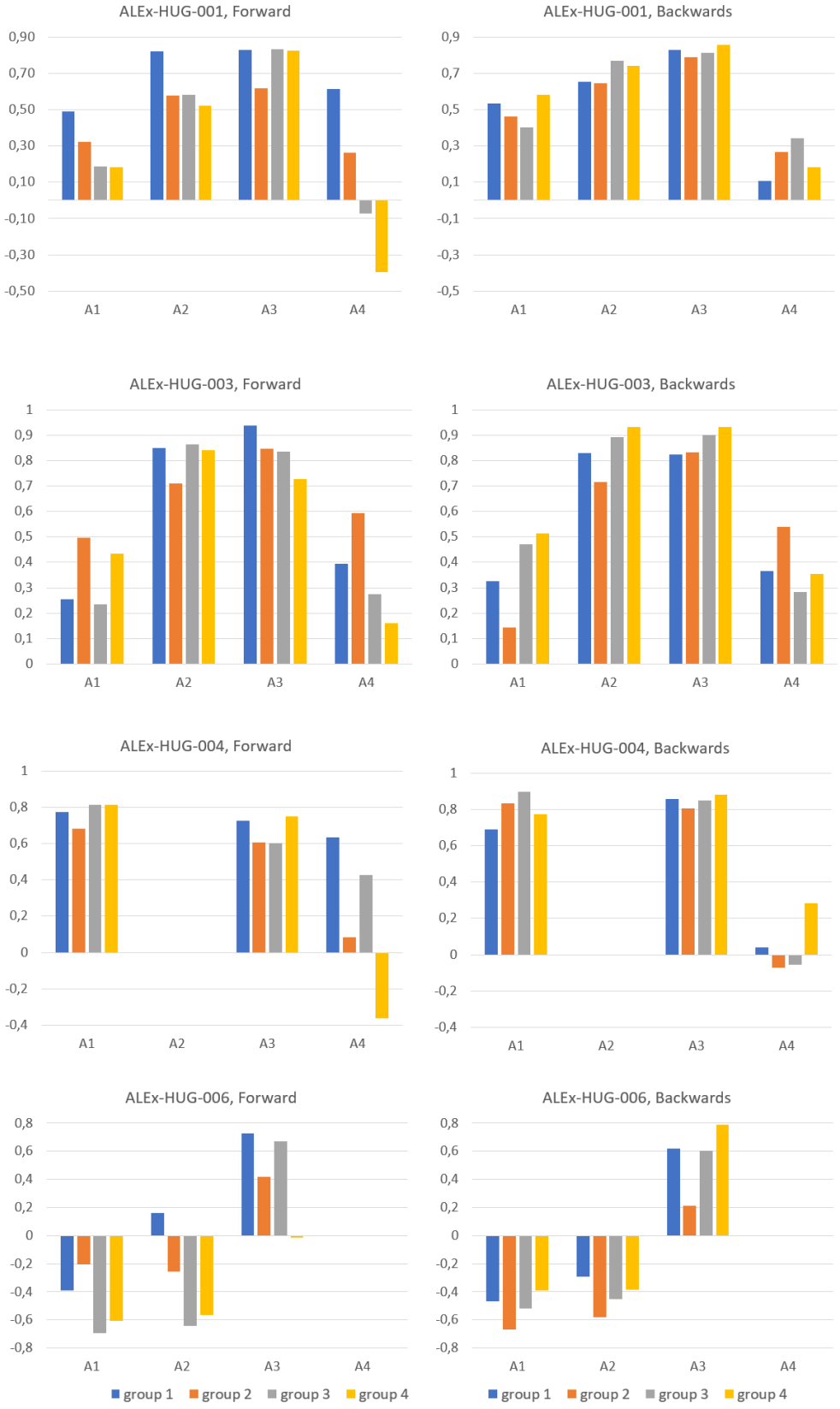

Figure G.1: 2-Dimensional correlation between the patients' spinal maps and the respective healthy ones.

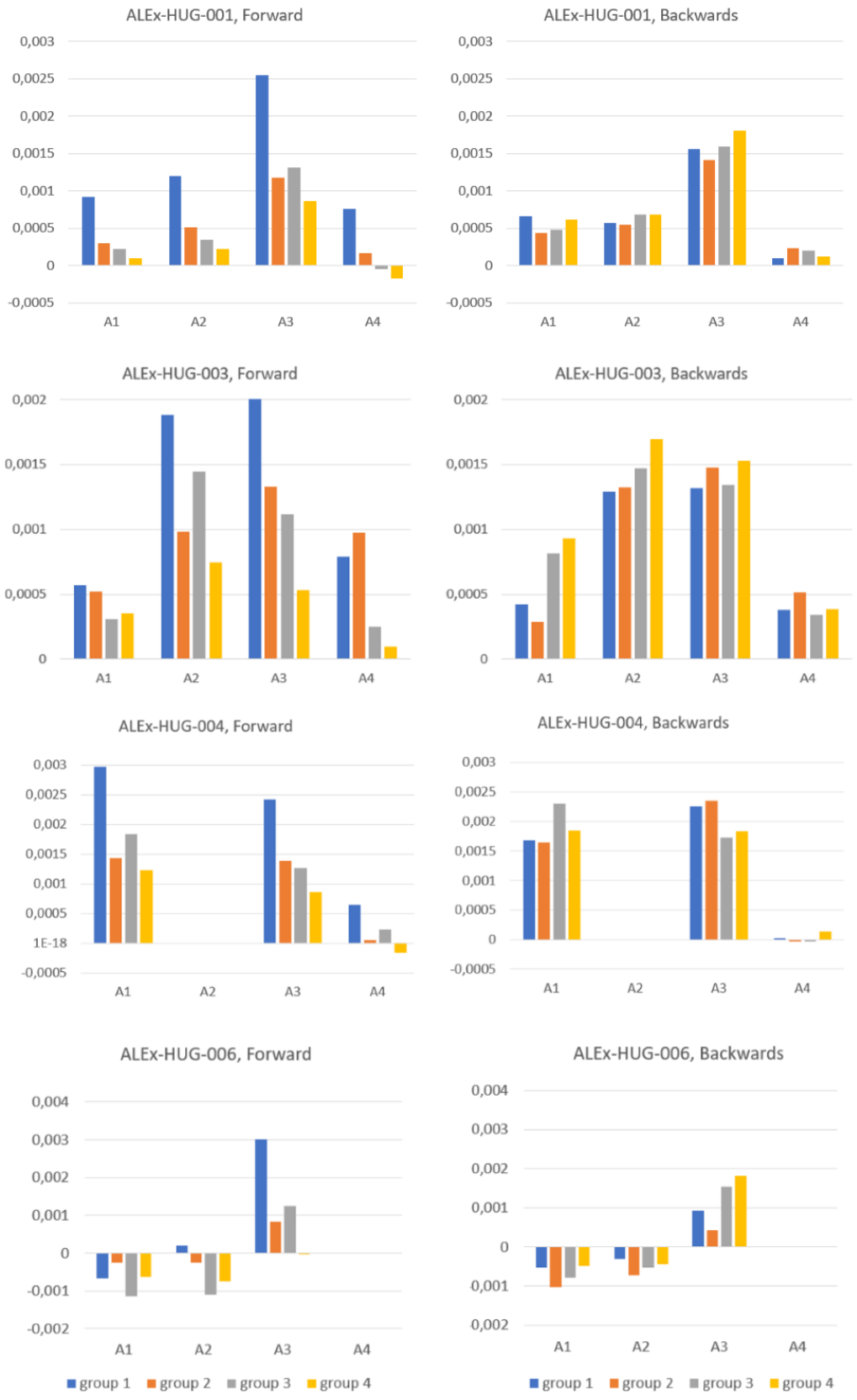

Figure G.2: Covariance between the patients' spinal maps and the respective healthy ones.

Appendix H

Kinematic metrics - results of stroke patients

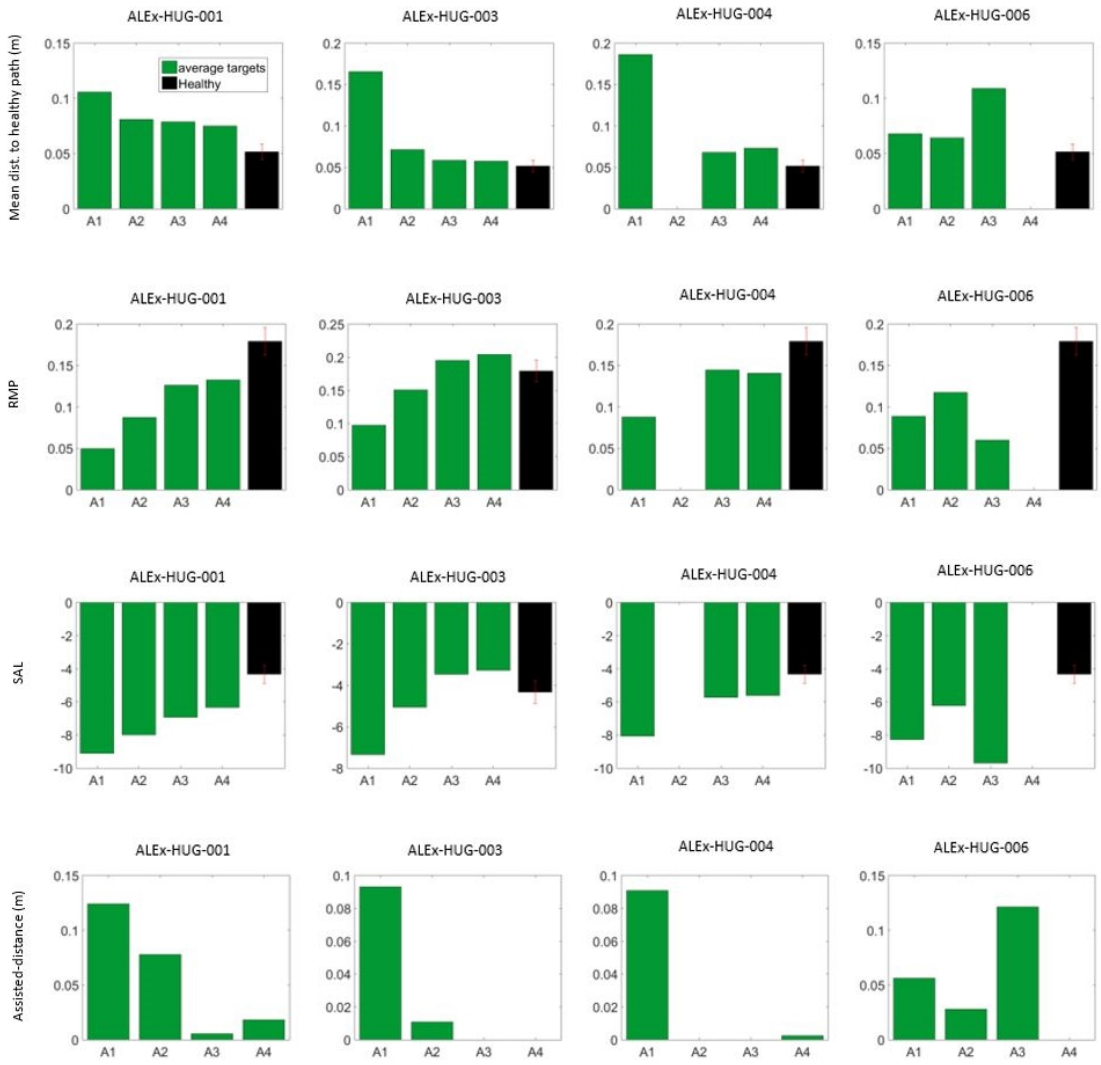

Figure H.1: Results of all patients (ALEx-HUG-001, 003, 004 and 006) in the Kinematic assessment, from assessment 1 (A1) to assessment 4 (A4). Represented values (in green) are the average across all targets (forward and backward movements). Healthy results (averaged across the 8 subjects, and across targets and directions) are presented in black. (continues in the next page)

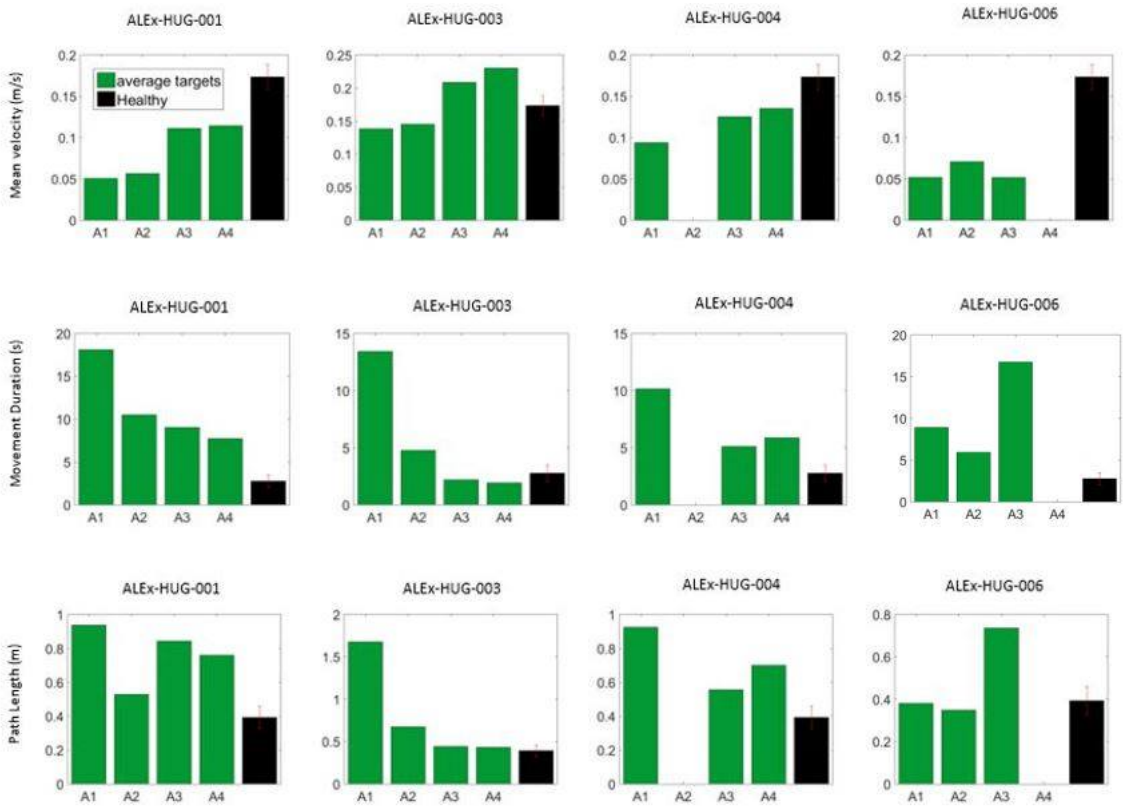

Figure H.2: Results of all patients (ALEx-HUG-001, 003, 004 and 006) in the Kinematic assessment, from assessment 1 (A1) to assessment 4 (A4). Represented values (in green) are the average across all targets (forward and backward movements). Healthy results (averaged across the 8 subjects, and across targets and directions) are presented in black.

Appendix I

Kinematics and motor performance

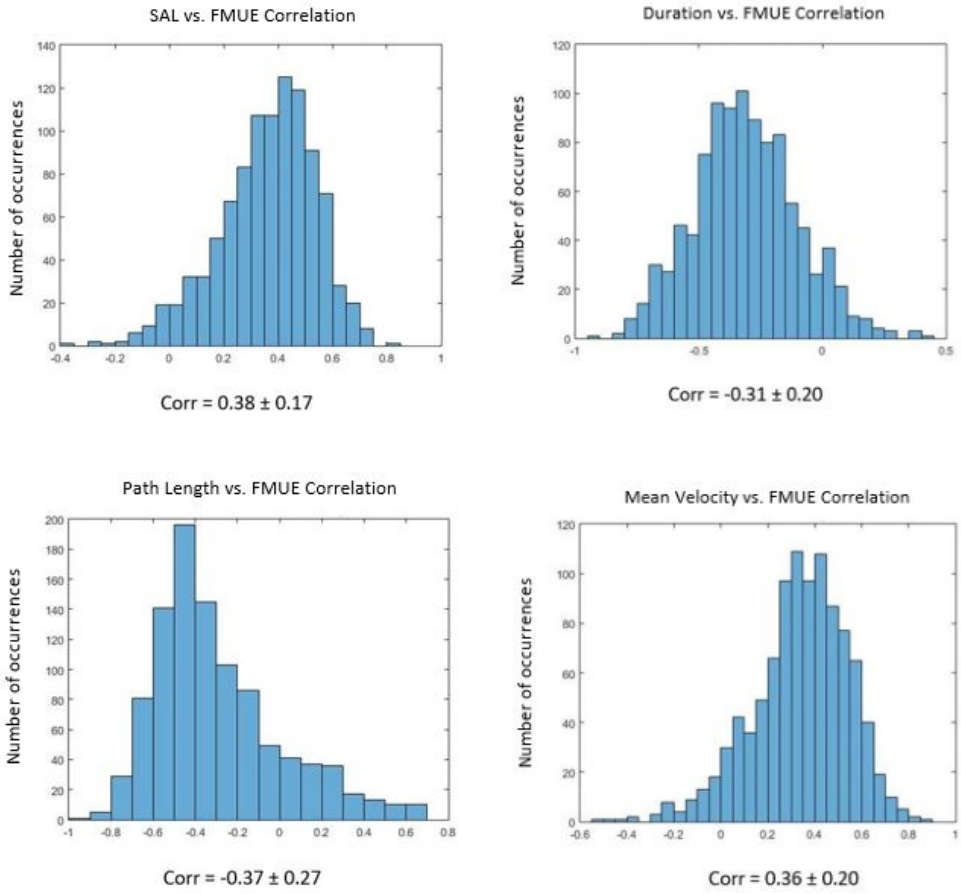

Figure I.1: Correlation between the clinical scale (FMUE) and metrics of the kinematic assessment. The average and standard deviation of the correlation are indicated below the respective histogram of the bootstrap method results. Histograms indicate the number of occurrences (bootstrap resamples / data sets) which resulted in a value of the correlation indicated in the x-axis. SAL is the spectral Arc-Length. This metric, the path length, the movement duration and the mean velocity did not achieve representative results, since their correlation with the respective FMUE score is very low.